Master Thesis

TVVR21/5006

Modelling of water and material transport in River Storån to Lake Bolmen

Hydraulic and water quality analysis in Storån river.

Imjal Sukupayo

Division of Water Resource Engineering

Department of Building and Environment Technology

Lund University

Modelling of water and material transport in River Storån to Lake Bolmen

Hydraulic and water quality simulation for the water quality analysis in Storån river.

By: Imjal Sukupayo

Supervisor: Clemens Klante

Co-Supervisor: Magnus Larson

Examiner: Rolf Larson

Master Thesis

Division of Water Resource Engineering

Department of Building and Environment Technology

Lund University

Box 118

221 00 Lund, Sweden

Water Resource Engineering

TVVR21/5006

ISSN 1101-9824

Lund. 2021

www.tvrl.lth.se

Master Thesis

Division of Water Resource Engineering

Department of Building and Environment Technology

Lund University

English Tittle	Modelling of water and material transport in River Storån to Lake Bolmen
Author	Imjal Sukupayo
Supervisor	Clemens Klante
Co-Supervisor	Magnus Larson
Examiner	Rolf Larson
Language	English
Year	2021
Keywords	Brownification, watercolor concentration, hydraulic analysis, Tracer Analysis, HEC-RAS, GIS.
Cover Photo	Storån River near Forsheda during field survey on August 05, 2020, captured by Imjal Sukupayo.

Acknowledgement

Firstly, I would like to express my sincere gratitude to Professor Magnus Larsson, Lund University, also my co-supervisor, whose expertise was invaluable in formulating the research ideas, objectives, and methodology. I truly appreciate his involvement, supervision and guidance and his insightful feedback since the preliminary phase of this study in June 2020.

Similarly, I extend my deep gratitude to my supervisor, Clemens Klante for his supervision, suggestions and sharing his ideas in the study. I would like to thank for his valuable efforts in measuring and collecting bathymetric data, organizing very fruitful site visit as well as providing vehicle during the visit. I also like to thank Sydvatten AB for arranging accommodation during the field study.

Furthermore, I am grateful to the Swedish Institute for providing me with an opportunity to study in LTH, Sweden with a scholarship that covers my tuition fee and living expenses. I am equally thankful to Lund University for providing a chance to gather in-depth knowledge in water resource engineering. I am also grateful to the university for providing working space and facility in V-Building during my thesis study.

Though the thesis is an individual work, I could never have reached the heights or explored the depths without the help, guidance, and efforts of Fainaz Inamdeen, who helped me in the understanding of the HEC-RAS software and helped me in solving problems that arose during simulations. Similarly, I would also like to thank my inspiring friend, Anjana Timilsina, who constantly motivated me to study and helped me in R- programming during bathymetric data compilation.

Lastly, my deepest appreciation belongs to my parents and my beloved friends for their constant support and encouragement throughout the study.

Popular Summary

Surface water exhibits large variation while transporting chemicals and other materials to downstream. The concentration of such material varies as per time as per the water discharge in the river and its tributaries. In lake Bolmen, some organic compounds and metal ions are causing the change in color of water to yellow or brown known, as brownification. For this, river Storån being the main tributary for the lake plays a significant role in the transport of these materials. The color concentration of water in river Storån has been increased about double in recent 35 years, and it has been a bad effect on the living organisms underwater, tourism and for drinking water purposes from the lake.

This study focuses on the transport of materials causing the brownification in the term of color concentration. Such watercolor variation due to the mixing of water in the river and tributaries has been analysed using mathematical modelling software. Storån river with seven major tributaries was set to study about the mixing mechanism and transport of materials from the south of lake Flatten to lake Bolmen. From the study, it was found that there is an increasing trend in the change in water color. Further, the change in water is seemed to be more in winter where there is high water flow in comparison to the low discharge in the river in spring and summer. The increase in the brownification might be due to the land use change, seasonal variation, and climate change.

Abstract

The change of color of water from yellow to brown termed as brownification process is mainly due to leaching of humus and iron concentrations. In recent years, this problem is increasing in lake Bolmen, a major source of drinking water in Skåne county, Sweden. This process has been a threat to aquatic life and increasing the water treatment cost too. Storån river being the main tributary of the lake has a significant contribution to this browning process.

This study deals with the hydraulic model and water quality model in the river system, modelled in HEC-RAS software to visualize the variation of brownification in Storån, for which color concentration was taken as a parameter to measure. Daily varying discharge and watercolor concentration were taken as input for the HEC-RAS model for the simulation. The 67 km reach of Storån river starting from downstream of Flatten Lake to Bolmen lake was modelled and multiple sources of color concentration from major tributaries were simulated with time-varying discharge data series.

For model setup, a Digital Elevation Model was created from bathymetric data from 18 measured cross-section and LiDAR data were taken and then merged and developed in Arc GIS and RAS mapper tools. For hydraulic analysis, daily discharge data from 2004-2019 were taken from SMHI. In the water quality model, color data from 2012-2016 were taken from SLU and analyzed. The actual transport of materials was mimicked by tracer analysis with multiple sources. The transport mechanism was solved through Advection Diffusion Equation. The hydraulic model was calibrated through velocity and elevation comparison of computed and observed values during the field survey. On the other hand, the water quality model was calibrated by steady analysis with some color data taken from SLU.

Result shows that there is an increasing trend of the brownification in river Storån. From year 1985 to 2019, the color concentration has been increased by more than 1.5 times (from 159 mg Pt./l in 1985 to 265 mg Pt./l in 2019, see *Figure 29*). The reason behind this could be the change in the land use pattern, climate change and seasonal variation in the catchment. From the model simulation, it was found that the watercolor concentration in the river is higher in a wet climate, like in autumn and winter, rather than in the drier season like in spring and summer. The possible reason for this is that high runoff draws more materials from catchments for the brownification process. Among all tributaries, it was found that catchment for the Lillån- Havridaån (R_7) has significant effect in the color variation. The study would have been better if there were more measurement stations as well as a high frequency of measurements in all tributaries.

Keywords: Brownification, Water Color, Dissolved Organic Matter, Discharge, hydraulic analysis, Tracer Analysis, Dispersion coefficient, Advection and Diffusion, Bolmen Lake, Storån River

Abbreviations

ADE	Advection Diffusion Equation
DOC	Dissolved Organic Compound
DEM	Digital Elevation Model
GIS	Geographic Information System
HEC-RAS	The Hydrologic Engineering Center- River Analysis System
HS	Humic Substances
MAWC	Mean Annual Watercolor Concentration
MARD	Mean Annual River Discharge
n	Manning's Coefficient
NOM	Natural Organic Matter
SGU	Geological Survey of Sweden
SLU	Swedish University of Agricultural Sciences
SMHI	Swedish Meteorological and Hydrological Institute
SONAR	Sound Navigation Ranging
TIN	Triangular Irregular Network
TOC	Total Organic Carbon
WCC	Watercolor concentration

Table of Contents

Acknowledgement i
Popular Summary ii
Abstract iii
Abbreviations iv
1. INTRODUCTION 1
1.1. General Background 1
1.2. Significance of the study 1
1.3. Research question and objectives 2
1.4. Structure of the report 2
2. STUDY AREA 3
2.1. Location and Geography 3
2.2. Catchment Characteristics and Landuse 3
2.3. Geology 5
2.4. River system 5
2.5. River Flow 5
2.6. Climatic conditions 5
3. LITERATURE REVIEW 7
3.1. Water quality and Brownification 7
3.2. Humic Substances, its measurement, and units. 8
3.3. Transport of material 9
3.4. River Flow and water quality modeling 12
3.4.1. HEC-RAS Software and Related theory 12
3.4.1.1. Module of study and related theory 13
I. Hydraulic Analysis 13
1-D steady flow analysis 13
1-D unsteady flow analysis 15
II. Water quality analysis 16
4. DATA COLLECTION AND PROCESSING 17
4.1. Field Survey 17
4.1.1. Bathymetric data collection by sonar method 17
4.1.2. Post Processing of the raw bathymetry data 19
4.2. Digital Elevation Model (DEM) and Shapefiles 19
4.3. Manning's value 19
4.4. Flow Data 20

4.5. Watercolor data 22
4.6. Water level of the lake 24
5. MODEL SETUP AND METHODS 25
5.1. HEC-RAS Model Development 25
5.1.1. Pre-Processing: Developing DEM and geometry of river in RAS Mapper 25
5.1.2. Processing of hydraulic analysis (steady and unsteady flow) 30
I. Steady flow analysis 30
Entering and Editing flow data. 30
Boundary Conditions 31
Flow Analysis 31
II. Unsteady Flow Analysis 31
Flow data and Boundary Conditions 31
Initial Conditions 32
Computation Option 32
Computation Intervals 33
Debugging and Model Stability 33
5.1.3. Processing of water quality analysis 34
Water Quality Constituent 34
Water Quality cells 34
Boundary condition: Watercolor concentration data 35
Initial Condition 35
Dispersion Coefficient 35
Simulation Options 36
5.1.4. Post Processing of HEC-RAS results 36
5.2. Calibration of the hydraulic and water quality model 36
5.2.1. Hydraulic Model 36
Data and processes involved. 36
5.2.2. Velocity Calibration 36
5.2.3. Water Elevation Comparison 37
5.2.4. Water Quality Model 38
6. RESULT AND DISCUSSION 41
6.1. River and Tributaries Flow 41
6.2. Long term watercolor data analysis 42
6.3. Variation in watercolor from lake Flatten to lake Bolmen 45
Regression Analysis between simulated WCC and Q at DS station 48

6.4. Tributaries contribution for color concentration 49
6.4.1. Contribution of Lilån, nedstorms Bredaryd (R_7) 51
6.5. Watercolor concentration in high/low flood events 52
7. MODEL LIMITATIONS AND UNCERTAINTIES 54
8. CONCLUSION AND RECOMMENDATION 55
BIBLOGRAPHY 56
APPENDIX 61
Appendix A: Tables and Figures 61
Appendix B: Simulation Result and Calibration results 72
Appendix C: Photographs 85

List of Figures

Figure 1 Location of study area, catchment area in the municipalities (Left) Overview of the study area. The river system was derived from the flow accumulation function of 2 m resolution DEM of the catchment in Arc- GIS (Right). 3
Figure 2 Landcover of the catchment area of Storån River 4
Figure 3 Browning of water in the river at about 40 km upstream of lake Flatten. 7
Figure 4 (Left)Sketch of the effect of Advection and Diffusion in the river. (Right) Illustration of Advection and Diffusion, Figure taken from Chapra, 1997 9
Figure 5 Molecular diffusion of a tracer through a unit area surface in water with no water velocity (Jönsson, 2006) 10
Figure 6 Energy levels at two points in a flow channel. 13
Figure 7 Main channel, Floodway, Right bank station and left bank station in a river 14
Figure 8 Deeper Smart Sonar CHIRP (Photo Credit: Deep Sonar, 2021) 17
Figure 9 (Left) Bathymetric measurement of river from deep sonar method. (Right) Measured points (yellow dots in the figure) from the sonar measurement near the B1. 18
Figure 10 Location, depth measurement and cross-section of the river Chainage of 157389 (Result from https://maps.fishdeeper.com/en-gb) 18
Figure 11 Cross section at chainage 158396 19
Figure 12 River Network and associated sub-catchments. 21
Figure 13 shows the color measuring stations, sketch of different reaches of Storån as main river the river joints of main tributaries named symbolically. 23
Figure 14 Stage hydrograph near to the outlet of Storån. 24
Figure 15 Model approach for HEC-RAS Analysis 25
Figure 16: DEM with only LiDAR file input (Left), Merged DEM with LiDAR and bathymetric data included (Right) 26
Figure 17 Sample cross section with merged DEM and LIDAR input. 26
Figure 18 Schematic diagram of rivers in HEC-RAS Geometry Editor 28

Figure 19 Cross-section editor in HEC RAS 29
Figure 20 RAS Mapper Layers 29
Figure 21 Steady flow data input for sample year 2019. 31
Figure 22 Boundary Condition for the unsteady flow analysis 32
Figure 23 HTAB properties of a sample cross-section. 33
Figure 24 Property table of a sample cross-section 34
Figure 25 Water quality cells, layers for water quality analysis in HEC-RAS 35
Figure 26 Comparison of the observed and computed water elevation in different river stations. The location of the stations can be located in Figure 18. 37
Figure 27 Color concentration in different river station with three dispersion values in water quality analysis for sample date 2015-12-15. 39
Figure 28 HEC- RAS results for maximum and minimum river profile in year 2004 to 2019 42
Figure 29: Yearly average color concentration near the outlet of Storån 43
Figure 30 Average yearly color concentration and yearly average discharge of corresponding year. 43
Figure 31 Regression Analysis for watercolor and water discharge from year 2004-2019 based on SLU data (r=0.24). 44
Figure 32 Comparison of color concentration between outlet of Flatten and outlet of Storån in Year 2012 45
Figure 33 Daily River discharge hydrograph for year 2012 46
Figure 34 Comparison of color concentration between outlet of Flatten and outlet of Storån in Year 2013 47
Figure 35 Daily River discharge hydrograph for year 2013 47
Figure 36 Regression analysis for simulated watercolor concentration and water discharge of the year 2012 and 2013 (Left: r=0.63, Right: r= 0.23) 48
Figure 37 : Correlation of river discharge and watercolor concentration for R7 (r=0.09) 50
Figure 38 Color concentration variation in different reaches of Storån river in year 2013. 51
Figure 39 Watercolor concentration for high and flow events for year 2012 and 2013. 52
Figure 40 Graphical Illustration of WCC variation on 6th April 2012. 53

***

Figure A. 1 Location of Bridges along in the Storån 64
Figure A. 2 Daily River discharge hydrograph for year 2014 65
Figure A. 3 Daily River discharge hydrograph for year 2015 and 2016 (Feb) 65
Figure A. 4 Long-term color trend of the main tributaries of Lake Bolmen (Source : Klante et al., 2021,(Remarks : Unpublished, Permission taken) 65
Figure A. 5 Correlation of river discharge and watercolor concentration for outlet of lake Flatten (r=0.32) 66
Figure A. 6 Correlation of river discharge and watercolor concentration for R3 (r=0.068) 66
Figure A. 7 Correlation of river discharge and watercolor concentration for River R5 (r=0.55) 66

Figure A. 8 Correlation of river discharge and watercolor concentration for R6 (r=0.06) 66
Figure A. 9 Land use for main tributaries of Storån (Source: SMHI). 67
Figure A. 10 Soil type for main tributaries in Storån (Source: SMHI). 67
Figure A. 11 Geological Map (Bedrock) of the study area (1/2) 69
Figure A. 12 Geological Map (Bedrock) of the study area (2/2) 70
Figure A. 13 River profile along with chainage and river 71

***

Figure B. 1 Depth mapping for simulation result for maximum water surface profile for year 2004-2019 (1/5) 72
Figure B. 2 Depth mapping for simulation result for maximum water surface profile for year 2004-2019 (2/5) 73
Figure B. 3 Depth mapping for simulation result for maximum water surface profile for year 2004-2019 (3/5) 74
Figure B. 4 Depth mapping for simulation result for maximum water surface profile for year 2004-2019 (4/5) 75
Figure B. 5 Depth mapping for simulation result for maximum water surface profile for year 2004-2019 (5/5) 76
Figure B. 6 Simulation Results for the watercolor concentration in 2014 for US and DS stations 77
Figure B. 7 Simulation Results for the watercolor concentration in 2015 and 2016 for US and DS stations 77
Figure B. 8 Calibration Results for color data of 2016-02-18 78
Figure B. 9 Calibration Results for color data of 2014-10-21 79
Figure B. 10 Calibration Results for color data of 2014-12-16 80
Figure B. 11 Calibration Results for color data of 2012-10-24 81
Figure B. 12 Calibration Results for color data of 2013-10-09 82
Figure B. 13 Comparison of the observed and computed velocity in different river stations 83
Figure B. 14 Velocity plot corresponding to the maximum water surface and lowest water profile (Aug. 7, 2018) 83
Figure B. 15 WCC variation in extreme events in year 2012 and 2013 84

***

Figure C. 1 Storån near river station 46536, Bridge code: B4 85
Figure C. 2 Storån near river station 56260, Bridge code: B5 85
Figure C. 3 Storån (upstream) near river station 70184, Bridge code: B6 86
Figure C. 4 Storån (downstream) near river station 70184, Bridge code: B6 86
Figure C. 5 Storån near river station 80977, Bridge code: B8 87
Figure C. 6 Storån near river station 87329, Bridge code: B9 87
Figure C. 7 Storån near river station 88088, Bridge code: B10 88
Figure C. 8 Storån near river station 128254, Bridge code: B13 88

Figure C. 9 Storån (downstream) near river station 154562, Bridge code: B16 89
Figure C. 10 Storån (upstream) near river station 154562, Bridge code: B16 89
Figure C. 11 Storån (downstream) near river station 157889, Bridge code: B17 90
Figure C. 12 Storån near river station 202425, Bridge code: B23 90
Figure C. 13 Storån near river station 209024, Bridge code: B24 91
Figure C. 14 Storån (downstream) near river station 212524, Bridge code: B25 91
Figure C. 15 Storån (downstream) near river station 213962, Bridge code: B26 92
Figure C. 16 Store Mosse National Park located in the catchment of river Storån. Picture credit: Clemens Klante 92

List of Tables

Table 1 River/Reaches and associated sub-catchment. 22
Table 2 Availability of the color data (The shades represent the frequency of data availability. Darker shades represent higher frequency data and vice versa) 22
Table 3 Comparison of observed and computed velocities. 37
Table 4 Comparison of the observed and computed water elevation in different river stations. 38
Table 5 Steady flow analysis water quality analysis result with sample data 2015-12-15 39
Table 6 Annual average flow and contribution of tributaries to Storån 41
Table 7 Tributaries contribution for average watercolor concentration for year 2013 49

Table A. 1 Manning's Value Chart 61
Table A. 2 Yearly, min, max color concentration for station Storån Inlopp Bolmen 62
Table A. 3 Information about bridges existing in Storån 63
Table A. 4 Land use and soil type area for each tributary and reach catchments (Source: SMHI). 68

Table B. 1 Calibration Results for color data of 2016-02-18 78
Table B. 2 Calibration Results for color data of 2016-02-18 79
Table B. 3 Calibration Results for color data of 2014-12-1 80
Table B. 4 Calibration Results for color data of 2012-10-24 81
Table B. 5 Calibration Results for color data of 2013-10-09 82

1. INTRODUCTION

1.1. General Background

Material transport in water bodies can be a serious challenge, especially if it implies the introduction of harmful chemicals or microorganisms (Conservative Energy, 2021). It may degrade the water quality and pose serious threats to the environment and the aquatic life (Inyinbor et al., 2018). The material transport can cause a change in color of the water, such as turning it into yellow or brown which is known as brownification (Lindgren, 2019). The change in the color is mainly due to leaching of humus, a brown substrate from peat or soil (SLU, 2003) and iron (Fe) concentrations (Weyhenmeyer et al., 2014), transported from soil or the geological substratum. Humus substance, a complex organic substance from terrestrial and wetland origin is a fraction dissolved organic carbon (DOC) that results yellow to brown color of water in lakes and rivers (Creed et al., 2018). Further, DOC couples with Fe to create browner color in water by (i) redox reaction (Knorr, 2013) and (ii) by preventing precipitations of Fe (Sundman, 2014). These two processes facilitate the transport of organic matter and Fe from soils into water bodies through runoff (Creed et al., 2018). The groundwater flow in the riparian zones in the boreal region may also play an important role to convey DOC in the hydrological streams (Ploum et al., 2019).

Rivers play important roles in the variation of the concentration of different substances in the lake. Furthermore, the river water exhibits large variations in the organic matter with respect to time and space (SLU, 2003). These flow processes and the natural substances to be transported or mixed in the surface water are mainly due to advection, diffusion, and chemical/biological reactions that may take place (Williamson, 2001).

The study of material transport causing brownification under varying discharges can be modelled thorough numerical modelling software with water quality model like HEC-RAS. Concentration of water color has been taken to study the as a parameter to study these brownifying materials. The variation of color concentration and its variation with the unsteady flow in the river system starting from lake Flatten to lake Bolmen has been studied in this report.

1.2. Significance of the study

Storån (“large river”) is the main tributary to the lake Bolmen, which is the main source of drinking water for the southernmost county in Sweden, Skåne (Persson, 2011). The lake also entails high value for recreation purposes and has high ecological importance (Borgström, 2020). It is also the largest source of runoff water to the lake, i.e., 40% of the total flow (Länsstyrelsen, 2006), and the largest contributor of natural organic matter (Persson, 2011). Based on 2007, the flux (product of color and discharge) from Storån to lake Bolmen was 66%. Rest of the tributaries are Lillån, Unnen, and Murån, which has the color contribution of 21%, 9% and 4% respectively (Tumdedo, 2010). The long-term color trend of the main tributaries of Lake Bolmen as shown in *Figure A. 4* also shows that Storån has highest color concentration with among other tributaries. In recent years, the problem of brownification of the water in lake Bolmen has been increasing (Borgström, 2020). Brownification also can have some environmental threats, such as warming and eutrophication (Kritzberg et al., 2019). Thus, it is of interest to study the transport of water and material from Storån to Lake Bolmen, as well as the variation in time.

1.3. Research question and objectives

The main objective of this project is to investigate concentration distribution of material transport with respect to time varying water discharge in different stretches of the river Storån and its tributaries. Through this, it will be possible to detect the concentration of materials in different time phases due to different solute sources along the river profile. Furthermore, the estimation of the water profile in different sections of the river under time varying water discharge will be determined.

1.4. Structure of the report

This thesis report consists of eight chapters. The first chapter, Chapter *1*, the "*Introduction*" describes the general background, description of the existing condition and problem in the study area, significance of study and study objectives. The second chapter is the "*Study Area*", which gives the idea of location, catchment characteristics, climatic condition and a general idea of hydrology, river system and discharge. The third chapter is "*Literature Review*" which highlights the theory involved in the transport of material and previous findings related to this research. In the same chapter, module of study in HEC-RAS software like hydraulic analysis and water quality analysis are also elucidated. The report continues further to Chapter *4 "Data Collection and Processing"* where the data collection and processing of these data taken from field survey, SMHI and SLU are discussed in detail. Aspects covered in Chapter *5* is the "*Model Setup and Methods"* used for the model development, calibration, and simulation of the results. The procedure and the parameters taken, and calibration are discussed in detail. The report further goes to Chapter *6 "Result and discussion"* which comprises the results and discussion of the analytical as well as model output. The report then dives into Chapter *7 "Model Limitations and Uncertainties"* which talks about the description of limitations of the study and model setup. The last chapter, Chapter *8 "Conclusion and Recommendation"* has contents of conclusion and recommendation of the study. Finally, the report ends with a list of references considered in the study and then comes the figures, as well as tables that could not be included in the main report, are included in the appendices.

2. STUDY AREA

2.1. Location and Geography

The study area is river Storån which is located in the Värnamo, Gnosjö and Vaggeryd municipalities in the southern part of Jönköping County, Småland province, Sweden. Both catchment of Storån and Bolmen lie in the river basin of Lagan (SLU, 2021), the second largest river on the Swedish west coast after the Göta älv (Degerman et al., 2011). Storån is originated from the forested area and large number of lakes near Bondstorp, Jönköping, and then runs through lake Långasjön and lake Flatten. Next, the river passes through the urban area of Hillerstorp and Forsheda, and finally gets mixed with the northern part of lake Bolmen *(Figure 1, Right)*. The total length of Storån is about 110 km, but this study will focus on the lower stretches of the river about 67 km south of lake Flatten to the lake Bolmen.

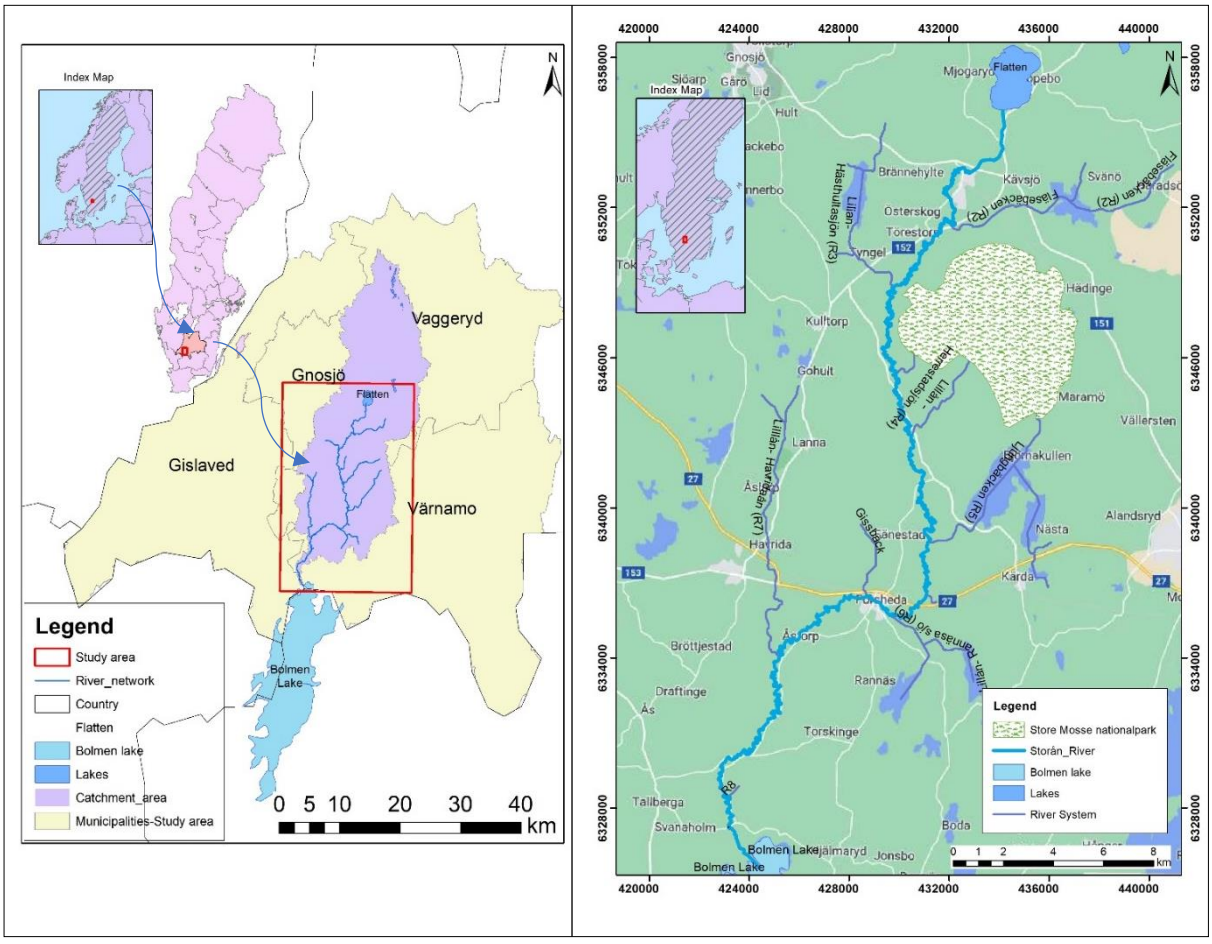

Figure 1 Location of study area, catchment area in the municipalities (Left) Overview of the study area. The river system was derived from the flow accumulation function of 2 m resolution DEM of the catchment in Arc- GIS (Right).

2.2. Catchment Characteristics and Landuse

The catchment area of the river is 676.8 km^2 of which almost 70 % is covered by forest and about 13 % is occupied by marshes and wetlands. Similarly, agricultural land covers about 8 % of total land, which is equal to half of the area covered by lakes and water courses present in the catchment. There is very little settlement area, just 1.04 % of all areas (SHMI, 2021). The population density in the catchment is 23 inhabitants per km^2 (Statiskmyndigheten, 2020). Store Mosse Nationalpark (*see Figure*

1 and Figure C. 16) of area 78.5 km^2 lies in the catchment, which is valuable wetland and Sweden's largest largely untouched raised bog area south of Lappland (Naturvardsverket, 2021).

The catchment area is dominated by glacial till (unsorted glacial sediment), 34 % followed by peat, 27 %. Thin soil and bare rock comprise 16 % and rest are silt, rough soil, sandy soils and light clay. (SHMI, 2021). The soil cover of the catchment is shown in *Figure 2*.

The lower stretch of the catchment area *(Figure 1, Right*) include large amount of fertile land, (area adjacent to the river) and the river has very mild slope (*Figure A. 14*); at the downstream end it joins the northern part of Lake Bolmen.

The details about land cover and soil cover in each tributary are shown in detail in *Table A. 4*

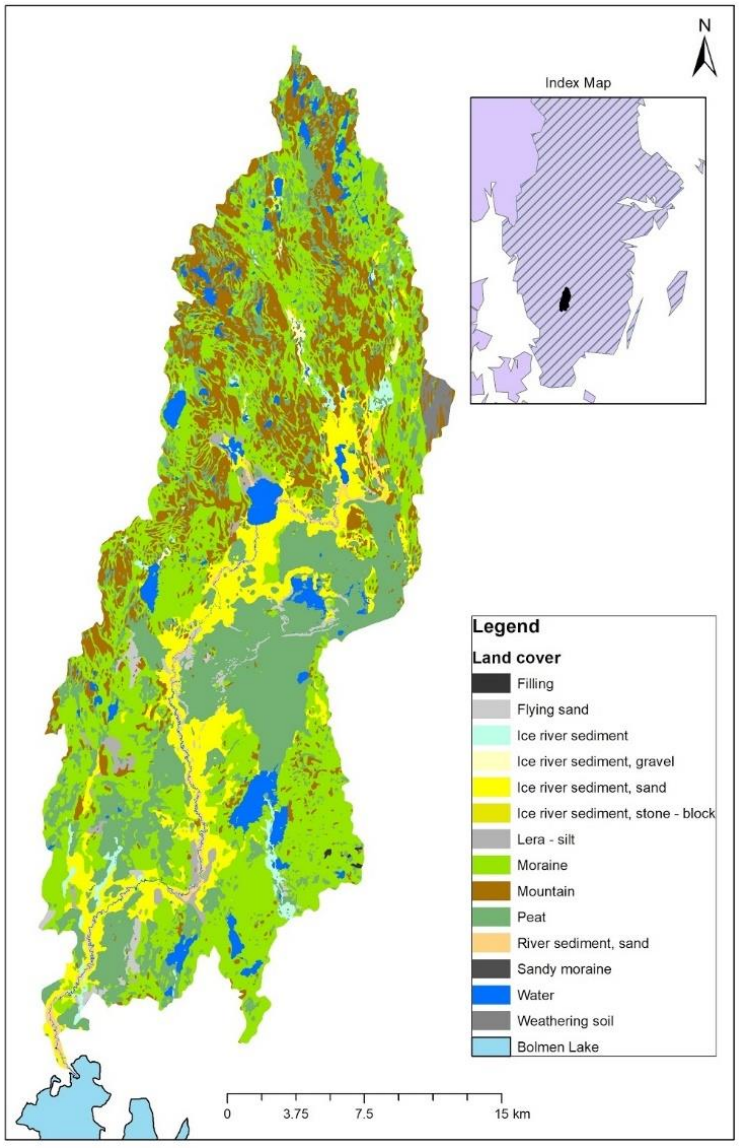

Figure 2 Landcover of the catchment area of Storån River

2.3.Geology

The area is generally covered by 1.5-1.6 billion years old crystalline rocks; gabbro, pyrozenite, anorthosite, diabase, granofric and other metamorphic equivalents. The tectonic belongs to Sveconorwegian orogen, subunit Eastern segment, middle unit (SGU, 2021). The geological formation map is shown in *Figure Figure A.* 11 and *Figure A. 12.*

2.4.River system

Storån watershed has a dendritic river system with rivers flowing from north to south and mix to the northern part of lake Bolmen. There are major seven tributaries identified. Among them, the main tributary to the river Storån is Havridaån originating from the lake Gölem, Kullerstorp followed by number of lakes which join the river in Åeke, Bredyard (Länsstyrelsen, 2006). River Fläsebäcken originating from lake Kävsjön, Store Mosse nationalpark connects to the river at Håkanstorp. Similarly, another small river commencing from lake Häasthultasjön joins the river near Simonstorp (*Figure 1).*

Other small river starting from the Store Mosse nationalpark near lake Herrestadsjön combines with the Storån river near to Frisborg (Länsstyrelsen, 2021). Other rivers are shown in *Figure 1.*

2.5. River Flow

The average flow of the river before discharging into Bolmen as per SMHI in the year 2019 was 9.5 m^3/s where minimum and maximum is 1.5 m^3/s and 30.2 m^3/s respectively. From year 2004 to 2019, as per the model data given by SMHI, the minimum flow is 0.7 m^3/s whereas the maximum is 40.3 m^3/s. From field visit and from Google Maps, it was found that there exist three small weirs built for hydropower generation in the river south of lake Flatten to lake Bolmen.

2.6.Climatic conditions

Storån river basin has four distinct seasons namely Spring (1st March to 31st May), Summer (1st June to 31st August), Autumn (1st September to 30th November) and Winter (1st December to 28th February), (Hikersbay, 2021). In Jönköping country, the average temperature is 7° C while the highest temperature of 25.0 °C has been recorded in July being the hottest month. The coldest month is January with the lowest temperature of -1.6 °C, followed by February and December. July has the highest precipitation, followed by September. February is the driest among all (Weather and Climate, 2021). It has a humid climate with average of 80 % of humidity throughout the year.

3. LITERATURE REVIEW

3.1. Water quality and Brownification

The quality of water refers to the condition of physical, biological, and chemical characteristics of water (Spellman, 2013), usually corresponding to its suitability for a particular purpose. The quality of water in rivers depends on many factors such as upon the catchment characteristics; soil type, vegetation, land management, topography, climate, season of the year, flow conditions and human activities (Lintern et al., 2018). Color is one of the parameters in water that shows the changes in physical or chemical characteristics of water. Dissolved organic compound (DOC) is considered as a main cause of change in watercolor and presence of both DOC and Fe increases the brown color significantly (Weyhenmeyer et al., 2014). Most studies performed in the boreal region of Nordic countries indicates increasing watercolor (Haaland et al., 2010).

In the boreal region like in Sweden, concentration of natural organic matter (NOM) is high due to cold and wet climate (Vogt et al., 2001). This NOM contains considerable amount of Dissolved Organic Matter (DOM). Further, DOM contributes to the formation of humic substance (HS) causing browning of the water. Brownification, an increasing watercolor to yellow or brown, has been increasing in recent decades (Ekström, 2013). A sample picture of brownification in Storån river is shown in *Figure 3*.

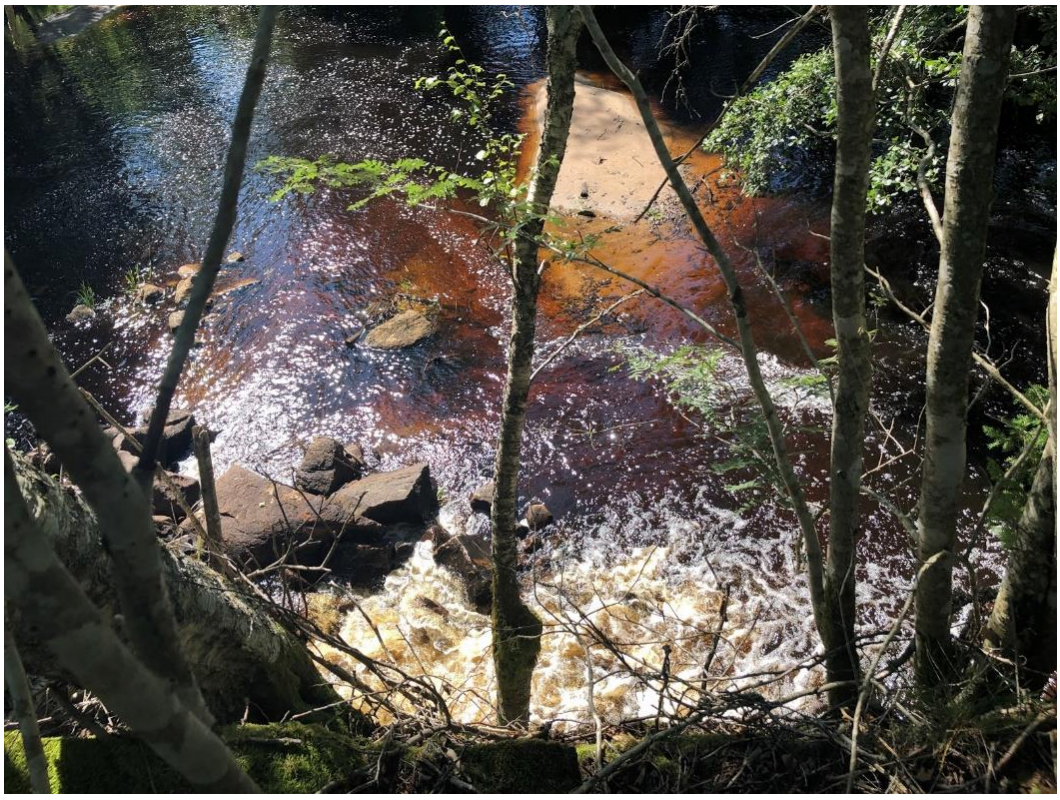

Figure 3 Browning of water in the river at about 40 km upstream of lake Flatten.

Drivers like climate change, acid deposition, increase nitrogen deposition and change in land cover, (Kritzberg et al., 2019, Meyer-jacob et al., 2019) have been contributing to generate the increased browning of inland waters. In addition, high precipitation in lowland rivers may cause floods after long dry periods that transport a high amount of DOC, which ultimately increase the color (Kazanjian et al., 2019). Further, high precipitation also increases groundwater level which helps in easy access of DOC from the organic soils (Kritzberg et al., 2019). The temperature on another hand

increases the microbial reaction by iron reduction, which results in more release of Fe (II) ions (Knorr, 2013). In a river, besides the input of water and material from the catchment, the brown color may be affected by different processes, including sedimentation, resuspension, and various biological and chemical processes (Klante et al., 2021).

Though brownification is a natural process, the yellow or brown colored water may have negative effect in tourism, may influence water quality for drinking purpose and eco-system (Kritzberg et al., 2019). For instance, it makes the water less pleasant in terms of recreational purposes like swimming and it only allows lower sunlight under the surface followed by eutrophication and cause less UV protection. The higher watercolor content can be a negative effect on the life expectancy of several fish species (Hedström et al. 2017).

Brownification also increases treatment costs when water is used for drinking purposes (approximately 5% in Sweden) (Kritzberg et al., 2019). In general, water treatment process, organic matters are removed by flocculation or any other filtering process as per the water quality inflow in the facility. If there are high amounts of organic matter, the filtration process should be done more frequently, and a high amount of coagulation materials may be needed. As the brownification is due to the higher organic compound, the rate for the filtration may get increased (Kritzberg et al., 2019).

3.2. Humic Substances, its measurement, and units.

The color in water may be the result of humic substances, peat, weeds, the presence of metallic ions such as iron and manganese, industries, etc. (APHA, 1999). In natural rivers, the absorption is mainly due to the presence of humic substances and certain iron and manganese compounds which result in the browning of water (SLU, 2021).

Humic substances (HS) are complex and heterogeneous mixtures formed due to the decay of plant and the transformation of plant and microbial remains known as humification (IHSS, 2020). HS are the major components of the natural organic matter in soil and water, as well as in the form of organic deposits as peat and sediments. At higher concentrations, HS can impart a dark color, especially in brown freshwater ponds, lakes, and streams (IHSS, 2020). Though plants decay, and microbial remains share the common properties, HS in the soil is different from the aquatic HS in chemical and structural compositions (Frycklund, 1998). Humic substances in soils and sediments can be divided into three main fractions: humic acids (HA or HAs), fulvic acids (FA or FAs) and humin, whereas aquatic HS contain only HA and FA. The aquatic humic substance is the largest fraction of natural organic matter in water, which constitutes 40 to 60 % of dissolved organic carbon (Thurman, E.M., 1985).

Humic substances can be measured in many ways like watercolor method, measuring total organic carbon, dissolved organic compound, etc. (SLU, 2003). In the method of watercolor, the color of sample water is measured against the known concentration of colored solutions. Then, watercolor number is determined by visual comparison of the sample with the standard solutions.

The method can be done by using a special and calibrated glass color disk. The standard method is the platinum-cobalt method of measuring color, the unit of color being that produced by 1 mg platinum/l in the form of chloro-platinate ion. Then, the sample of water color is then compared with dilution series of platinum cobalt chloride (the Pt/Co scale or Apha-Hazen Scale) (SLU, 2021). Thus, the unit of watercolor concentration is mg Pt./l. The turbidity should be removed, as even slight turbidity can cause the apparent color to be noticeably higher than the true color. As the color value is highly pH-dependent, pH should be measured during the standard test.

3.3. Transport of material

The material in the river is mainly due to the surface runoff. These materials can be in dissolved form as well as in suspended form. In the storm time, the soil materials can be washed away into the water. The material can be flushed away from the catchment during the first heavy rainfall of the year or heavy rainfall after a significant amount of time. Within the river, the possible modes of transport include advection and diffusion (Williamson et al., 2001). If the contamination of concern (COC) moves in a unidirectional path because of fluid motion, and the concentration of contaminant remains the same, the mode is called Advection *(Figure 4)*. It is the transport of as substance or quantity due to imposed current system (Jönsson, 2006). On the other hand, diffusion mode of transport occurs when COC moves from high concentration to the region of low concentration (*Figure 4*). It is scattering of particles or contaminants due to (i) effect of shear and (ii) transverse diffusion caused by turbulent motion (Jönsson, 2006). Diffusion process can be molecular as well as turbulent nature (Jönsson, 2006). The molecular diffusion is the random motion of molecules in a fluid and does not depend on the flow velocity. Turbulent diffusion, on the other hand results from turbulent eddies and dependent on flow velocity. It occurs as turbulent fluid systems reach critical conditions in response to the shear flow. The molecular diffusion can be demonstrated by using the Fick's law. The combined effect of Advection and Diffusion is shown in *Figure 4.*

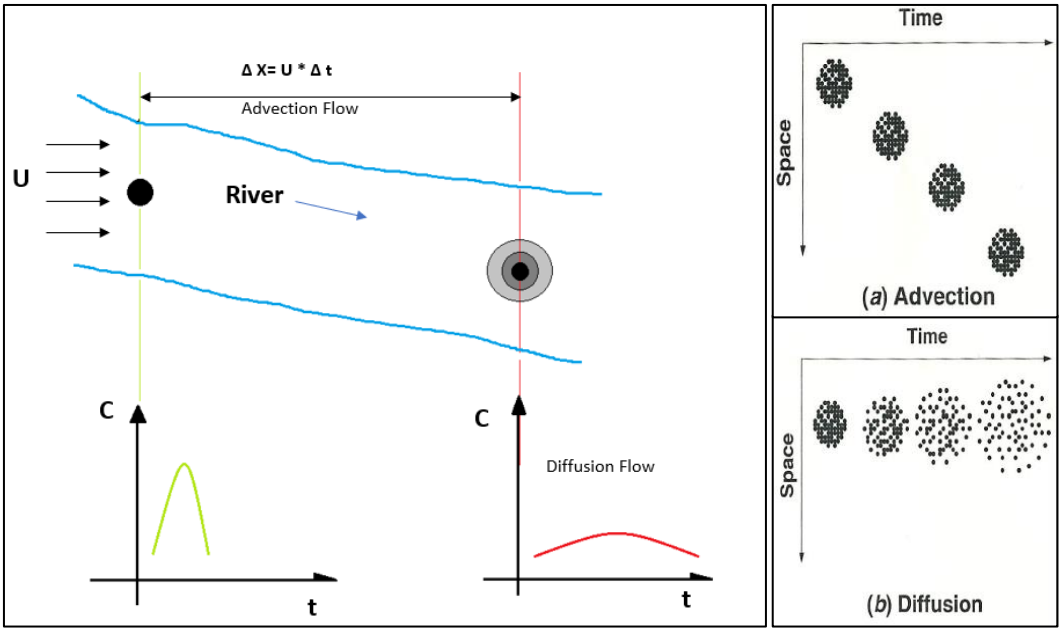

Figure 4 (Left)Sketch of the effect of Advection and Diffusion in the river. (Right) Illustration of Advection and Diffusion, Figure taken from Chapra, 1997

Fick's law

Fick's law describes about molecular diffusion in a mathematical form as

$$q = -D_{mol}\frac{dc}{dx} \qquad (1)$$

Where,

q	= flux of the diffused tracer through an imaginary unit are surface (mass of tracer/ unit area and unit time [mol/m^2/s].
D_{mol}	= molecular diffusion coefficient for the tracer (material constant) [m^2/s]
c(x)	= the concentration along of tracer along the x-axis [mol/m^3]

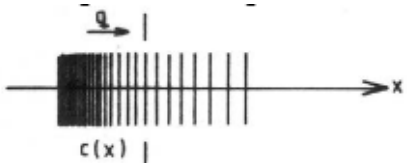

Figure 5 Molecular diffusion of a tracer through a unit area surface in water with no water velocity (Jönsson, 2006)

Advection-Diffusion Equation

The transport of contaminants in surface water can be described with advection-Diffusion equation (ADE). The mathematical form of the equation can be written as:

$$\frac{\partial \bar{c}}{\partial t} + \bar{u}\frac{\partial \bar{c}}{\partial x} + \bar{v}\frac{\partial \bar{c}}{\partial y} + \bar{w}\frac{\partial \bar{c}}{\partial z} = \frac{\partial}{\partial x}\left(D_x \frac{\partial \bar{c}}{\partial x}\right) + \frac{\partial}{\partial y}\left(D_y \frac{\partial \bar{c}}{\partial y}\right) + \frac{\partial}{\partial z}\left(D_z \frac{\partial \bar{c}}{\partial z}\right)$$

Change in concentration with time at x,y,z

Change due to advection.

Change due to diffusion.

(2)

This is the general equation for turbulent flow. If the pollutant can be produced or degraded in the flow field, it should be added in the form of source or in sink term as Q_c (mass of pollutant per mass unit of water and unit time) on the right-hand side.

In a river the mixing and transport of solute particles normally occurs in all three directions: transverse, vertical and longitudinal direction (Czernuszenko, 1987). Here in this study, the transport of solute particles is studied in one-dimensional process, the longitudinal direction. One dimensional transport equation is written as in simplified equation as

$$\frac{dc_m}{dt} + U\frac{dc_m}{dt} = \frac{d}{dt}\left(E_d * \frac{dc_m}{dx}\right) \qquad (3)$$

Where c_m = tracer concentration in a cross cross-section of river (considered as homogeneously distributed across the cross-section)

E_d = dispersion coefficient [m^2/s]

U = velocity of flow in X-direction [m/s]

The solution of the differential *Equation (2)* for this case is

$$C_m(x,t) = \frac{M}{A\rho(4\pi E_d t)^{0.5}} e^{-\frac{(x-Ut)^2}{4E_d t}t} \qquad (4)$$

M = mass of the tracer homogeneously distributed across the plane x=0 at time t=0 [kg]
A = river cross-sectional area [m^2]
t = time [s]
ρ = density of the fluid [kg/m^3]

Dispersion Coefficient

Dispersion coefficient is the spreading coefficient of tracer concentration. It is the most crucial parameter in the mass transport in the river (Antonopoulos et al, 2015). Dispersion coefficient along the longitudinal direction is called longitudinal dispersion coefficient. It varies from one river to another due to hydrodynamic and geometrical parameters of the river (Zeng & Huai, 2013). This can be calculated by the integral method, dye tracing and empirical formulae (Zeng & Huai, 2013). Some of the empirical formula from Elder (1959) and Fischer (1979) are given below.

Elder (1959) has determined the dispersion coefficient for the flow in a wide channel as

$E_d = 5.9 * H * u^*$ (m^2/s) *(5)*

Where H is the average channel depth [m]

u* = shear velocity

Also, Fischer (1979) has an estimate of dispersion coefficient based on hydraulic and geometric quantities (velocity, channel width, depth and slope) as

$D = 0.011 \frac{u^2 w^2}{y u^*}$ *(6)*

Where,

u= cross-sectional average velocity [m/s]

y= average channel depth [m]

w= average channel width [m]

u*= shear velocity [m/s]

Shear velocity is calculated by $u* = (g.d.S)^{0.5}$ *(7)*

g=gravitational constant [m/s^2]

d= average channel depth [m]

S= friction slope

This empirical formula is used by HEC-RAS v.5 as the formula for computation of E_d.

Fischer (1966) has shown that the dispersion coefficient in the natural rivers should be in the interval of $50Ru^* < E_d < 700Ru^*$ *(8)*

3.4. River Flow and water quality modeling

A hydraulic model is a mathematical model of a fluid flow system generally used to analyse hydraulic behaviour such as depth-velocity relationship and flooding (Marinwatersheds, 2021). Topographical data is also required to represent the ground surface to acquire flow behaviour in a river or a lake. Input data such as flow series, GIS files like DEM, contours shape files, river shapefiles as well as CAD files of plan, river profile and river cross-sections of the river are fed into the model to create a physical representation of the real-world system. In natural channels such as rivers, unsteady and non-uniform flow complicates the flow behavior (Galina et al., 2015). The simplified model for such complexities can be done as a river flow modelling using software such as HEC-RAS, LISFLOOD-FP and TELEMAC-2D, etc.

Water quality modeling involves water quality based on mathematical representation of pollutant fate, transport, and degradation within a water body (Tang et al., 2019). A variety of properties like temperature, color concentration, acidity (pH), dissolved solids, TOC, particulate matter (turbidity), dissolved oxygen, hardness, and suspended sediment among others are measured to determine the water quality. Those parameters can be taken to simulate in a model to determine correlations to constituent sources and water quality along with identifying information gaps (Tang et al., 2019). Quantitative models help local communities and environmental managers to better understand how surface waters change in response to pollution and how to protect them. Water quality modeling can be done in software like HEC-RAS, Delft3D, QUAL2E, irIC, MARINA, PCLake, etc.

In this study, HEC-RAS has been used for hydraulic modelling as well as water quality model. Arc GIS was employed as a platform for the merging of the cross-sectional data obtained from the sonar depth survey and LiDAR data downloaded from SLU (https://zeus.slu.se/), which was used as input in HEC-RAS. Furthermore, Arc GIS was used for demarcation of the project area, preparation of maps, spatial analysis, and hydrologic analysis.

3.4.1. HEC-RAS Software and Related theory

HEC-RAS is a free computer tools developed for the hydraulic analysis of natural river, channel and harbours developed by Hydrologic Engineering Centre, U.S. Army Corps of Engineers. It can be used for one and two-dimensional steady as well as unsteady flow, water quality, and sediment transport analysis (Brunner, 2016). The analysis is based on the input of geometry data, flow data, water quality and sediment data. Having a good graphical interference and facility of including numerous data entry, its storage and management, and good graphing and reporting facilities, it is widely used since its public release in 1995. The geometry of the river and digital elevation model can also be created and edited through HEC RAS mapper in this tool (Brunner, 2016).

RAS mapper is inbuilt module accessed from HEC-RAS which not only provides geospatial visualization but also facilitate to edit different combination of geometric data like river, joints, terrain, cross-section location, flow lines and so on. Further, the simulation results like water surface, velocity, water depth can also be viewed under this graphical interference (Brunner, 2016). The disadvantage with HEC-RAS is that a large amount of input data is required, making the model difficult to calibrate.

In this study HEC RAS v5.0.7 was used for the 1D steady and unsteady flow and water quality analysis though the DEM merging from LiDAR point source and bathymetric source was done in RAS Mapper in HEC RAS 6 beta version for better interpolation.

3.4.1.1. Module of study and related theory

In this project, one dimensional (1-D) steady and unsteady flow analysis has been performed to calculate the water level, velocity of water in different locations of the river. Then water quality model was built to find the color concentration at the different locations of the river. This chapter deals with the related theory for the hydraulic and water quality analysis.

I. Hydraulic Analysis

1-D steady flow analysis

Steady flow is defined as that in which the various parameters like velocity, pressure, and density of a flow at any point do not change with time. In 1-D steady analysis, a flow is assumed gradually varied in the river. The hydraulic water surface profile, velocity and other hydraulic parameters for subcritical, supercritical, and mixed flow condition are analysed based on inputs by the software using finite difference method (Brunner, 2016). For this, the energy equation method is employed, given as below and illustrated in the *Figure 6.*

$$Z_2 + Y_2 + \frac{\alpha_2 V_2^2}{2g} = Z_1 + Y_1 + \frac{\alpha_1 V_1^2}{2g} + h_e \qquad (9)$$

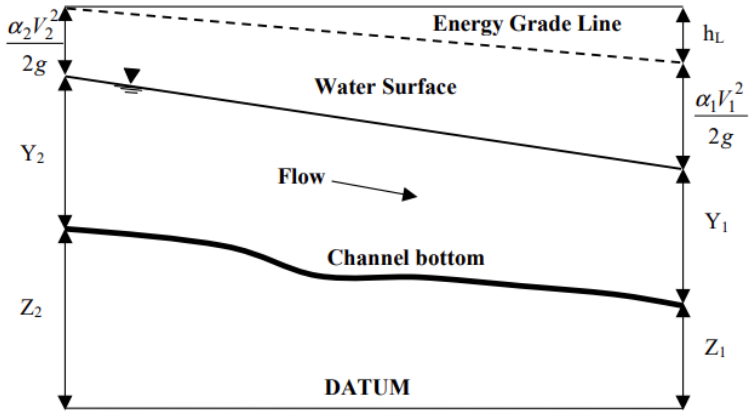

Figure 6 Energy levels at two points in a flow channel.

Where, Z1 and Z2 = elevation of bottom of the channel at cross-section 1 and 2 [m]

Y_1 and Y_2 = depth of water at cross-section 1 and 2 [m]

V_1 and V_2 = velocity of water at cross-section 1 and 2 [m/s]

α_1 and α_2 = velocity weighing factors

g = acceleration due to gravity [m/s^2]

h_e = energy head loss [m]

While doing 1-D steady analysis, each input of cross-section is divided into three parts namely left-over bank (LOB), main channel (Ch.), and right-over bank (ROB) separated by assigned manning's value (*Figure 7*). Then the water level is calculated in all these three divisions by solving the above *Equation 9* iteratively in a standard step method. As HEC-RAS assumes that the energy head is the same across cross-section and the water flows right angle with it, the final energy in the cross-section is the average of these energy levels (Brunner, 2016). After the velocity and water surface is established in one cross-section, the same will be calculated in adjacent cross-sections.

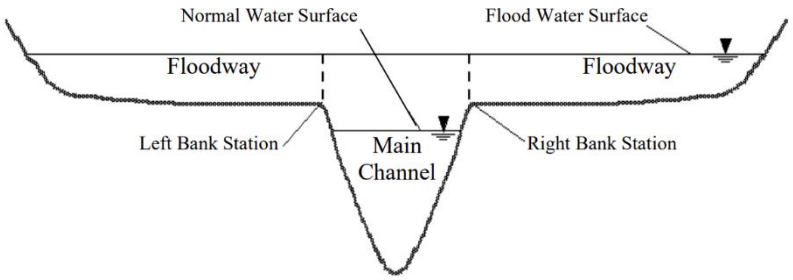

Figure 7 Main channel, Floodway, Right bank station and left bank station in a river

For subcritical flow, a boundary condition is needed in the downstream end and the computations also starts from the downstream boundary and proceed upstream. On the other hand, for supercritical flow a boundary condition is set up at the upstream from where the computations start and proceeds to downstream. But in the mixed flow regime, both subcritical and supercritical regime occurs, so boundary conditions must be taken in upstream as well as downstream. In the model, mixed regime was taken as the flow may be supercritical or subcritical as per the varying cross-sections in the river course (Paige, 2021).

Further, the energy head loss is the sum of friction loss and loss due to contraction or expansion. This is solved by the equation as per as the HEC-RAS manual.

$$he = LSf + C\left|\frac{\alpha_2 V_2^2}{2g} - \frac{\alpha_1 V_1^2}{2g}\right| \quad (10)$$

Where,
L = distance weighted reach length calculated by

$$L = \frac{L_{LOB}Q_{LOB} + L_{ch}Q_{ch} + L_{ROB}Q_{ROB}}{Q_{LOB} + Q_{ch} + Q_{ROB}} \quad (11)$$

L_{LOB}, Lch ,L_{ROB} = cross-section reach length in left overbank, main channel and right overbank respectively [m].
Q_{LOB}, Qch ,Q_{ROB}= average mean flow between sections for left overbank, main channel and right over bank respectively [m^3/s].

Q = Flow in the channel length calculated by

$$Q = KS_f^{½} \quad (12)$$

K = conveyance factor calculated by

$$K = \frac{1.486\, AR^{2/3}}{n} \quad (13)$$

Sf = representative friction slope (slope of energy grade line)

n= Manning's roughness coefficient
A = Area of the channel [m^2].
R = hydraulic radius which is calculated as area per wetted perimeter [m].
C = coefficient for expansion or contraction loss

Velocity weighing factor, α is calculated by $\alpha = \frac{Q_1 V_1^2 + Q_2 V_2^2}{(Q_1 + Q_2) V^2}$ *(14)*

V = mean velocity of the reach length [m/s].

1-D unsteady flow analysis

The 1-D unsteady flow is quite complex unlike 1-D steady analysis. In this flowrate, velocity and water depth varies in time and space throughout the river or watershed. For the boundary conditions a tabulated flow hydrograph, stage hydrograph, stage and flow hydrograph, rating curve, normal depth, time series gate openings and many more can be taken.

The analysis uses a numerical solution for St. Venant Equations that governs the flow of water, namely the continuity equation based on conservation of mass and the momentum conservation equation based on Newton's second law of motion (Ponce, 2021). HEC-RAS uses a four-point implicit finite difference scheme, also known as box scheme using the Newton Raphson iterative technique.

Unlike in steady analysis, unsteady analysis in HEC-RAS combines the left and right over bank elevation and water conveyance in a single flow compartment called as floodplain. It stores the combined properties into a one to build a single set of relationships for such flood plains (Brunner, 2016). Moreover, the reach length is also taken as the average of left bank and right bank reach lengths in each cross-section for the numerical solution, of the continuity equation and momentum equations.

Continuity Equation

The continuity equation can be written as

$$\frac{\partial Q}{\partial x} + \frac{\partial A}{\partial t} + \frac{\partial S}{\partial t} = q \qquad (15)$$

Where x= distance along the channel [m].

t = time [s]
Q = flow [m^3/s]
A = cross-sectional area [m^2]
q = inflow per unit distance [$m^3/s/m$]
S = storage from non-conveying portions of cross-sections [m^3]
V= velocity

The above equation can be written for the channel and the flood plain as

$$\frac{\partial Q_c}{\partial x_c} + \frac{\partial Q_c}{\partial t} = q_f \qquad (16)$$

$$\frac{\partial Q_f}{\partial x_f} + \frac{\partial A_f}{\partial t} + \frac{\partial S}{\partial t} = q_c + q_i \qquad (17)$$

Where c and f refer to the channel and flood plain

q_c and q_f are the exchange of water between the channel and flood plain.

q_i = lateral inflow per unit distance [m^3/s]

Momentum equation

Momentum conservation equation states that sum of all external forces acting on the system equals to the change in the momentum. Mathematically F = M Â', where F= Force acting on the system, M = mass of the fluid and "Â" is the rate of change of velocity. It can also be expressed as in Brunner, 2016.

$$\frac{\partial Q}{\partial t} + \frac{\partial (VQ)}{\partial x} + gA(\frac{\partial z}{\partial x} + S_f) = 0 \quad (18)$$

Where g= acceleration due to gravity
S_f = friction slope
V= Velocity [m/s]
Q= discharge [m^3/s]
It can be written in the channel and flood plain as

$$\frac{\partial Q_c}{\partial t} + \frac{\partial (V_c Q_c)}{\partial x_c} + gA_c\left(\frac{\partial z}{\partial x_c} + S_{fc}\right) = M_f \quad (19)$$

$$\frac{\partial Q_f}{\partial t} + \frac{\partial (V_f Q_f)}{\partial x_f} + gA_f(\frac{\partial z}{\partial x_f} + S_{ff}) = M_c \quad (20)$$

Where M_c and M_f are the momentum fluxes per unit distance exchanged between the channel and flood plains, respectively. A_c and A_f are the cross-section area of channel and the flood plain respectively. An assumption of these equations is that the water surface is horizontal (in channel and in floodplain) at any cross-section perpendicular to the flow. The resultant profile is the sum of all the forces with friction as an external boundary condition.

For the unsteady flow, varying discharge interacts with channel and floodplain flows in a such a way that when the river stage rises, then water moves laterally away from the channel inundating the flood plain and fills the water in it. These off-channel areas are modelled as storage areas and the water is filled in the available storage areas. These areas convey the discharge downstream along the shorter path available than that of the main channel. Such flows can be approximated as a flow through a separate channel. Further, when the river stage falls, the main channel is supplemented by the water through the over bank flood plains (Brunner, 2016). The flow in channel and flood plain is simplified by taking the same water level in the cross-section so that the exchange of momentum between channel and flood plain is negligible, and the discharge is distributed as:

$Qc = \phi * Q$ *(21)*

Where Q = total flow [m^3/s] $\Phi = K_c/(K_c+K_f)$

Qc= flow in channel [m^3/s] K_c K_f = conveyance in the channel, and channel

II. Water quality analysis

For water quality analysis, HEC- RAS solves one dimensional advection-dispersion equation (Brunner, 2010) using QUICKEST-ULTIMATE explicit numerical scheme. QUICKEST stands for quadratic upwind interpolation for convection kinematics with estimated streaming terms, whereas ULTIMATE stands for universal limited for transient interpolation modelling of advective transport equation. The details of the scheme are given in the HEC-RAS User's Manual (Brunner, 2016) which explains the algorithms used for the evaluation of water quality parameters. In this study, the module of non-decaying that performs conservative tracer analysis was taken, which is based on ADE. ADE equation is based on the principle of conservation of mass and Fick's law (Jönsson, 2006). The theory related to the transport of solute is given in *Section 3.3*.

4. DATA COLLECTION AND PROCESSING

Collection of data and its processing in a right order is an important step in the study. It consumes significant portion of time as per the nature of the data and its source. Open-source data from SMHI and SLU were utilized for collection of necessary data. Field survey was also conducted to collect data during the study.

4.1. Field Survey

The field survey was conducted with Clemens Klante on 5th and 6th August 2020. During the visit, the bathymetry survey of different cross-sections was done by deep SONAR method. In addition, the vertical distance from water surface to bridge surface were also measured manually in those cross-sections to determine the bottom elevation and water depth of the river and for post-processing of the raw data obtained from sonar. Furthermore, the vegetation of the catchment, browning of river discharge were roughly observed for about 100 km stretch upstream of the river starting from lake Bolmen.

4.1.1. Bathymetric data collection by sonar method

During the field work, a deeper Smart SONAR (Sound Navigation Ranging) CHIRP+ (*Figure 8*) was used to determine the depth of water in 18 different locations in the river. It was quite useful and handy as it is precise, GPS enabled with Wi-Fi attached sonar which floats in the water surface and emits a continuous flow of high and low range frequencies (Deeper, 2021).

SONAR produces a pulse of sound waves down through the water and when it hits the vegetation or bottom of the channel, the wave gets reflected to the surface. The depth of water is calculated by the relation of velocity of wave propagation and the time taken to travel down, hitting an object, and coming back to the surface (Deeper, 2021b).

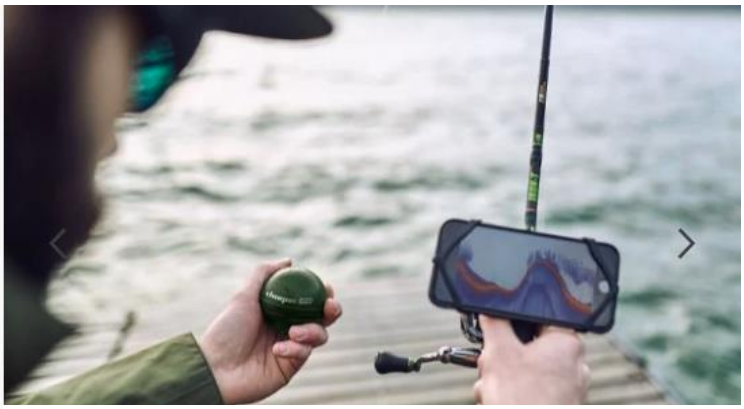

Figure 8 Deeper Smart Sonar CHIRP (Photo Credit: Deep Sonar, 2021)

The observations retrieved by sonar include time, geographical coordinates of the sonar and sonar depth measurements. The location map, profile and measurement details are displayed in the smart device connected to sonar by means of an app called Fish Deeper (Deeper, 2021).

This kind of bathymetry observations through SONAR has been successfully tested in inland water bodies of Denmark. A single beam sonar can retrieve accurate water depths with an accuracy of ca. 2.1% of the total depth for observations up to 35 meters, without effect of water turbidity (Bandini et al., 2018). The accuracy in water depth measurement is not affected by structures at bottom turbidity of water if the sound wave is correctly processed (Bandini et al., 2018).

During measurement, a thin fishing string was attached on the top of the sonar, and it was slowly released from the bridges to the water surface after connecting to the smartphone. Then the floating sonar was dragged slowly to travel from left bank to right bank of the river and vice versa (*Figure 9*). The yellow dots in the figure represents the point of measurement by the SONAR during the survey. The water depth in the periphery of the bridge were also measured, majorly in the downstream of the

river, as the sonar was left driven by the velocity of the river for a period. The measurement was recorded and then uploaded online instantly. In this process, water depth and velocity in some cross-sections were also measured. Velocity of the surface water was also measured in several locations.

Figure 9 (Left) Bathymetric measurement of river from deep sonar method. (Right) Measured points (yellow dots in the figure) from the sonar measurement near the B1.

Below in *Figure 10* shows a location, plan and cross-section of the river showing vegetation and the bottom of river near High Chaparral Camping, (in Chainage of 157389). The green and brown color in the cross-section (bottom of the figure) denotes the vegetation and soil or hard bottom, whereas some yellow spots indicate the presence of fishes. The orange polygon in the *Figure 10* shows the surveyed area in the plan. The same process was done for the remaining 17 cross-sections.

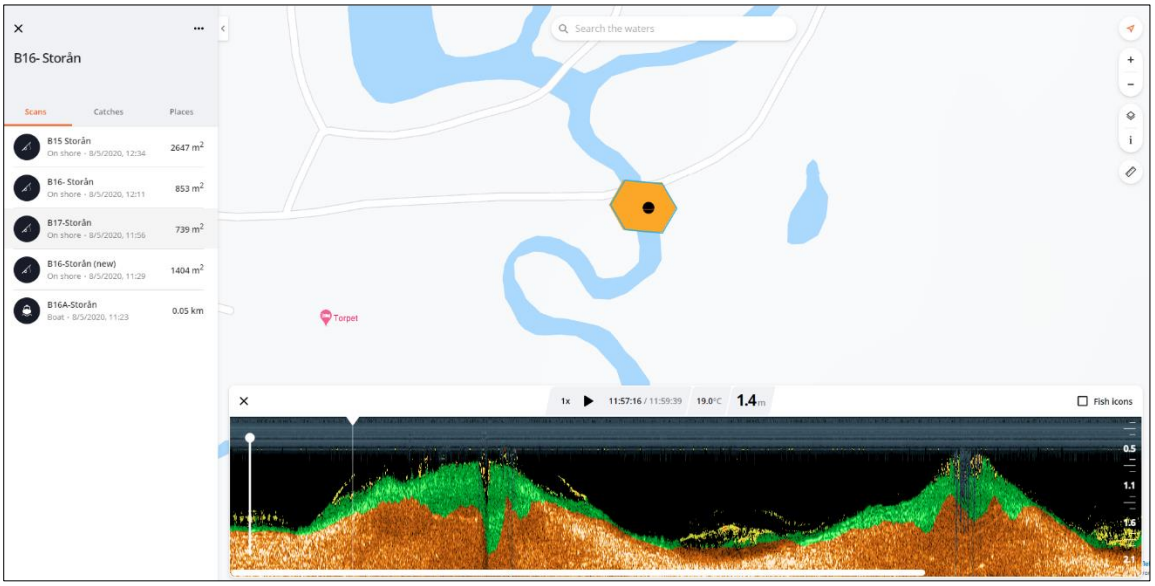

Figure 10 Location, depth measurement and cross-section of the river Chainage of 157389 (Result from https://maps.fishdeeper.com/en-gb)

4.1.2. Post Processing of the raw bathymetry data

The raw data from SONAR contains large amount of data and need to be processed further for compatibility. Software like R and MS Excel were used to process it. In the field, it was noticed that the instrument gives false measurements in the banks of the river. These data were eliminated during the process.

As the SONAR data provide the water depth instead of elevation, the elevations of each depth were computed manually. For the calculation, first the elevation of a bridge was noted from the LiDAR data taken from SLU and then the elevation of water surface was calculated by subtraction of the manual measurement of vertical distance between bridge surface and the water level from the elevation of the bridge from where the sonar measurement was done. An example of the elevation calculation of the bottom of water surface is illustrated below.

Example 1

In the *Figure 11,* the elevation of the bridge deck is 159.558 m and the vertical distance from the deck to water surface measured manually is 4.45 m and the depth of water measured from sonar is 2.75 m for one spot. Then,

Water surface elevation: 159.558 m - 4.45 m = 155.108 m

Bottom of the river = 155.108 m- 2.758 m = 152.35 m

The coordinates of the measured points were converted to X, Y coordinates of SWEREF99_TM projection. In this way, details of each surveyed points were extracted.

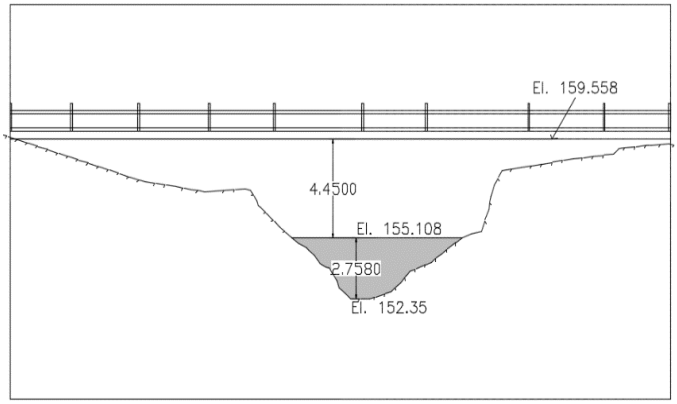

Figure 11 Cross section at chainage 158396

4.2. Digital Elevation Model (DEM) and Shapefiles

DEM represents the topographic feature of the area. For the study area, LiDAR data of 0.5 m resolution was taken. Then, the DEM was merged with bathymetry data collected during field survey. The merging of these two has been discussed in the *Section 5.1*. As the DEM was of 0.5 m cell size resolution, the river channel, riverbanks, and the flood plains were clearly visible. Such geometry was drawn manually in Arc GIS software.

For the delineation of the catchment area and river network formulation 2 m cell resolution DEM file was downloaded from Swedish Agricultural University (SLU). The raster tiles were downloaded and combined to one. Further, shape files of rivers, administrative boundary, landcover, schematic maps and other relevant maps were downloaded from geodata extraction tool from SLU.

4.3. Manning's value

The Manning's coefficient denoted by "n" is the roughness of the surface of a channel against the flow. The value is generally selected from *Table A. 1* but can be back calculated from field measurements, provided the discharge and hydraulic parameters. The selection of manning's coefficient in a model may have great effect in computational results (Brunner, 2016). In this study, the manning's value was

initially taken from the table and then they were calibrated using hydrological model as discussed in sub-chapter *5.2*.

The value can also be referenced to the pictures of the river along the river chainage as shown in *Figure C. 1 to Figure C. 15*.

4.4. Flow Data

In the study area, no gauge stations for river discharge exit at current date. Thus, the river flow data were taken from the website Swedish Meteorological and Hydrological Institute (SMHI) website: https://vattenwebb.smhi.se/ in which one can find the modelled discharge in the river modelled as per HYPE model. The Hydrological Predictions for the Environment (HYPE) model is a semi-distributed catchment model for simulation of water flows and nutrients developed by SMHI (SMHI, 2021).

The HYPE application for Sweden known as S-HYPE model is a catchment-based, process-oriented model which describes the river flow generation from precipitation and temperature values. The model calculates evapotranspiration, snow storage and melting, soil moisture, groundwater fluctuations, routing in lakes and streams in river network starting from the source till the end at sea (SMHI, 2021).

The model parameters in the S-HYPE model are calibrated manually, and it is being improved and developed continuously using the maximum use of hydrological judgements and experiences (SMHI, 2021).

The discharge generated in each sub-catchment (as shown in *Figure 12*) of a river or rivulets can be downloaded from above-mentioned website. Here, the whole catchments have been divided into sub catchments and works similar as of “Box Model”. The inflow to the sub catchment can be treated as a box, which gives the output discharge based on the S-HYPE model and the same output value becomes input to another sub catchment treated as a box located downstream in the river. From there, one can download the river flow data from the pop out window. For the study, daily and monthly discharge data of Storån river and its main tributaries were downloaded from year 2004 to 2020.

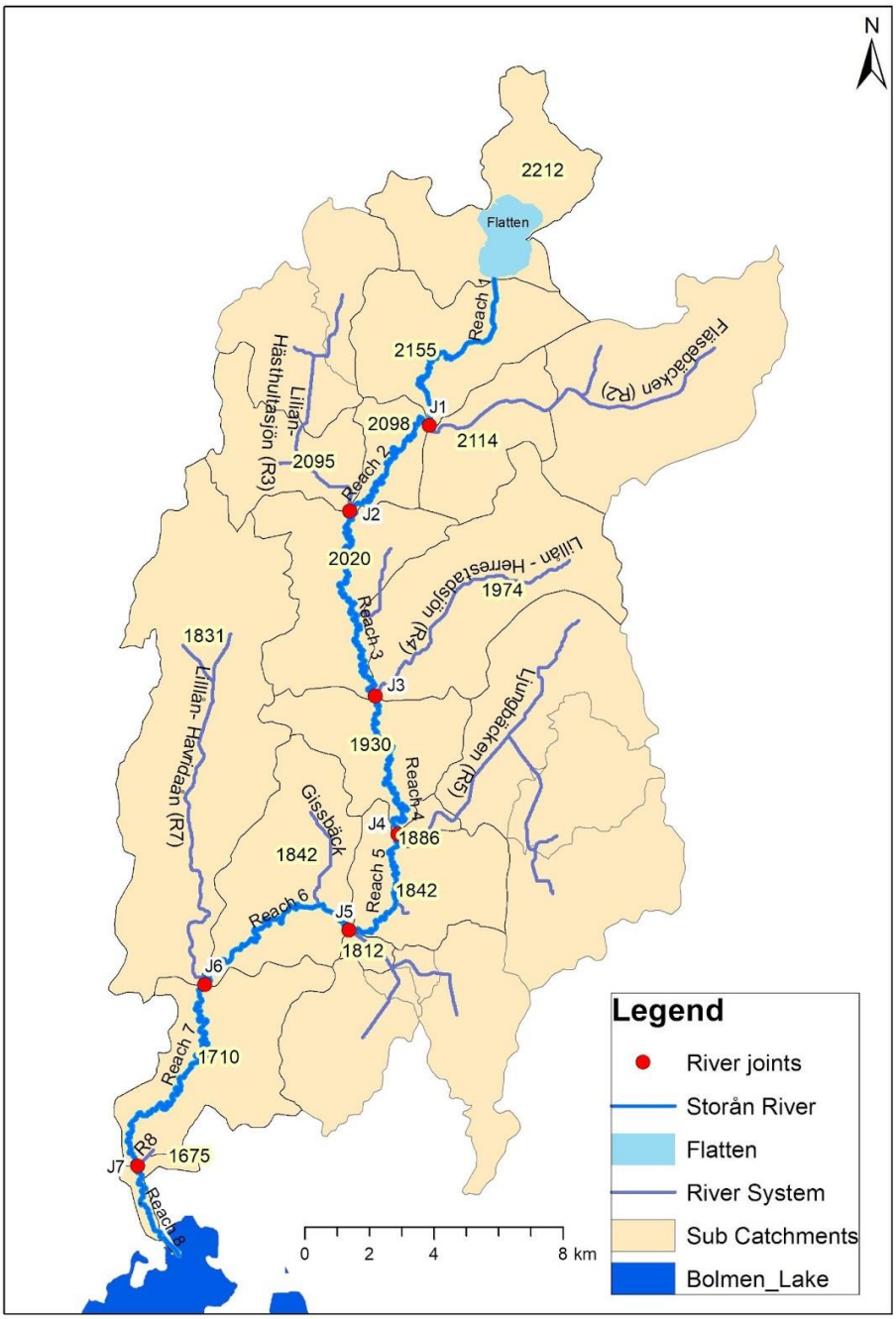

Figure 12 River Network and associated sub-catchments.

The Storån river runs through eight sub-catchments and hence they are divided into eight reaches as shown in *Figure 12*. The tributaries of Storån were symbolized as R_2, R_3, to R_8 *(Table 1)*. The flow from the other small tributaries (not considered in HEC-RAS) and direct precipitation to the river which sums to roughly 20% of the total flow (see *Table 6*) were divided as per their inflow ratio to the Storån river and added to the input of these seven tributaries flow in the model.

When the major tributaries meet the main river, a joint is made. These river joints are symbolized as J_1, J_2 up to J_7. The sub-catchments of each tributary and reach of the river is named after SUB ID as shown in the *Figure 12*.

Table 1 River/Reaches and associated sub-catchment.

SUB ID	Reaches/ River	Length (m)
2155	Storån - Reach 1	8558.17
2098	Storån -Reach 2	8108.15
2020	Storån - Reach 3	12588.04
1930	Storån - Reach 4	8386.19
1842	Storån - Reach 5	6247.57
1825	Storån - Reach 6	9193.06
1710	Storån - Reach 7	11683.40
1675	Storån - Reach 8	4303.049
2144	Fläsebäcken (R_2)	174.80*
2095	Lillån -Hästhultasjön (R_3)	67.24*
1974	Lillån - Herrestadsjön (R_4)	56.95*
1886	Ljungbäcken (R_5)	74.25*
1812	Lillån- Rannäsa sjö (R_6)	59.87*
1831	Lillån- Havridaån(R_7)	155.71*

**Only few metres of tributaries were taken in the model to feed the discharge and color concentration.*

4.5. Watercolor data

For the analysis of material transport, watercolor data is taken to be used in a conservative tracer analysis in HEC- RAS. For this, color measuring stations in the vicinity of project area were identified. A total of 10 stations *(Figure 13*) located in the river and its tributaries were taken and color data preferably after 2004 were collected from them as discharge data from SMHI is only available from 2004. From the observation, it was found that the time interval of measuring and the frequency of measurements in all stations differs from each other. Also, the data availability years is not same for all the stations. The data stations, the yearly data availability and frequency of measurements are shown in *Table 2*. From the table, it was found that from year 2012-2015 are the common years for all stations for the availability of color data.

Table 2 Availability of the color data (The shades represent the frequency of data availability. Darker shades represent higher frequency data and vice versa)

SN	Stations	2004	2005	2006	2007	2008	2009	2010	2011	2012	2013	2014	2015	2016	Frequency (per year)
1	Flatten														1
2	Storån, Flatens utlopp														6
3	Storån, nedströms Törestorp														6
4	Storån, nedströms Forsheda							N/A	N/A	N/A	N/A	N/A	N/A	N/A	6
5	Storån, nedströms Forsheda ARV	N/A	N/A	N/A	N/A	N/A	N/A								6
6	Lillån, nedströms KAPE														6
7	Lillån, nedströms Bredaryd														6
8	Storån inlopp Bolmen														12
9	Bolmen Norra														1
10	Herrestadssjön utlopp	N/A	N/A	N/A	N/A	N/A	N/A	N/A	N/A					N/A	4
11	Lillån Perstorp	N/A	N/A	N/A	N/A	N/A	N/A	N/A	N/A						4

The tabular data provided by SLU has color concentration data measured in different depth but for the analysis, measurement at 0.5 m in depth were employed to the model.

For the simulation, color data was necessary to feed in every computation time corresponding to the flow series. In this study, the daily flow series were taken, so at least daily color concentration data was required. But due to the lower frequency of color measurement in the sub-catchments, a linear interpolation method was approached for the filling of the missing data for simplification of the model. For instance, there were just six color data in every year for station "Storån Flatens utlopp", but in the model, a continuous data of computation time step was required for the simulation. Hence a linear interpolation of color data between two measuring dates was taken for simplicity However, it is important to note that such data filling can only provide data that are lower than the typically measured color data. Further discussion about the color data has been done in sub-section *5.1.3*.

For analytical analysis for river Storån, the color data available from the year 1987 to 2019 was taken for station Storån inlopp Bolmen. For analytical analysis for river Storån, the color data available from year 1985 to 2019 was taken for station Storån inlopp Bolmen. The analysis is shown in *Chapter 6.*

Assumptions

Following assumptions were taken while handling and processing the data water quality analysis.

1. In *Figure 13*, most of the color measurement stations identified in tributaries are not nearby the river joints (red dots in the figure) but lies somehow upstream of the tributaries (Green dots in the figure). For the simulation of the watercolor concentration (WCC) source should be in the river joints where tributary meets the river Storån. To overcome this, the concentration of color in each tributary are assumed to have the same concentration throughout its water course. It means that, no matter how far is the color measuring station is from the river joint, the same WCC will be taken as input for tracer analysis.

2. Color data in the lake Flatten was not sufficient for the analysis due to lesser frequency of sample measurement. But the hydraulic analysis starts from Flatten Lake. There exists a next color measuring station just 1.4 km downstream of the lake. So, the concentration of water

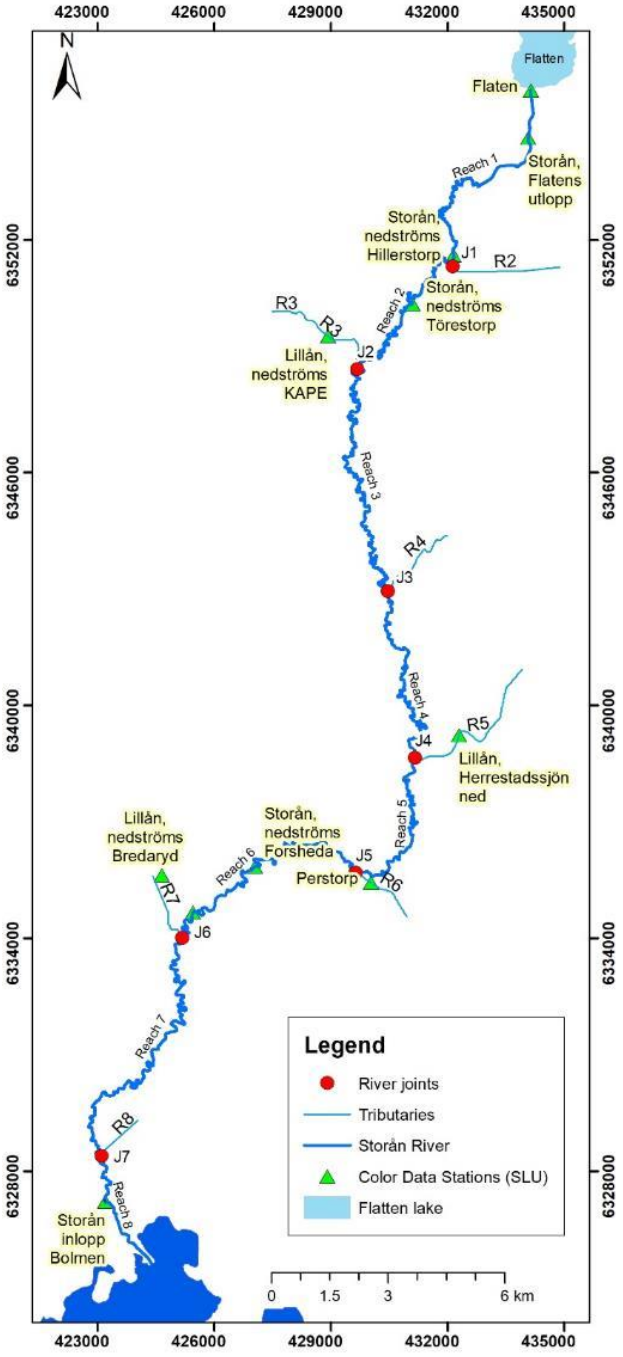

Figure 13 shows the color measuring stations, sketch of different reaches of Storån as main river the river joints of main tributaries named symbolically.

flowing from Flatten were assumed to have the same color concentration as station Storån Flatten Utlopp.

3. Rivers R_2, R_4 and R_5 originates from the Store Mosse National Park. Unlike in the river R_5, there are no data observation found in the vicinity of the rivers R_2 and R_4. To solve this, the color concentration was taken as taken as the same of as R_5.

4.6. Water level of the lake

Water level of the Bolmen lake was taken from the measuring station present in the northern part of the lake. *Figure 14* shows the water level at the northern part of the lake assumed as the water level at the outlet of the river. This water level is taken as the downstream boundary condition for the model. The horizontal line in the figure is the average level of water from year 2004 to 2007. After that, daily water level variation can be seen up to 2019.

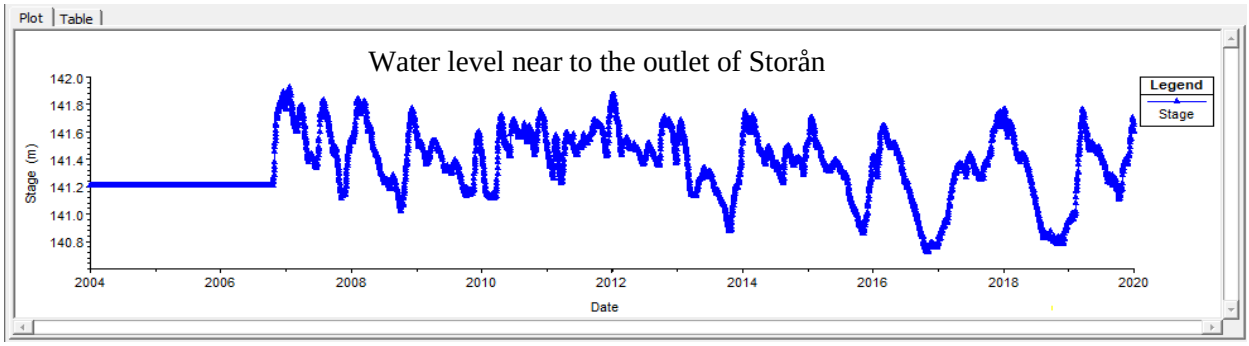

Figure 14 Stage hydrograph near to the outlet of Storån.

5. MODEL SETUP AND METHODS

In this chapter, the step and procedure for the model setup in HEC- RAS has been described in detail in sub-chapter wise. Furthermore, calibration of hydraulic model as well as water quality model has also been described.

5.1. HEC-RAS Model Development

Model setup includes several steps while inserting the inputs and model parameters. Schematic approach of the model building for performing hydraulic analysis and water quality analysis is shown in *Figure 15.*

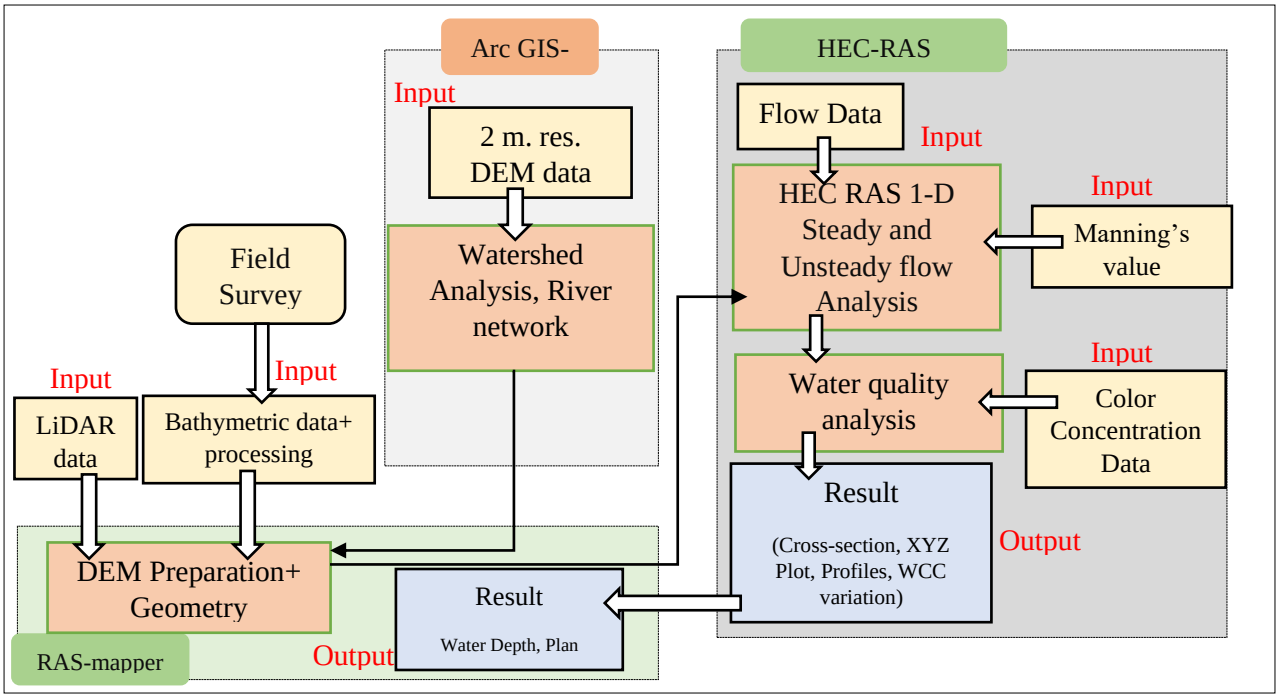

Figure 15 Model approach for HEC-RAS Analysis

The methodology used for performing the simulation analysis can be mainly divided into four process as follows :

a) Pre-Processing : Developing DEM and geometry of river
b) Processing of hydraulic analysis (steady and unsteady flow)
c) Processing of water quality analysis (conservative tracer analysis)
d) Post Processing of HEC-RAS results

Apart from it, long term data analysis of color data for Storån river and its tributaries were also done analytically with an aim to study the trend of color concentration varitaion over the years.

5.1.1. Pre-Processing: Developing DEM and geometry of river in RAS Mapper

Digital Elevation Model (DEM) Preparation

The LIDAR file was processed in Arc GIS while the cross-section data were merged with the DEM in RAS mapper, HEC-RAS. Before downloading the LiDAR file, a project boundary was demarcated on the website and the data tiles inside the project area were downloaded in the form of *.las file. Then it

was converted to compatible *.laz file by software "*lastool*", then merged into one. Further, the digital elevation model in *.TIF format was made in Arc GIS with cloud points of "Ground" class among all.

As the digital elevation model made from LiDAR file lacks bathymetric data, the DEM then was modified in HEC-RAS. For this, the bathymetric data of 18 cross-sections were taken and interpolated throughout the river. Then terrain of the bathymetric data was created and finally merged in RAS Mapper with DEM created in Arc GIS. This process took a substantial amount of time in the model preparation. During this process, the bathymetric data of the main river was merged with DEM, other tributaries of the Storån was left unchanged in the terrain merging process.

The illustration of this data merging process in shown in *Figure 16*. In the left image, the DEM is presented prepared from the LiDAR file in which, the actual depth of river is not computed whereas the right image shows the merged DEM of LIDAR file and bathymetric data. A sample cross-section is also shown in the *Figure 17*. In the figure, cross-section of the river before processing of bathymetric data and after processing are shown. While developing the model, bridges, hydropower weir and other structures were not modelled to make the model simple to study and analyze.

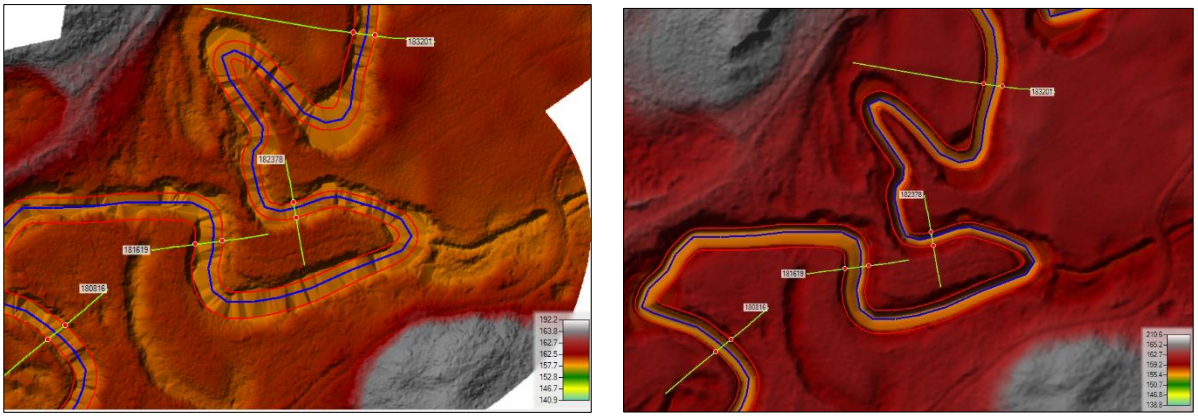

Figure 16: DEM with only LiDAR file input (Left), Merged DEM with LiDAR and bathymetric data included (Right)

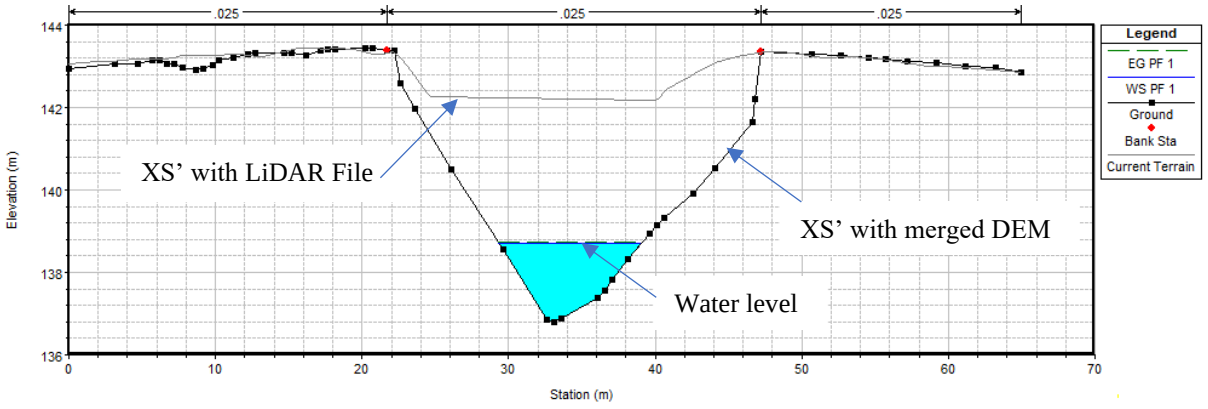

Figure 17 Sample cross section with merged DEM and LIDAR input.

Projection System

The projection system was set to SWEREF 99 TM in both Arc GIS and HEC-RAS. It is a national projection system for Sweden (Lantmäteriet, 2021b).

Most of the data downloaded from SMHI and SLU were from the same projection, but the data obtained from Google Earth and field work were in WGS1984 and were projected to SWEREF99_TM later in Arc GIS.

Geometry Preparation

River system geometry was first developed in Arc GIS and then exported to HEC-RAS. At first, watershed analysis in Arc GIS was done to delineate a catchment of the river Storån. After that, the geometry was fed to HEC RAS in the RAS Mapper.

Catchment delineation

For the catchment delineation, DEM of 2 m cell size was taken from SLU. Following process in sequence in Arc GIS were followed for watershed analysis and to develop river network.

1. *Fill:* It removes raster cells which does not have any associated drainage value known as sinks, present in the DEM. A similar DEM is added after this step and it is used for flow direction step.

2. *Flow direction*: It computes the grid value to each cell to indicate the direction of the flow as per the topography present. It is fed as input for the flow accumulation process.

3. *Flow accumulation*: It calculates the flow into each cell by identifying the upstream cells to the downs lope cell. After this step, a new file will be added which contains a grid value that represents the number of cells upstream from that cell.

4. *Stream segmentation*: This allows assigning the same unique value to stream cells located within the same stream segment Threshold of the cell size in flow accumulated file is taken in order to limit the size of the river present in the topography.

5. *Create outlet /Snap pour point:* This process includes the creation of a cell/raster point manually to which all the water is poured. It should exist in the higher flow accumulation value cell. In this study, the snap pour point was taken at the mouth of the river just before joining the lake Bolmen.

6. *Stream segmentation and processing*: It creates the drainage grid having the unique value.

7. *Delineation of watershed*: It comprises developing the watershed area prior to the pour point based on flow accumulation and flow direction. Later the raster file was converted into vector data.

The river network formed due to DEM were also compared with the schematic maps, shape files and LiDAR file provided by SLU.

River Geometry

This includes data related to the river system, river joints, cross-section geometry, bank lines and reach length information. For this, river system obtained from flow accumulation step in Arc GIS was taken. While importing geometry, the river stretches only from lake Flatten to lake Bolmen was imported (*Figure 13 and Figure 18*). As the study is more focused on the Storån only, small stretch of tributaries and three cross-sections in each tributary were only drawn to feed water and color concentration into the main river as shown in *Figure 13*.

Following layers were taken in the RAS Mapper for model set up. The interference of the RAS Mapper is shown in *Figure 20.*

- *Rivers*: This layer shows the river network and the orientation of water flow in it. The main Storån river was divided into eight reaches based on the river joints and sub-catchments of the river provided by SMHI.
- *Joints*: Joints denotes the merging of two or more than two rivers joining. The rivers were joint in the geometry editor and then imported in the RAS Mapper. There are altogether 7 joints in the model (*Figure 13*).
- *Bank Lines:* Bank lines are used to establish the main channel bank stations for the cross-sections. It was drawn in the RAS-mapper manually following the DEM of the study area. During the model set up, they were adjusted later for some specific cross- sections lying in the river curve.

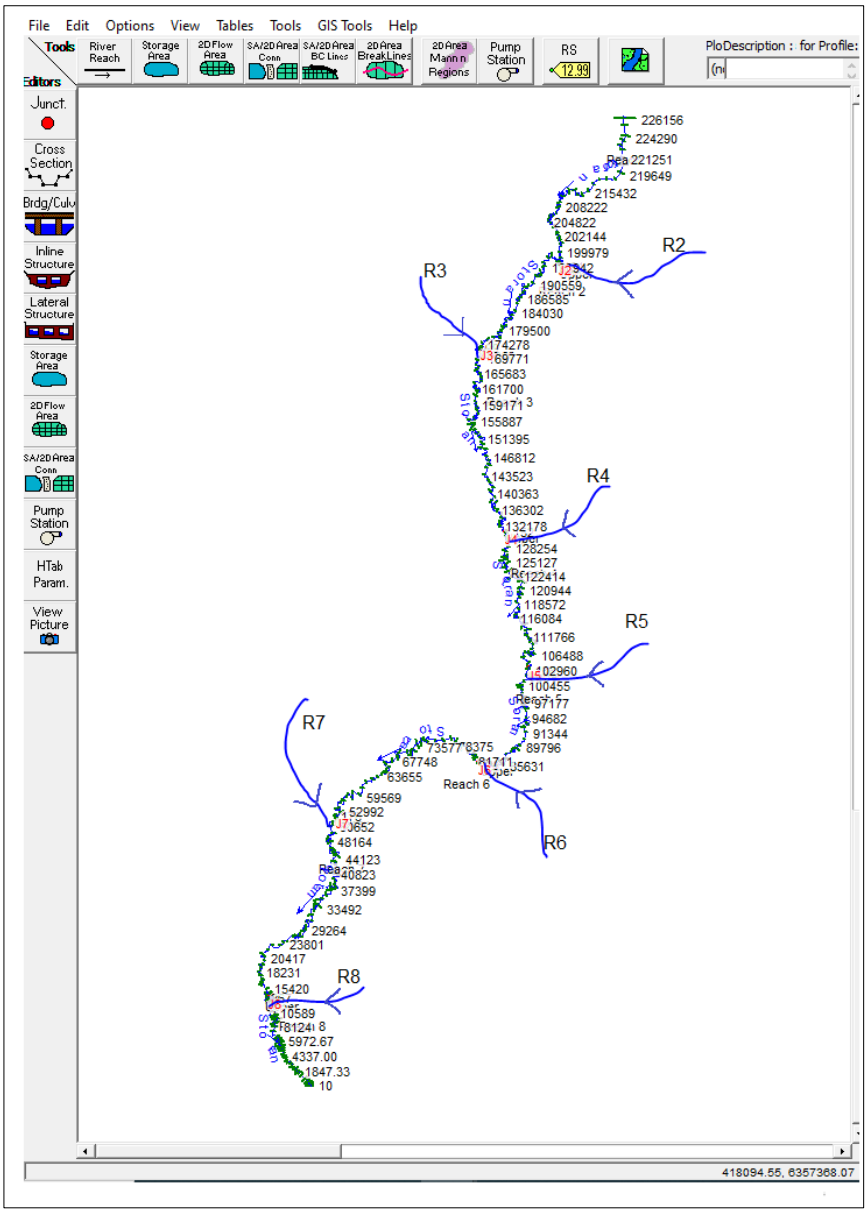

Figure 18 Schematic diagram of rivers in HEC-RAS Geometry Editor

- *Flow Paths*: Flow paths were drawn to calculate the reach length between two cross-sections. It was also drawn manually. Reach length is the distance between two consecutive cross-sections.

- *Cross-sections:* River cross-sections give the spatial location and alignment across the river. Cross-sections were drawn manually as per the merged DEM. Cross-section elevation profiles were created from the terrain model attached with the RAS Mapper and tabular form were also extracted and was further modified in cross section editor *(Figure 19)*. The spacing of the river cross-sections were not fixed. In river reaches with meandering curves, large number of cross-sections were assigned, whereas spacing between cross-sections was made higher in the straight reaches of the river. Total number of 333 cross-sections were taken for 67 km river, in average of one cross section per 200 m.
- *Bank stations*: Bank stations are the indication of the bank lines in each cross-section and are created automatically after drawing cross-sections in RAS mapper.

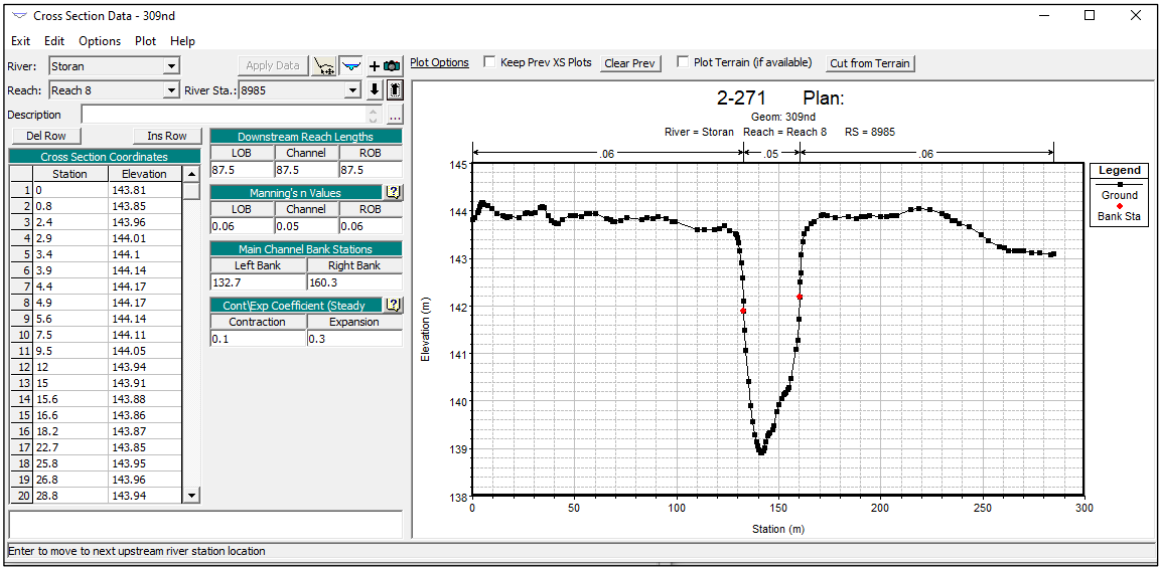

Figure 19 Cross-section editor in HEC RAS

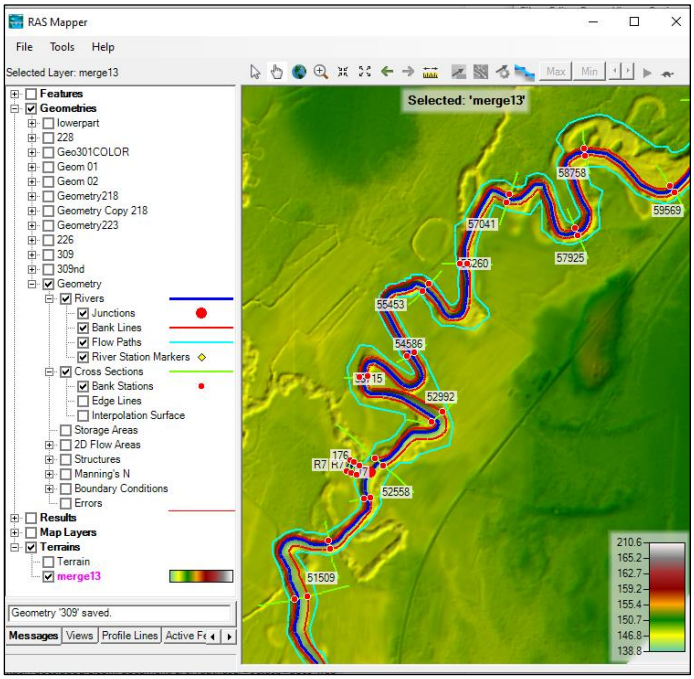

Figure 20 RAS Mapper Layers

- *River Edge lines:* It is also computed automatically based on the shape of the river center line connecting the outside edge of the cross-sections in the right and left edge.
- *XS interpolation surface:* It is the interpolation surface based on the cross-sections, river center line, cut lines, bank lines, and edge lines used for the mapping of the HEC-RAS results.
- *Error:* This layer shows the error while building the river geometry. These results must be addressed before the simulations.
- *Map layers:* It is used as a base map in the interference. Google Maps, satellite maps, USGS imaginary and Arc GIS base maps are some base layers.
- *Terrain*: This layer option was used for the terrain modification and merging of DEM.

- *Results*: This layer comprises different layer showing results of each simulation RAS plan. After the simulation, output layers like depth, velocity, and water surface elevation are automatically generated and these results can be seen on top of the terrain, google or satellites maps associated with the area.

Manning's value

Following manning's value were taken from the calibration process described in sub-chapter *5.2* for the analysis.

- Main Channel-sluggish reaches, weedy, deep pools = 0.0525
- Flood plains: High grass and cultivation in some places = 0.04

Contraction and Expansion Coefficient

The default value of contraction and expansion as 0.1 and 0.3 were taken.

5.1.2. Processing of hydraulic analysis (steady and unsteady flow)

This section discusses the process involved in the calculation of steady and unsteady flow water profile. The theory involved in both analyses has been described in Chapter 3. Steady flow was used for the calibration of the model whereas the unsteady analysis was used for the actual analysis. Here is the procedure applied while computing the results in steady and unsteady flow.

I. Steady flow analysis

Entering and Editing flow data.

After the preparation of geometry, the model was fed the steady and unsteady flow series. The process of entering the flow series in steady and unsteady are different.

Steady analysis was done for the calibration of the hydraulic model and the water quality model. So, few sample dates were only taken for this analysis. For a particular sample date, the daily flow at the outflow of lake Flatten and steady flow corresponding to each sub-catchment were taken from SMHI. Then these corresponding steady flow data were fed starting from the upstream to downstream in the corresponding river station near the joints.

During the entering of a steady flow of a sample date, the output discharge from the lake Flatten was inserted in the upstream most river station (RS) 226131 at first (*Figure 18*). Then the sum of steady flows from tributary R_2 and flow accumulated in Reach 1 was added in the river chainage of that specific sub-catchment. In this case, for tributary R_2, the sum of flow regarding the sub-catchment 2114 and discharge accumulated in sub-catchment 2155 (see *Figure 12)* was fed at RS 191 (near to the joint "J2") as shown in *Figure 18* and *Figure 21*. Once a flow value is inserted at the upstream end of a reach, HEC- RAS assumes the flow is constant until another flow is encountered downstream of the reach. Then the process was followed up to R_8.

The tabular data presentation in HEC-RAS for the steady flow is shown in *Figure 21*.

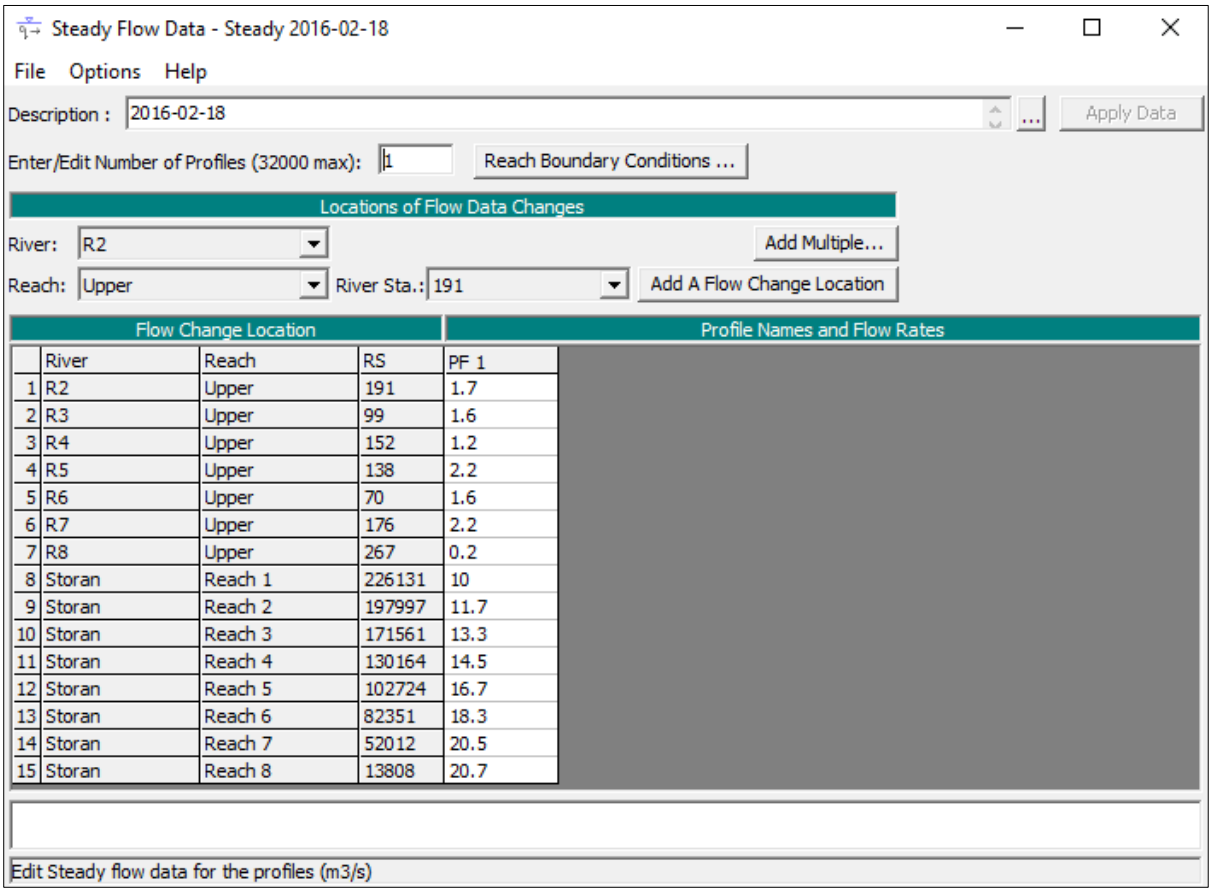

	River	Reach	RS	PF 1
1	R2	Upper	191	1.7
2	R3	Upper	99	1.6
3	R4	Upper	152	1.2
4	R5	Upper	138	2.2
5	R6	Upper	70	1.6
6	R7	Upper	176	2.2
7	R8	Upper	267	0.2
8	Storan	Reach 1	226131	10
9	Storan	Reach 2	197997	11.7
10	Storan	Reach 3	171561	13.3
11	Storan	Reach 4	130164	14.5
12	Storan	Reach 5	102724	16.7
13	Storan	Reach 6	82351	18.3
14	Storan	Reach 7	52012	20.5
15	Storan	Reach 8	13808	20.7

Figure 21 Steady flow data input for sample year 2019.

Boundary Conditions

The boundary conditions for the steady analysis were taken both from upstream and downstream to perform mixed flow regime. From downstream, the boundary condition was taken as the average normal water level of the northern part of the lake. For the upstream boundary condition, the average slope of the river channel and river junctions calculated from the DEM were taken.

Flow Analysis

After associating the geometry file and steady data inflow, flow regime as set to mixed flow. The flow condition of the river is yet to be known whether it is supercritical or subcritical. Then the steady flow analysis was computed. For steady state flow, no errors were found.

II. Unsteady Flow Analysis

Flow data and Boundary Conditions

In this model, daily inflow hydrograph data from 2004-2019 provided SMHI was inserted in the first reach of Storån (Reach 1) as to represent runoff from the river's most upstream cross-section. Then the river inflow hydrograph for all tributaries was taken as upstream external boundary.

The model starts with the inflow hydrograph from the first reach at the outlet of lake Flatten, then a river R_2 merge to the river then the discharge gets added and it goes to the second reach. The inflow gets added in the same manner to the last reach.

Furthermore, for downstream external boundary conditions, water level stage hydrograph series measured in the northern part of the lake Bolmen was taken in the most downstream cross-section, XS 2. The cross-section/ river station 2 (Downstream Stations) is located far from the river Lillån, another river joining the lake. So, it is assumed that that there is no effect of the Lillån over Storån. Also, there is no structure built up there which would possess some effects if present. The boundary condition for the unsteady hydraulic analysis is shown in *Figure 22.*

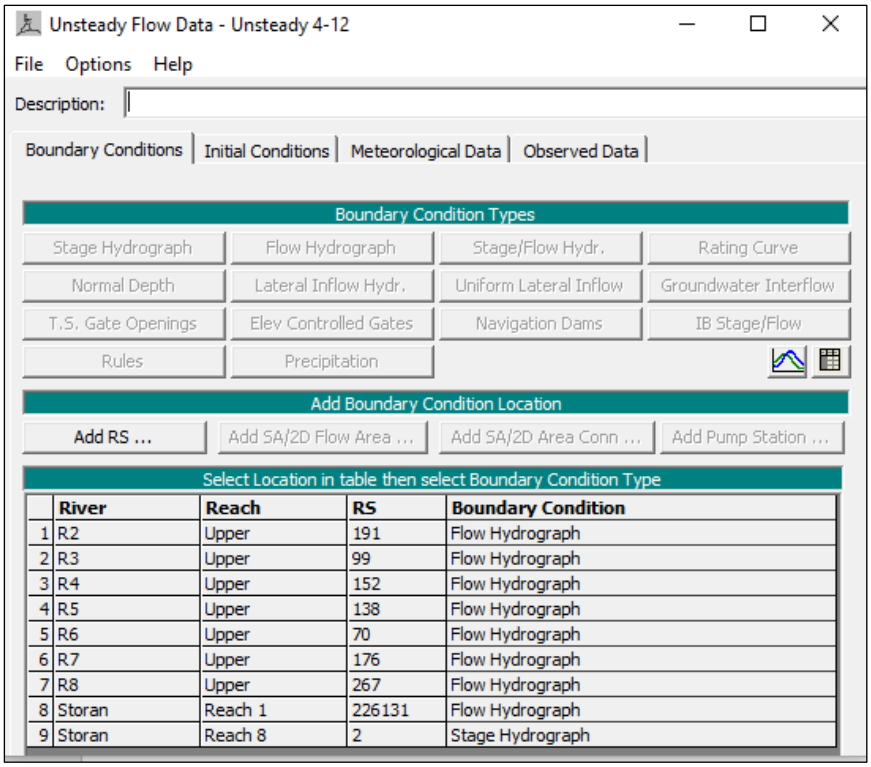

Figure 22 Boundary Condition for the unsteady flow analysis.

Initial Conditions

Initial condition flow helps to compute the initial steady flow and helps to achieve a stable and realistic water surface elevation (HCFCD, 2018). Initial flow values and stage values from the flow hydrograph were taken in the upstream boundaries and upstream cross-sections of the tributaries. Similarly, the initial condition of stage hydrograph in the lowermost cross-section was taken.

Computation Option

Computation options play an important role in the model stability and to maintain computational accuracy (HCFCD, 2018). Following values for the unsteady flow options are taken in the analysis.

- Maximum number of iterations = 20
- Implicit weighting factor (Theta) = 1
- Implicit weighting factor (Theta for warm up) = 1
- Water surface calculation tolerance = 0.006
- Time step = 1 hour
- Flow tolerance = 0.1 %
- Minimum flow tolerance = 0.03 m^3/s

These values were adjusted by hit and trail method by small increment / decrement while debugging and stabilizing the model.

Computation Intervals

Computation interval denotes the time difference between one to another simulation or calculation. Smaller interval may give the better results but may also result to unstable model (Brunner, 2016). It should be chosen with care and consideration so that it includes the change in the rise and fall of the hydrograph being routed. A general rule of thumb is to use a computation interval that is equal to or less than the time of rise of the hydrograph divided by 20 (Brunner, 2016). In this study, the computational interval was taken for one hour. This computation step was also taken due to limitation of software while employing large amount of flow data.

The output interval is time interval to write down the computed stage, flow hydrograph and other results in the output file, HEC DSS in case of HEC-RAS as an output file. This should have an enough number of points to define the shape of output hydrograph considering the peak and the total volume of the hydrograph. It should not be lesser that the computation interval (HCFCD, 2018).

Debugging and Model Stability

While computing unsteady flow, the model may go unstable due to rapid change of geometry and sudden change in flow (Brunner,2016). Improper geometry results in sudden change in the cross-section, flow area and top width. A model is said to be unstable when certain type numerical errors grow and the solution begins to oscillate, or the errors are so large that the computation process fails (Brunner, 2008).

Unsteady flow analysis in HEC -RAS needs more precise and proper geometry as compared to steady flow analysis (HCFCD, 2018). For stabilizing the model, additional cross-sections in the major river and tributaries were drawn for better interpolation. Additional cross-sections were built during the model preparation by XS interpolation tool in the Geometry Data Editor.

After the geometry preparation, HEC RAS develops hydraulic table property (HTAB) for each cross section. HTAB shows the horizontal discretization of cross section for velocity mapping and vertical discretization of elevation for generating hydraulic properties (*Figure 23)* in the rating curve or property curve. A sample property curve is shown in *Figure 24.* While computing, the starting elevation of the vertical discretization was taken at least the lowest channel elevation. Some of the unstable cross-section had starting level lower than that of minimum channel elevation which were casing the model instability. Later they were updated.

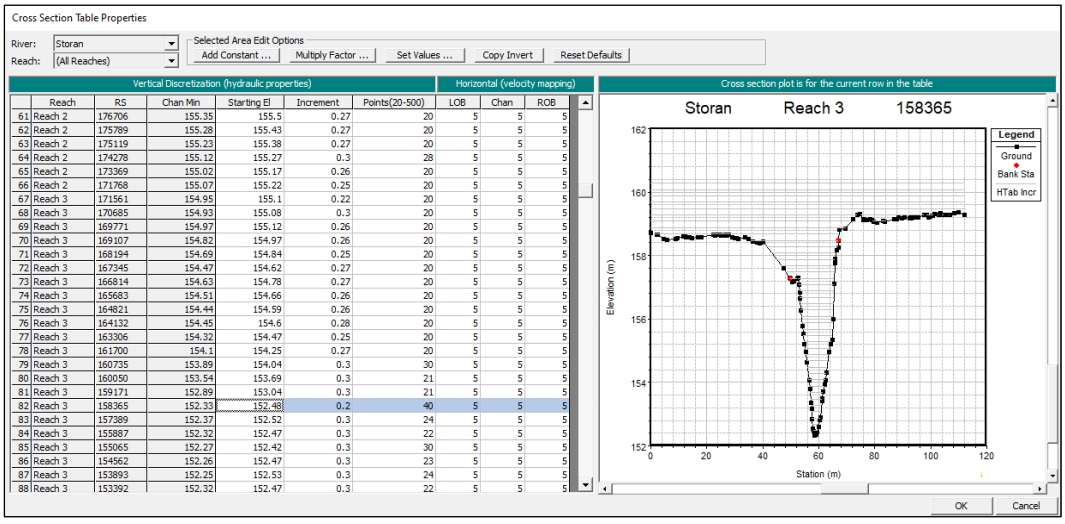

Figure 23 HTAB properties of a sample cross-section.

The property curve has curve for area in channel, area in banks, conveyance in channel and overbanks, top width which are used for the computation of the results. The small discretization of the elevation results in a finer curve resulting in finer outputs. Some of the unstable cross-sections were made stable in this way.

Other errors that occurred were in the geometry data and they were rectified and corrected from the Geometry Editor and in the RAS-Mapper.

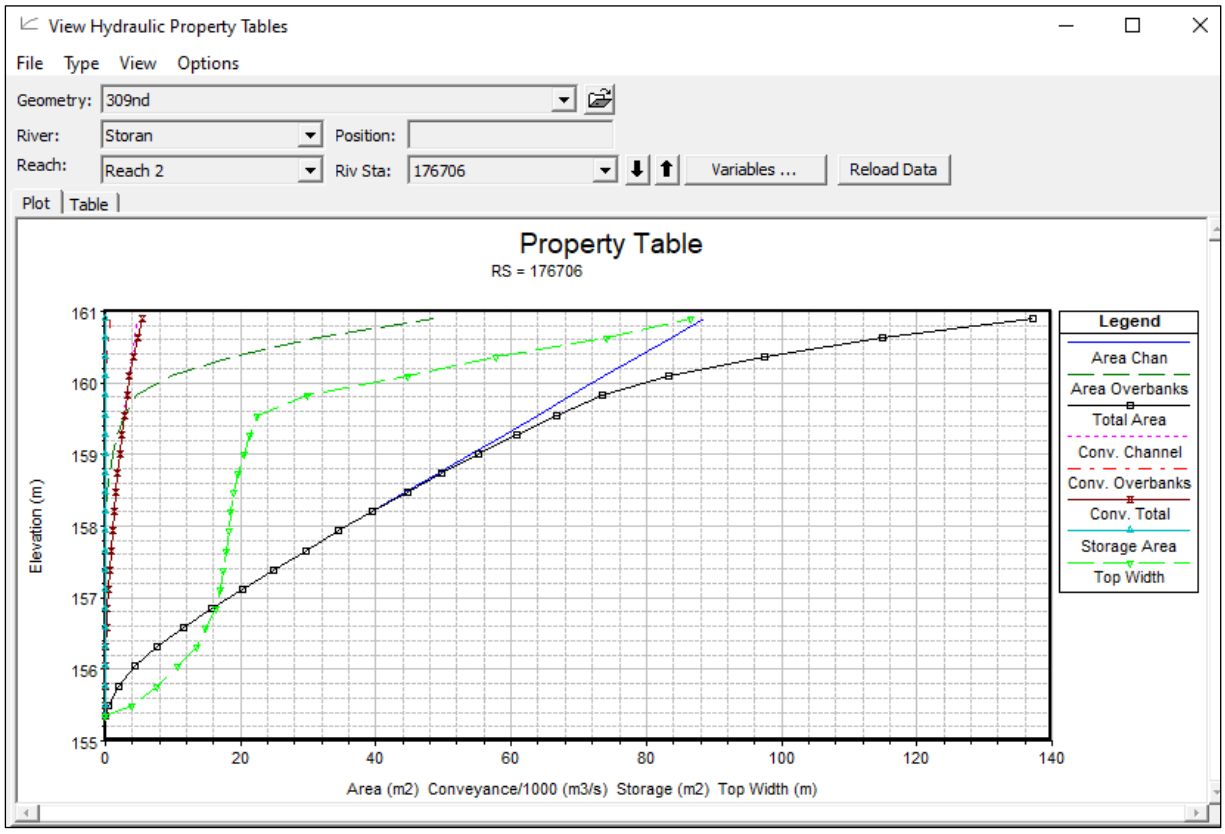

Figure 24 Property table of a sample cross-section

5.1.3. Processing of water quality analysis

Conservative tracer analysis as a part of water quality analysis was run after the model was calibrated with steady hydraulic flow. The variation of color concentration in the ricer was done with unsteady flow data series. The process involved in this analysis are briefly discussed in the following topics.

Water Quality Constituent

A water quality file was created, and arbitrary constituent option was chosen among all water quality constituents. The fate of constituents is taken as conservative as the color concentration data is taken as conservative in nature. These arbitrary constituents are independent of water temperature and nutrients.

Water Quality cells

Water quality cells of alternate green and yellow color are created automatically between the cross-sections initially (*Figure 25).* For the river Storån, altogether of 313 water cells were taken, varying from length 5.7 m to 600 m. For tributaries, only two cells were present as there exists only three cross-sections in each tributary. Every water cell is located at the centre of the cell and acts as a single unit and gives only one output no matter how big the cell is (Brunner, 2016).

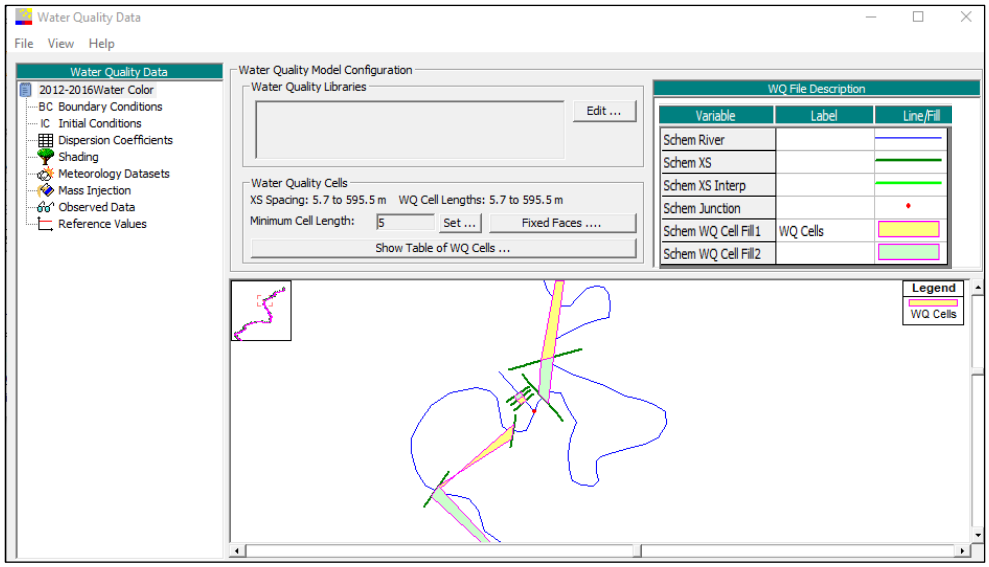

Figure 25 Water quality cells, layers for water quality analysis in HEC-RAS

Boundary condition: Watercolor concentration data

From *Figure 13* and *Table 2*, it can be seen that there are the 11 color measuring stations in which stations Flatten lies near the first boundary condition. The color data for Reach 1 (Starting of Storån, south of lake Flatten), R_2, R_4 were fed as per the assumptions discussed in *Section 4.5 "Watercolor data"*. The remaining rivers, R_3, R_5, R_6, and R_7, color data were taken from the nearest color data stations existed in the corresponding sub-catchments. For example, river R_3 corresponds to the sub-catchment 2095 (*Table 1*). The rest of these rivers were fed the color concentration data in similar fashion. A total of 4 years of data with frequency of 4-12 per year (varying with stations, *Table 1*) were inserted in tabular format for the simulation. While inserting the data in the tabular format, the HEC-RAS automatically does the linear interpolation to fill the gaps between two measuring dates.

Initial Condition

Initial distribution is required for each reach to initiate the simulation. For this, the starting value of color concentration at the starting of 2012 for all stations was taken.

Dispersion Coefficient

Dispersion coefficient were computed internally in HEC-RAS by empirical formula of Fischer, 1979 as discussed in *Section 3.3.*

For the calibration of water quality model, both diffusion and dispersion coefficient have lesser significant role as the steady flow analysis with constant color value was taken for the calibration and final output of watercolor concentration was compared to the provided one by SLU. So basically, simulation results show the weightage average watercolor concentration at each joint or station and then it will be compared with the measured one.

But, when it comes with the simulation of the color data of four years, the unsteady flow was taken, and varying color data was fed to the model. So, the simulation result will give the instantaneous result of watercolor concentration as per the ADE equation from the model.

Simulation Options

The time step of 60 minutes was taken for the analysis, but output time interval was taken for 2 hours due to software limitations. The whole simulation was run from 23rd February 2012 to 18th February. 2016 as the data available for every station is just 4 years.

5.1.4. Post Processing of HEC-RAS results

After the simulation, the result was obtained in graphical and tabular formats. The post-processing here refers to the plotting of the results in RAS-Mapper. After each simulation was done, a separate result layers with specific name were plotted in the "Result" section of RAS Mapper where one can visualize the results of hydraulic and water quality analysis. Also, all the results are written in DSS file, and the result of each simulation can be extracted from there in tabular as well as graphical format. The results are discussed in *Chapter 6* "Results and Discussion".

5.2. Calibration of the hydraulic and water quality model

5.2.1. Hydraulic Model

The hydraulic model was calibrated by (i) comparing computed velocities with observed one and (ii) comparing computed water levels with the observed ones in different stages of the river.

Data and processes involved.

For both comparison, modelled discharge data from SMHI of date 2020-08-05 (date of sonar measurement in site) was taken and HEC-RAS steady analysis was done. For the comparison, velocity and water level measured through bridges during field visit were taken. The river system of the study area, nodes, river stations are shown in the *Figure 13*. The total length of the river modelled is around 67 km.

5.2.2. Velocity Calibration

For velocity comparison, observed velocity was calculated by using a simple relation of velocity (v), distance (d) and time (t) as v= d/t. In the field, the sonar was left to be floated downstream under the free action of water, then the location of the sonar was traced and plotted in Arc GIS. The time taken for travelling between two points were noted and then the velocity was calculated using the above relation. Usually, the distance between two positions plotted were about 30 meters. Though the elevation of water surface was measured in 13 cross-sections, the velocity was measured in fewer river stations.

For the computed velocity, steady analysis with modelled discharge (of the same day) was carried out. To calibrate the model, the manning's value was chosen from the manning's table provided in the HEC-RAS manual *(Table A. 1)*. The manning's coefficient for main channel was varied from 0.05-0.08 with increment of 0.0025 and optimized. For optimal results, only one value for the entire river course was taken. Using optimization of the error in velocity, manning's coefficient with the least-root-mean square error was selected. The comparison of the observed and the computed velocities in different river stations are given in *While comparing*, it was assumed that the surface velocity in the river represents the average velocity at the cross-section, as the velocity calculated by HEC-RAS is the average one, but the velocity measured in this process is just the surface velocity.

Table 3. While comparing, it was assumed that the surface velocity in the river represents the average velocity at the cross-section, as the velocity calculated by HEC-RAS is the average one, but the velocity measured in this process is just the surface velocity.

Table 3 Comparison of observed and computed velocities.

Reach	River Station	E.G. Elev. (m)	E.G. Slope	Velocity Calculated (HEC RAS) (m/s)	Velocity Measured (m/s)	Froude Number
1	US 213160	160.23	0.000018	0.10	0.11	0.03
1	212524	160.23	0.000018	0.10	0.10	0.03
3	143523	153.17	0.000163	0.22	0.23	0.08
4	128254	152.80	0.000027	0.14	0.14	0.03
6	80977	148.91	0.000162	0.27	0.28	0.06
6	79200	148.81	0.000077	0.20	0.2	0.04
6	56260	143.65	0.000116	0.24	0.24	0.05
7	46536	143.45	0.000093	0.21	0.21	0.05
7	19190	142.52	0.000697	0.43	0.42	0.1
8	DS 7452	141.37	0.00003	0.15	0.15	0.04

The root-mean-square was found to be 6.325. E-03. The river chainage with corresponding the river stations is shown in Figure A. 14.

In this *Table 3 and Figure B. 13*, the velocities computed in the HEC-RAS are in good agreement to the measured one in most of the river cross-sections/ river stations.

5.2.3. Water Elevation Comparison

While doing the same steady analysis as stated in *Section* 5.2.2, the water elevation was also noted and compared to the one that were measured in the field survey. *Figure 26* and *Table 4* gives the comparison of elevation in tabular and in graphical view. *Table 4* also provides the information of the water depths in those sections for the comparison. For the calibration of water level also, different manning's coefficient was taken to calculate the root-mean-square (rms) error with the computed and observed elevation value. Manning's value of 0.0525 gave the least rms error.

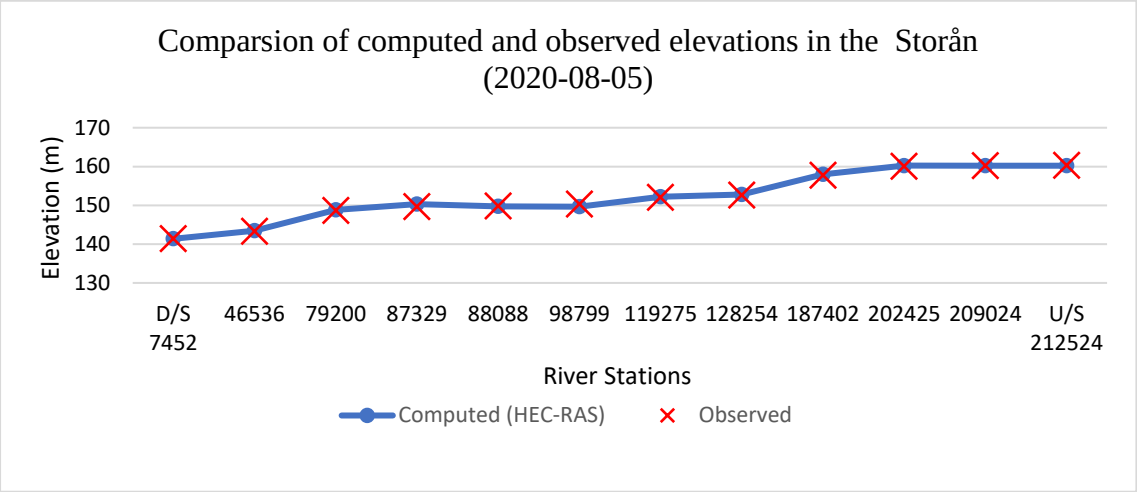

Figure 26 Comparison of the observed and computed water elevation in different river stations. The location of the stations can be located in Figure 18.

Table 4 Comparison of the observed and computed water elevation in different river stations.

SN	Bridge Code*	Reach	River Station	Water height (Observed)	Water depth-Computed(m)	Elevation Computed (HEC-RAS) in meter	Elevation Observed in meter
1	B1	Reach 8	DS 7452	2.853	2.46	141.4	141.793
2	B4	Reach 7	46536	1.59	2.12	143.33	142.8
3	B7	Reach 6	79200	2.445	1.99	148.63	149.085
4	B9	Reach 5	87329	1.88	1.97	149.67	149.58
5	B10	Reach 5	88088	1.749	2.12	149.78	149.409
6	B11	Reach 5	98799	1.74	1.68	150.35	150.41
7	B12	Reach 4	119275	1.83	1.49	152.07	152.41
8	B13	Reach 4	128254	2.08	1.6	152.64	153.12
9	B20	Reach 2	187402	1.404	1.31	157.74	157.834
10	B23	Reach 1	202425	2.1	1.38	160.01	160.73
11	B24	Reach 1	209024	1.77	1.81	160.24	160.20
12	B25	Reach 1	US 212524	1.88	1.93	160.25	160.20

The root-mean-square error with the computed elevation was found to be 0.372.

**The location of the bridges is showed in the Table A. 3.*

5.2.4. Water Quality Model

After the model was calibrated hydraulically, it was calibrated for water quality. Six different dates were chosen with the steady flow to calibrate the model for water quality. The SMHI data were taken and fed into in HEC-RAS. Then, the constant continuous color data of that specific sample date was fed from the starting of the river at the lake Flatten and from each tributary. Steady discharge in each reach and each tributary were also fed. Then, conservative tracer analysis was done in a steady flow regime for a certain day.

Then the simulation was carried out with the computed value of dispersion coefficient used in the HEC-RAS model itself. HEC-RAS uses the empirical Fischer (1979) relation as shown in *Equation 6*. The maximum limit in the computed dispersion has been limited to 100 m^2/s as max $E_d < 700u*R_{max}$ (*Equation 8*). For the calibration process, dispersion coefficient does not play significant role as discussed previously in *5.1.3*

As the flow is steady and constant color data was fed, the simulation output at the downstream station became constant after a certain time, a total of 2 days, and 9 hours in this case. The phase at which, the output becomes constant is termed as equilibrium phase in this report. Then the model output and observed color data in stations Storån Inlopp Bolmen (Stn. 6510), Storån nedströrms Forsheda ARV (Stn. 57041) and Storån nedströrms Törestorp (Stn. 187402) (*Figure 13*) were plotted in the graph for comparison. The watercolor concentration simulation for starting date 2015-12-15 has been shown in *Figure 27 and Table 5*. The rest of the results are shown *in Appendix B.*

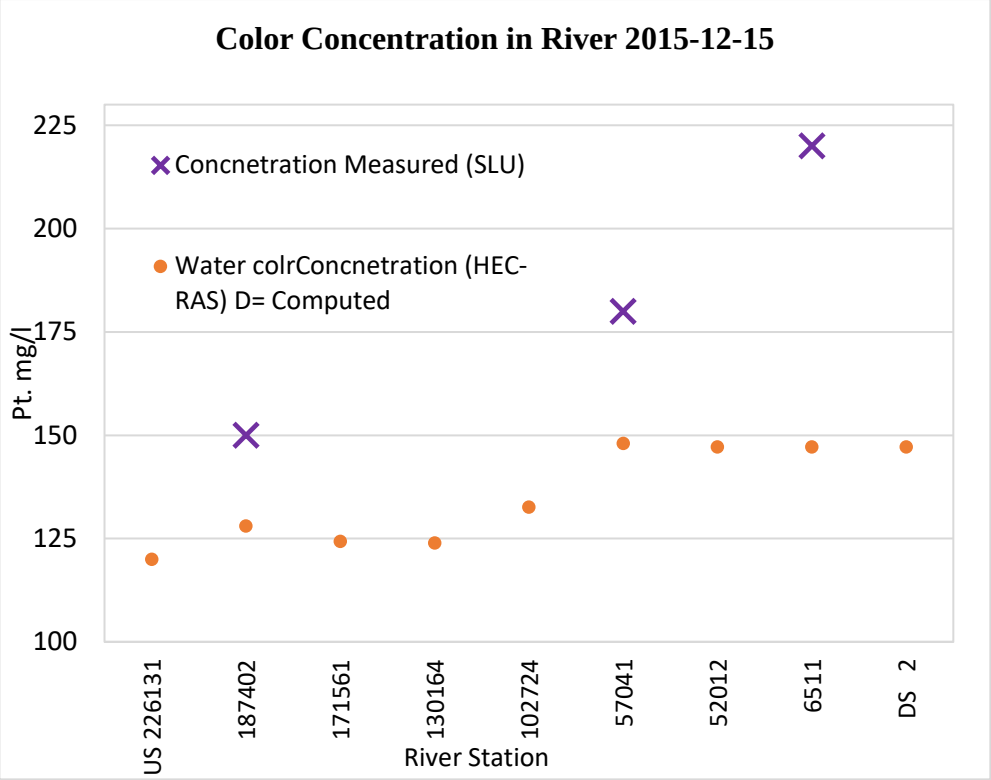

Figure 27 Color concentration in different river station with three dispersion values in water quality analysis for sample date 2015-12-15.

Table 5 Steady flow analysis water quality analysis result with sample data 2015-12-15

RS	Station	Discharge (m^3/s)	Dispersion Coefficient (Computed)	Concentration (HEC-RAS) D= Computed (mg Pt./l)	Concentration Measured (SLU) (mg Pt./l)
1	US 226131	8.71	8.900	120.00	
2	187402	9.949	3.998	117.35	150
3	171561	11.5	5.209	115.01	
4	130164	12.6	4.255	113.61	
5	102724	13.9	3.894	112.32	
6	57041	15.2	1.645	124.05	180
7	52012	17.5	2.740	140.62	
8	6511	17.6	8.130	139.82	220
8	DS 2	17.6	22.700	139.82	

The calibration of the watercolor concentration was difficult to accomplished as the model does not include the actual color data from sub catchments of rivers R_2 and R_4. Also, the frequency of color data was also limited as discussed previously. So, the qualitative approach of the calibration was done instead. In *Figure 27 and Table 5*, the observed and calibrated watercolor concentration is in increasing order. If *Figure B. 11* and *Table B. 4* is studied, it was seen that the observed and computed watercolor concentration is in good for stations 57041 and 6511, but the observed data varies for station 187402.

Similarly, for the next sample data of 9th October 2013, the observed and computed watercolor concentration is comparatively matching with *stations 57041 and 6511 (Figure B. 12 and Table B. 5.* The other sample simulation results are shown in *Table B. 1* to *Table B. 3* and *Figure B. 8* to *Figure B. 10.* From these it was concluded that model seems to be working fine qualitatively, and dispersion coefficient with Fischer's empirical formula was adopted for further simluation.

6. RESULT AND DISCUSSION

The results from analytical as well as from model simulation has been presented in charts and tables. The discussions from these results regarding brownification and material transport area are portrayed in sub-chapter wise.

6.1. River and Tributaries Flow

The main tributaries of Storån in chronological order as per water discharge available are Lillån-Havridaån (R_7), Ljungbäcken (R_5), Fläsebäcken (R_2), Lillån -Hästhultasjön (R_3), Lillån - Herrestadsjön (R_4), Lillån- Rannäsa sjö (R_6) (*Figure 12, Figure 13 and Table 6*). The sum of all discharges from tributaries and main river itself as per S-HYPE is about 81 % (in average) of the total flow of Storån at the outlet before drained to lake Bolmen. The rest of the discharge could be from the other smaller tributaries and direct precipitation in the river. A detail contribution of all main tributaries from year 2004-2019 are shown in *Table 6*. In this period, year 2013, 2016 and 2018 are the among the drier years whereas year 2007, 2008 and 2012 are among the most wet years in comparison based on river discharge.

Table 6 Annual average flow and contribution of tributaries to Storån

Year	Annual average flow (m^3/s)	Contribution of tributaries to the total discharge in %							
		Storån at Flatten Outlet	Fläsebäcken (R_2)	Lillån - Hästhultasjön (R_3)	Lillån - Herrestadsjön (R_4)	Ljungbäcken (R_5)	Lillån- Rannäsa sjö (R_6)	Lillån- Havridaån(R_7)	Other small tributaries+ Direct Precipitation
2004	11.8	40.9	7.9	5.2	5.1	8.4	4.8	8.7	18.9
2005	7.29	38.8	8.3	5.1	5.6	8.7	4.8	8.8	19.9
2006	9.80	41.7	7.8	5.3	5.2	8.1	4.6	8.7	18.7
2007	12.2	40.0	7.8	5.2	5.2	8.7	4.9	8.7	19.5
2008	12.1	42.2	7.6	5.3	5.0	8.1	4.6	8.5	18.7
2009	7.71	41.8	8.3	5.1	5.5	8.1	4.3	8.2	18.7
2010	9.91	40.7	8.1	5.1	5.2	8.8	4.8	8.4	18.8
2011	10.8	41.4	8.0	5.3	5.4	8.0	4.5	8.7	18.9
2012	10.7	41.7	8.1	5.2	5.1	8.5	4.6	8.4	18.4
2013	6.97	40.7	8.1	5.2	5.7	7.9	4.3	8.7	19.4
2014	10.8	41.9	8.1	5.2	5.3	8.3	4.5	8.5	18.3
2015	8.58	41.1	8.0	5.2	5.4	8.2	4.5	8.6	19.0
2016	6.67	41.7	8.3	5.1	5.4	8.6	4.5	8.0	18.5
2017	8.97	40.9	7.9	5.3	5.4	7.8	4.6	9.0	19.2
2018	6.66	42.2	7.9	5.1	5.1	8.6	4.4	7.9	18.7
2019	9.47	39.8	7.9	5.3	5.4	8.1	4.8	9.1	19.5

The daily discharge from 2004-2019 was taken for unsteady flow analysis to study the hydraulic parameters like velocity, depth, and river profile of the flow. Unsteady flow analysis was performed as described in *Chapter 4: Model Setup and Methods*. Below is the description of simulation results for the maximum water surface and for the minimum water discharge.

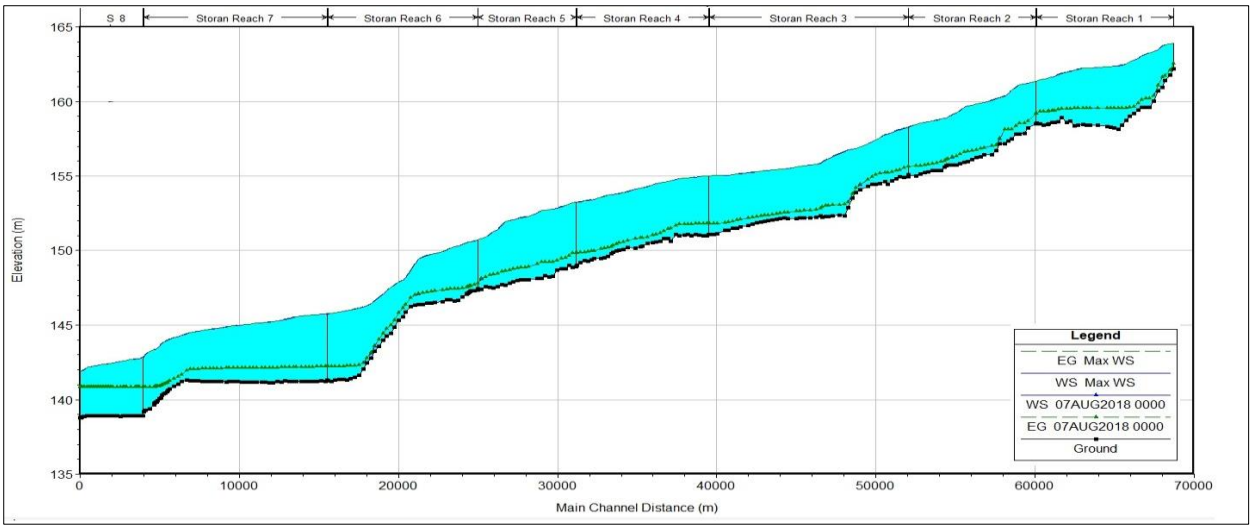

Figure 28 HEC- RAS results for maximum and minimum river profile in year 2004 to 2019

The maximum water depth of 4.65 m (for years 2004-2019) was obtained from discharge of 29.17 m^3/s in river station (RS) 56260 (16.74 km upstream of lake Bolmen) in Reach 6 *(Figure 28)*. The maximum discharge 40.3 m^3/s was obtained for river Storån at the river outlet on 14th July 2004. Similarly, the maximum water velocity was 1.3 m/s was found as per the HEC-RAS simulation for RS 70184, reach 6 (21 km upstream of lake Bolmen) for river discharge of 29.26 m^3/s. The graphical RAS Mapper result as areal plan is shown in *Figure B. 1* to *Figure B. 5*.

The minimum water depth of 0.27 m was obtained in RS 160050 *(Figure 28)* in Reach 3 for river discharge of 0.36 m^3/s (48.53 km upstream of lake Bolmen) from the simulation of water flow for the daily discharge series of 2004-2019. The velocity plot regarding the maximum and minimum water surface has been shown in *Figure B. 14.*

6.2.Long term watercolor data analysis

The yearly variation of material causing browning of water can be best explained by variation in watercolor concentration (WCC). For long term analysis, the yearly data of color concentration for 35 years of station Storån Inlopp Bolmen, located near the outlet of Storån *(Figure 13)* has been analyzed analytically and presented in *Table A. 2.*

The change in the watercolor can be broadly studied by detecting changes in color value from decade to decade. The mean annual watercolor (MAWC) in year 1990-2000 was 163 mg Pt./l. Following the data, the MAWC for year 2001-2010 was 199 mg Pt/l. And, from the years of 2011 to 2019, the MAWC was 206 mg Pt./l. Though the increment is found to be less each year, there is an increasing trend of the concentration as shown in *Figure 29 as* indicated by the broken red line.

Referring to *Table A. 2.* The MAWC in the river also varies from year to year. For example, the MAWC for year 2004 was 209 mg Pt./l but for year 2006, it was just 167 mg Pt./l. Also, the MAWC for year 2008 it was just 152 mg Pt./l. which is only 75% of the average color concentration of that decade. In the years between 2011 and 2019, there has been a significant variation in the color, up and down in every other year. For instance, year 2012 has MAWC of 215 mg Pt./l but for 2013, it dropped to 170 mg Pt./l and in the next year, 2014, it was 235 mg Pt./l again. Then the following year, 2015, MAWC was found to be 179 mg Pt./l. This alternating fashion continued to 2019 (*Figure 29 and Figure 30*). This alternating up and down behavior can be related with the mean annual river discharge (MARD) of the river.

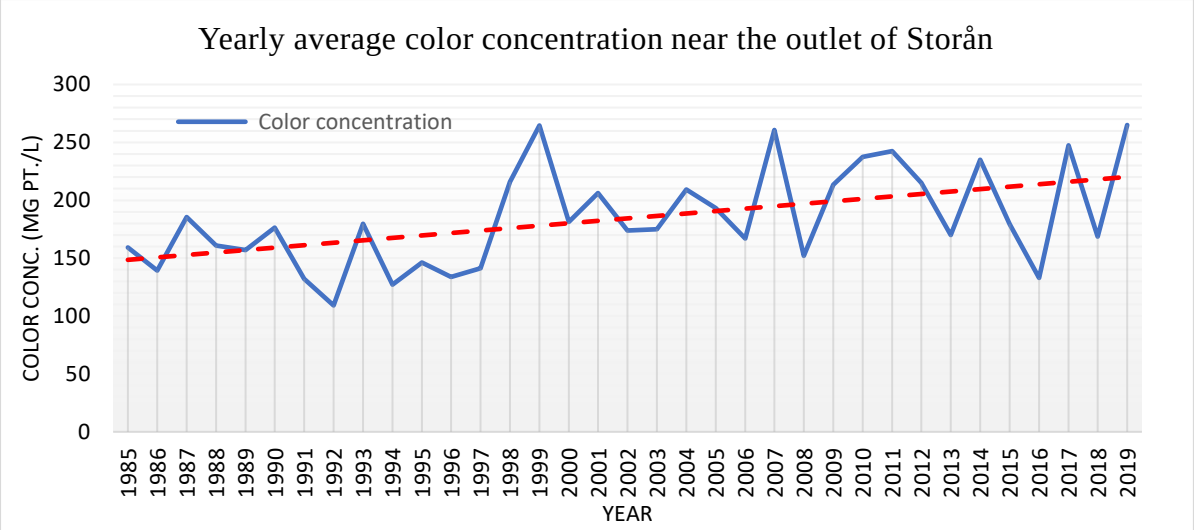

Figure 29: Yearly average color concentration near the outlet of Storån

The comparison of the MAWC and MARD from year 2004 to 2019 has been illustrated in *Figure 30*. Here, the year with lower MARD also has the lower MAWC and vice versa except for year 2006 and 2008. The graph also shows that wet years followed by dry years have more MAWC. For instance, year 2016, the MAWC is 133 mg Pt./l and for year 2017, it was 248 mg Pt./l respectively, which was nearly double than that of year 2016. The MARD for these two years were 6.67 m^3/s and 8.97 m^3/s, respectively. Here both MAWC and MARD for 2016 is lower than for year 2017, but in later year, the average discharge is more and hence resulted higher MAWC. Similar fashion of relation of MAWC and MARD can be found in a couple of years like year 2013 and 2014. It seems that drier years have lower transport of materials to the river than that of years having higher discharge. The similar results due to change in climatic condition have been observed by Meyer-Jacob, et al. (2019) for study of browning and re-browning of lakes located in boreal region of northern America.

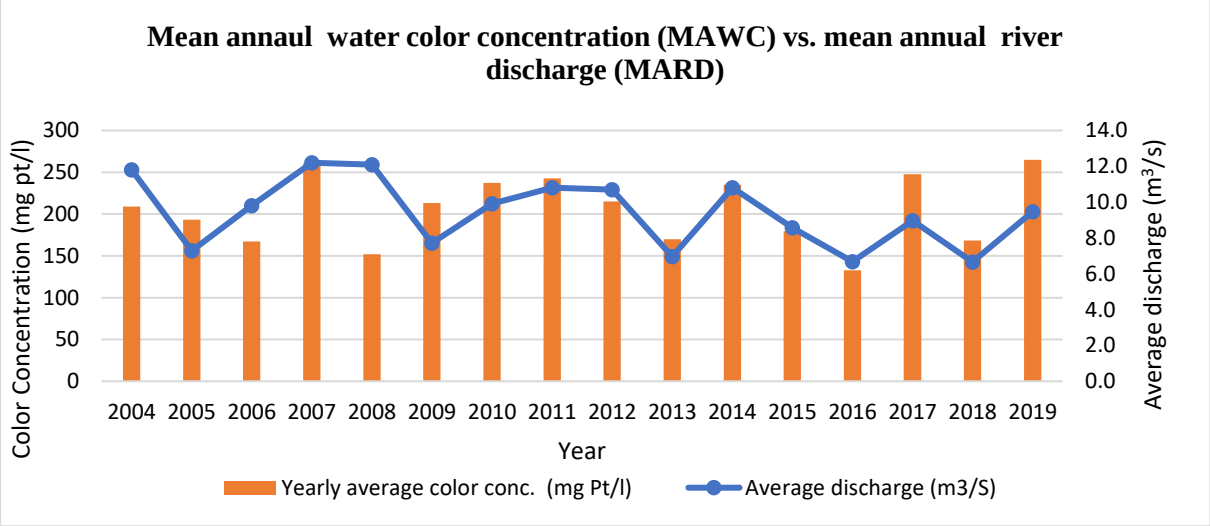

Figure 30 Average yearly color concentration and yearly average discharge of corresponding year.

Referring to *Table A. 2*, In recent 35 years data, almost all years have the peak color value more 1.5 times of the minimum value except year 2018 which is the driest year in year 2004-2019 (*Table A. 2).* In 2018, the MARD value was 6.66 m^3/s and the ratio of maximum to minimum MAWC is just 1.3 (*Table A. 2*). The standard deviation of the watercolor in this station varies from 18.6 to 163.3. In year

2017 and 2018, the frequency of the measurement was just two times a year whereas other years have representing color concentration data of recorded in every month. Year 2019 has the maximum ratio of max. concentration/min concentration of 6 times (*Table A. 2*). The month in which maximum or minimum watercolor concentration is present varies from year to year but most of the maximum color concentration were in the month of July or August in summer, whereas most of the minimum watercolor were observed in the month of October.

The transport of materials in a catchment starts from water picking up nutrients, minerals, humic substances, organic substances, and other chemicals. Then the water discharges wash out these substances in the river. This washing out is an important process of transport from the catchment to the river, which might be revealed by the positive correlation between the watercolor and flow (Naden, 1989). The material causing brownification measured as watercolor concentration has been correlated with the water discharge in the river to see if there exists any relation between them. Due to the low frequency of color measurement, the result may be considered as indicative instead of being conclusive. The daily watercolor data taken from SLU was correlated with the daily discharge for the same day taken from SMHI. Though the color data was collected from 1985 to 2019, due to unavailability of discharge data, regression analysis was carried out from 2004-2019 only. A simple regression analysis in MS Excel was carried out as shown in *Figure 31*.

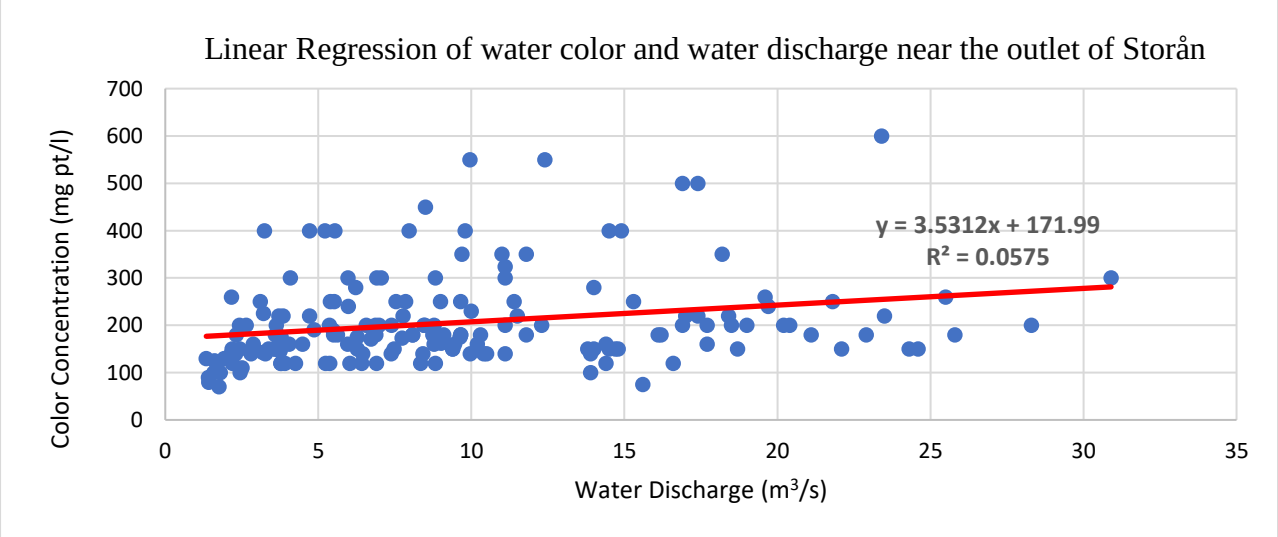

Figure 31 Regression Analysis for watercolor and water discharge from year 2004-2019 based on SLU data (r=0.24).

The analysis shows that the river discharge and watercolor were positively correlated, even the correlation is weak with r= 0.24 (*Figure 31*). Though the surface runoff carryout the watercolor, the relation is not linear. It shows that not only discharge but, there exists other factors too, responsible for variation of watercolor concentration (WCC). Other mechanisms related to land cover, climate, and acidification history are responsible for the ongoing browning of surface waters (Temnerud et al., 2014). Among the different factors responsible for this its seasonality, precipitation and temperature have been found to be the most significant factors (Temnerud et al. 2014, Kritzberg et al. 2019). The increase in temperature accelerates the organic matter decomposition process in soil (Davidson and Janssens, 2006), which contributes to the production of more humic substances. The surface runoff in the study area is predicted to increase in future due to climate change (Arheimer et al., 2013). As runoff has a positive correlation with watercolor, it could increase in the future. Tumdedo, 2010 also showed that there is positive correlation between WCC and surface runoff, and with WCC and temperature for most of the years from 1997-2007.

6.3. Variation in watercolor from lake Flatten to lake Bolmen

The comparison of WCC simulated from the model between starting station (outlet of lake Flatten) and last station in the model (outlet of river to the lake Bolmen) was done with an aim to study the variation of the WCC in two ends in different seasons and years. Among the four years of simulation, year 2012 with daily average discharge of 10.7 m^3/s (wet year) and year 2013 with daily average discharge of 6.97 m^3/s (dry year) has been discussed in this sub-section.

Based on the simulation of WCC from February 2012 to February 2016, it was found that the WCC in at the starting of the river is lower to that of downstream (DS) station near Bolmen lake in spring and summer seasons. But in the season of autumn and winter, during higher river discharge, there is increment of WCC in both Upstream (US) and DS. Further, the simulation in such wet periods, the WCC at DS station is generally lower than that of US station.

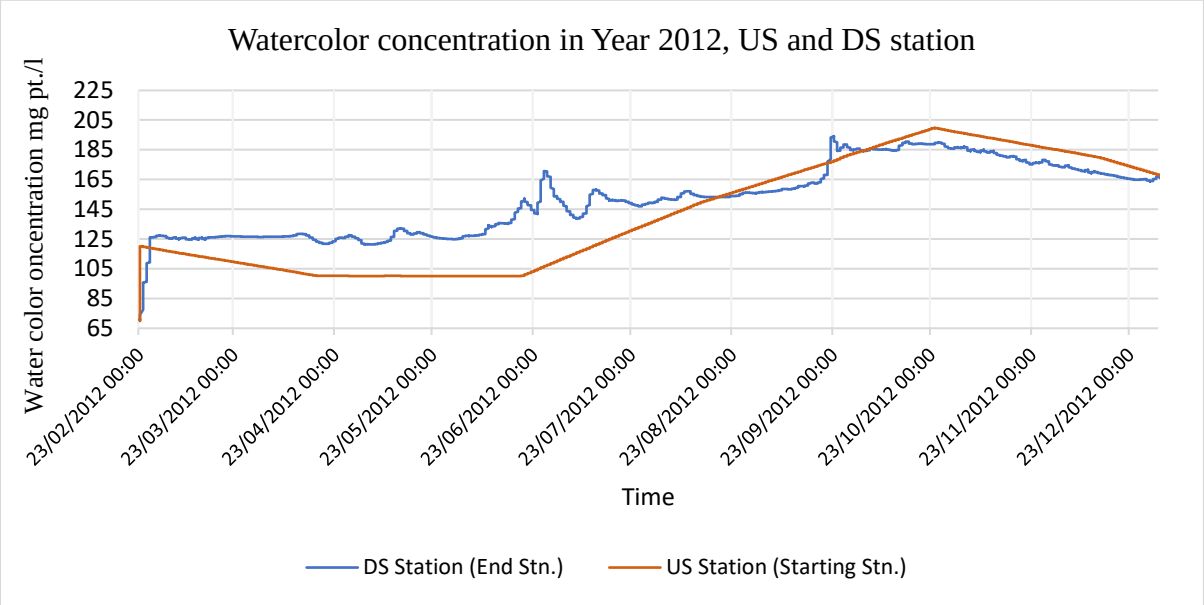

Figure 32 Comparison of color concentration between outlet of Flatten and outlet of Storån in Year 2012

Figure 32 shows the WCC for two stations from February 2012 to end of the year, in which the orange curve shows the WCC of US station whereas the blue curve is the WCC at DS station after the simulation after mixing of WCC from tributaries and the river itself. At first, there is a sudden increase in WCC in both stations after the start of the simulation as the initial condition was taken 70 mg Pt./l only. The initial condition was taken as the minimum color reading in all these four years. Overall, the WCC was in increasing order for both US and DS to the end of October, despite WCC for US was declining from February to mid of April. Then from the end of October, WCC has been decreasing order up to the end of the year. The maximum WCC for US stations was around 200 mg Pt./l but for US station, the maximum was 192 mg Pt./l only. The minimum WCC for US and DS was 121.57 mg Pt./l and 100.1 mg Pt./l respectively.

Following the graph, WCC in US station is lesser than that of DS station from end of February till end of month August 2012, then WCC in the US station became less than the that of WCC value in the DS Station. At the end of October, WCC in both stations dropped, but the WCC in US was little more than of DS. This trend continued up to the end of the year. This result can be roughly related with the variation of river discharge of the year. *Figure 33* shows the daily discharge hydrograph of the year 2012. Starting from the end of February, the discharge for both US and DS stations were in lower range

with small ups and down in the spring and then in July, there was a little spike in the discharge. From mid of September, there was an increase in the discharge in the river. At the end of the year in December, WCC in both stations also declined as water discharge dropped in December as shown in *Figure 33*.

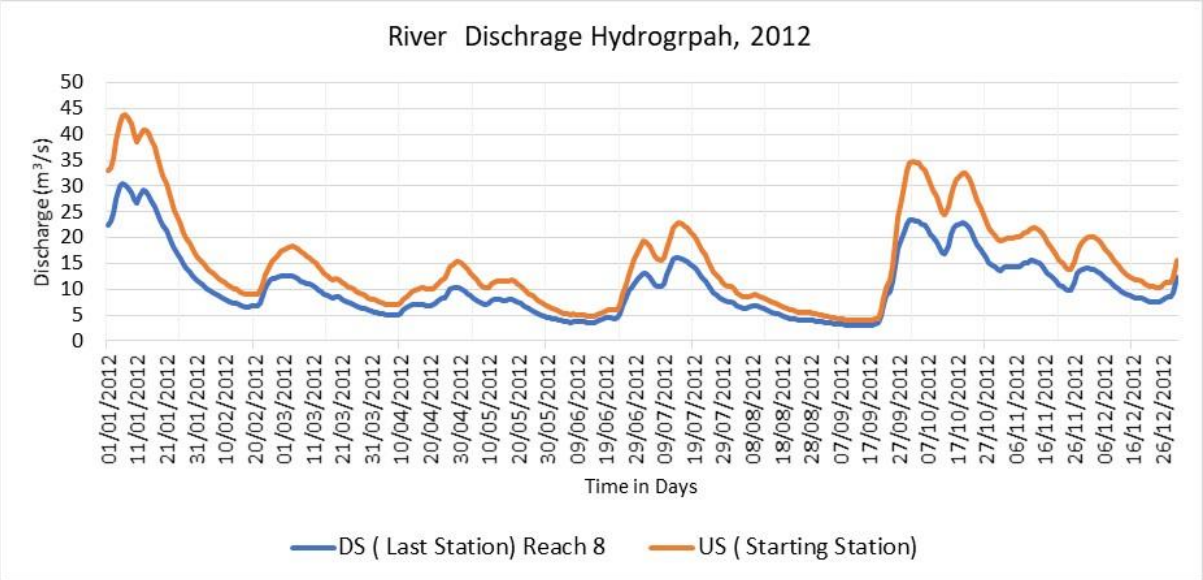

Figure 33 Daily River discharge hydrograph for year 2012

Figure 32 and Figure 33 are taken a close look, it can be seen that lower discharge is followed by lower WCC, and higher water discharge was followed by higher WCC. In winter and autumn, there was increase in WCC for both US and DS conditions, so as increase in river discharge. This phenomenon can be described as the higher discharge sweeps away the materials causing watercolor like DOM and other metal concentration like Fe, as positive correlation between WCC and discharge as shown in *Figure 31*. During the longer precipitation events or wet period, the groundwater level becomes higher, and the organic soil gets saturated. Similar results have also been demonstrated by Meyer-Jacob et al. in 2019, in which higher magnitude of color was found in wetter climate and lower in the dry seasons. Water in close contact with the deposited organic matter within the surface peat leaches the organic matter pool (Nieminen et al. 2018). During such high flows, DOM get increased immediately whereas Fe gets delayed (Ekström, 2013). This can be possibly related to the higher WCC even after the discharge started decreasing from early November in 2012 (*Figure 33*).

For the year 2013 *(Figure 34)*, Both US and DS stations has a declining trend of WCC from starting of the year until mid of October, probably due to less water discharge or drier year in comparison to previous year, 2012 *(Figure 30, Figure 33 and Figure 35).* WCC at US station has continuous fall up to end of June. After a small increment at the starting of September, it continued to fall up to the end of October and rose from there as the river discharge got increased from that time.

WCC in DS has also decreasing order up to end of October though, it has some increment in the reading due to slight increase in river discharge in mid-May and other few dates (*Figure 34 and Figure 35).* After the increment in river discharge in the end of October, the concentration started increasing.

Even the WCC of both US and DS stations has somehow decreasing order up to end of October, the WCC at DS was more than that of US as similar case to the Year 2012. Also, after the increment in discharge in winter, in October and November *(Figure 35)* the WCC in DS station became less than that of US station.

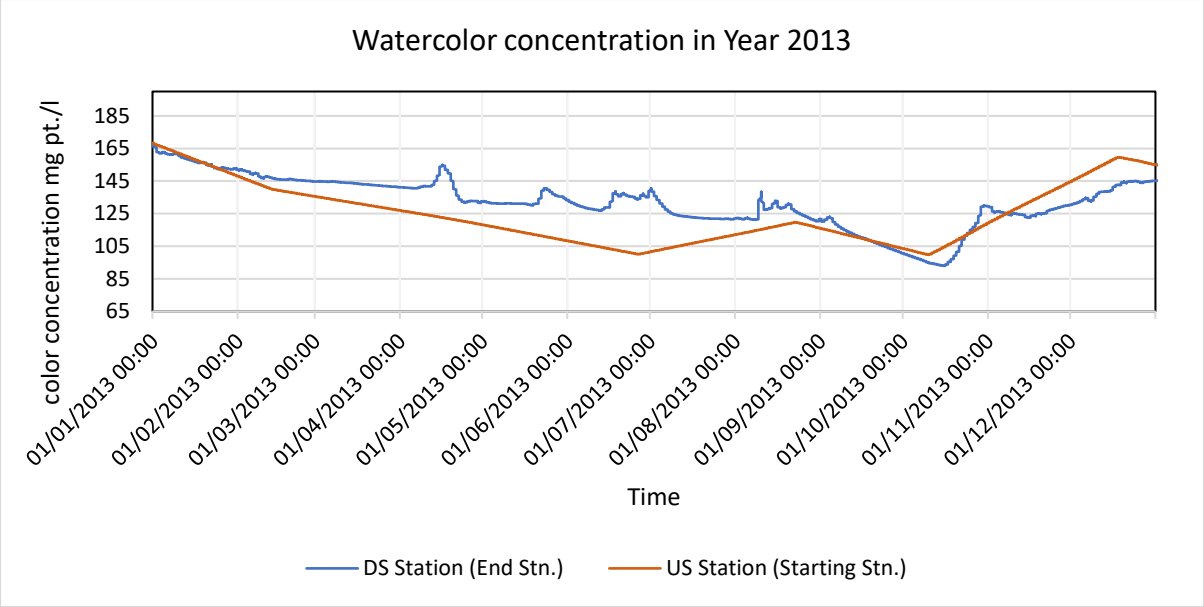

Figure 34 Comparison of color concentration between outlet of Flatten and outlet of Storån in Year 2013

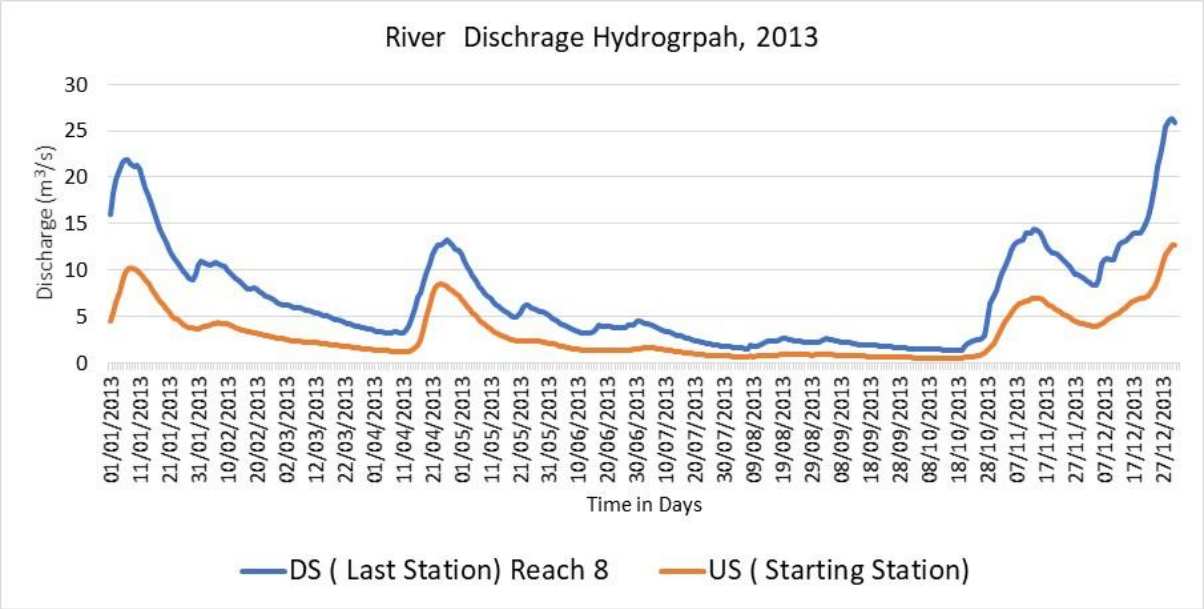

Figure 35 Daily River discharge hydrograph for year 2013

The WCC for year 2014 to 2016 (up to Feb.) has been shown in *Figure B. 6 and Figure B. 7* respectively in *Appendix A*: Tables and Figures. The daily discharge hydrograph for those years is shown in *Figure A. 2* and *Figure A. 3* respectively in *Appendix A*: Tables and Figures. Here, year 2014 can be considered as wet year and year 2015 and 2016 (up to Feb.) can be considered as dry year.

In year 2014 the variation in WCC was of roughly like the case of 2012 except that, year 2014 had gentle trend of increment. Among all four-year, year 2014 had the highest WCC in the DS i.e., 293 mg Pt./l in the month of September and for US, the maximum value read was 239.19 mg Pt./l in the month of November 2014. The year 2014 was one of the most wet year with average daily discharge of 10.8 m^3/s. This may be the reason for obtaining maximum WCC in 2014 among other three years simulation results.

For the year 2015 and 2016 (up to Feb.) can be correlated with the year 2013 as both are drier years. But for year 2015, WCC at DS station decreased gradually from the starting of the year till mid of August. Then it rose gradually and reached maximum at the end of October and finally decreased from there. WCC at DS stations was in between 100 mg Pt./l to 130 mg Pt./l up to mid-August but increased sharply in mid-October that started falling.

In the year 2015, the effect of the increasing river discharge seems to have less influence in the variation of WCC unlike in previous years. Though the river discharge was maximum at the end of December, the maximum WCC was attained at the mid-October. Also, despite high discharge in February in 2016, there was no significance change in WCC in that period. There is no strong reason found to describe this irregular pattern with comparison to previous three years. It might be due to lots of reasons like seasonal variation in precipitation temperature and other landuse mechanisms in that year. Due to data limitations in 2016, the variation pattern of WCC in entire year could not be discussed.

Regression Analysis between simulated WCC and Q at DS station

Two scatter diagrams between the daily flow data from SMHI (X-axis) and simulated WCC (Y-axis) at DS one for the spring and summer (drier seasons) and another autumn and winter (wetter seasons) was plotted ash shown in *Figure 36.* The plot was carried out to observe the correlation between WCC and Q in drier and wetter seasons. The dates for the seasons were taken as the same as discussed in sub-chapter *2.6.*

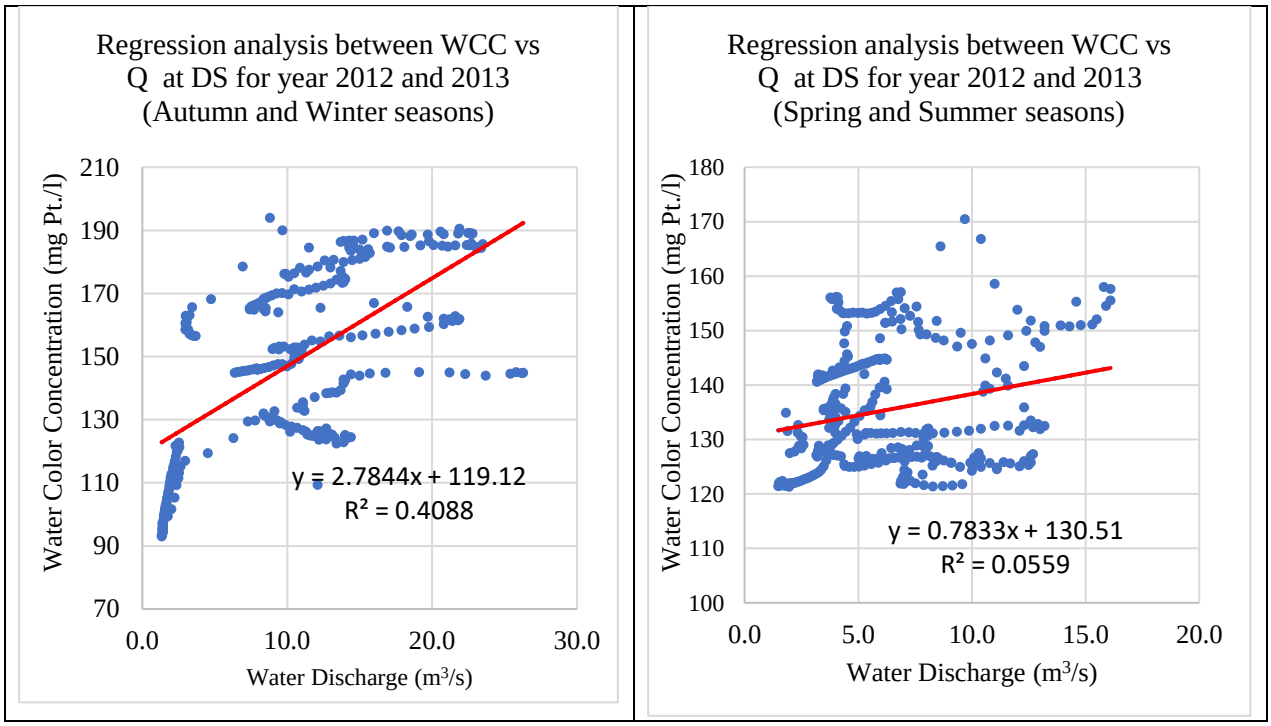

Figure 36 Regression analysis for simulated watercolor concentration and water discharge of the year 2012 and 2013 (Left: r=0.63, Right: r= 0.23)

From the observation in *Figure 36*, it was found that there exists a stronger correlation between WCC and Q in wetter seasons (left in the figure) with compared to the drier ones (Right in the figure). This result also supports that the higher discharge results in higher WCC, as discussed previously in this sub-chapter.

6.4. Tributaries contribution for color concentration

The main tributaries of the river Storån from the south of lake Flatten are analyzed analytically to study the tributaries' contribution in WCC of water. Among the major seven tributaries, WCC data for only four stations are available. For R_2 and R_4, although discharge value was taken from SMHI, the same color concentration was used as of R_5 as mentioned in the "Assumptions" in the previous chapter. The tributary R_8 is not discussed as the flow input from this river is almost negligible that is just 0.3 % but it was enlisted as the tributaries due to different sub-catchment as divided by SMHI (*Figure 12)*.

Table 7 Tributaries contribution for average watercolor concentration for year 2013

SN	River name	River Code	Color Concentration (WCC) mg Pt./l	Avg. Discharge (Q) m^3/s	Flux WCC* Q
1	Fläsebäcken	R_2	104.00	0.570	59.280
2	Lillån -Hästhultasjön	R_3	130.00	0.363	47.132
3	Lillån - Herrestadsjön	R_4	104.00	0.390	40.560
4	Ljungbäcken	R_5	104.00	0.549	57.086
5	Lillån- Rannäsa sjö	R_6	250.40	0.299	74.865
6	Lillån- Havridaån	R_7	228.33	0.607	138.535

The 2013 mean annual color value was used to compare the color contribution of tributaries, as shown in *Table 7*. Among the main tributaries, the maximum WCC was found in R_6 followed by R_7, R_3 and R_5, respectively. But the maximum average water discharge of the year was found in descending order in R_7, R_5, R_3, R_6, respectively. This resulted that the even R_6 has the highest average WCC in the year, and R_7 has maximum flux which almost double of R_6. Hence, it can be considered that it has the highest contribution for the WCC variation and thus presented as the major tributaries for the material transport in the catchment of Storån (*Table 7*).

Even though the climatic condition like temperature and precipitation are similar for the entire catchment of the river, the occurrence of WCC in each tributary was seen different. It might be due to different land use patterns and soil types present in each sub-catchment. The color-magnitude of outgoing water quality is influenced by the difference in land use of a sub-catchment (Klante et al., 2021), as mobility of DOC and Fe are influenced by land use (Kritzberg et al., 2019). For example, the cultivation of spruce forest means can result in higher accumulation of organic material in the water than that of pine and birch trees (Klante et al., 2021). The reason for higher WCC of R_6 and R_7 may be due to the presence of a larger area of peat, i.e., 24 % and 20 % respectively in the area as compared to R_3 and R_5. Details about the landcover are shown in *Table A. 4.*

In the Boreal region, peatlands with high connectivity with streams are the most important source for producing DOC (Laudon et al., 2011) causing brownification. The effect of Store Mosse Nationalpark, in river R_2 and R_4 is not integrated into this report as this study lacks the color data in the rivers originating from the park. The other parameters for the variation of the WCC may be due to temperature too, but it is not discussed in this study. The detailed information of the land use and soil type is shown in *Table A. 4.* Further discussion about the effect of R_7 has been done in Sub-chapter *6.4.1.*

A correlation between WCC and discharge was also done to see if there is any correlation or effect of washing out of humic as well as substances from tributaries flow which can cause brownification. Similarly, as in Section 6.2, correlation between the watercolor and flow was done for all tributaries except R_2 and R_4. *Figure A. 5 to Figure A. 8* shows the plot of discharge and WCC measurements at the same day for the tributaries outflow from lake Flatten to R_7, respectively. Regression analysis

showed that correlation factor "r" varies from a minimum of r = 0.06 for R_6 to a maximum of r = 0.55 in R_5. Even though there is no good correlation between WCC and Q, a positive correlation was found in every sub-catchment. The data plot for R_7 is quite interesting and discussed below.

Figure 37 shows the correlation between the WCC and discharge from a catchment of R_7. A linear regression analysis shows that even though there is a positive correlation between discharge and WCC, a good correlation between them could not be achieved. But it was observed that for R_7, even the discharge was lower, most of the discharge has high WCC (*Figure 37*). This had a significant effect on the WCC in Storån river. This distinct behavior of this sub-catchment may be due to larger agricultural area as a source for carbon (Mattsson et al., 2005) compared to other catchments, i.e., 15% *(Table A. 4)*. Among the four years of simulation, the sample year 2013 has been taken for the illustration of the effect of R_7 in the following sub-chapter *6.4.1*.

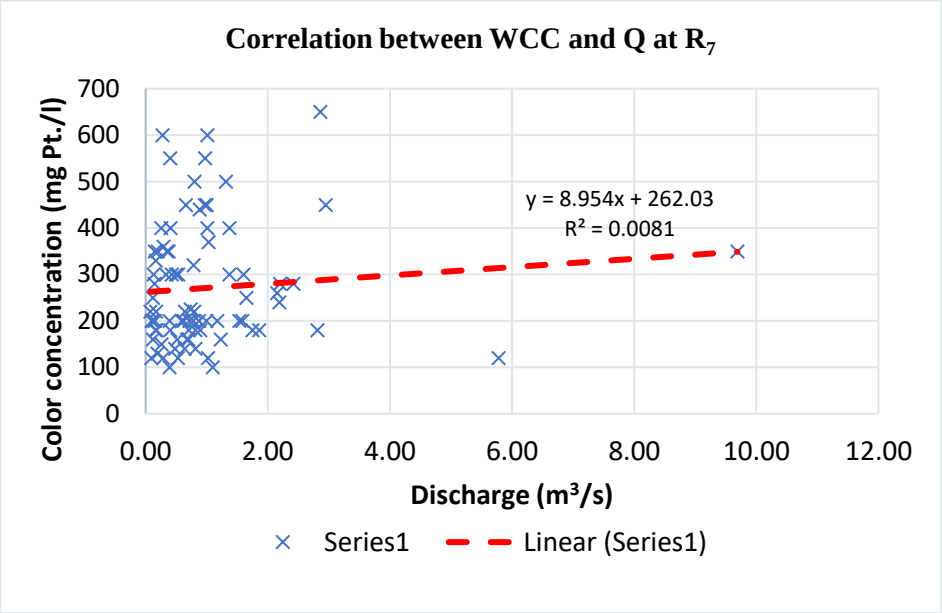

Figure 37 : Correlation of river discharge and watercolor concentration for R7 (r=0.09)

6.4.1. Contribution of Lilån, nedstorms Bredaryd (R_7)

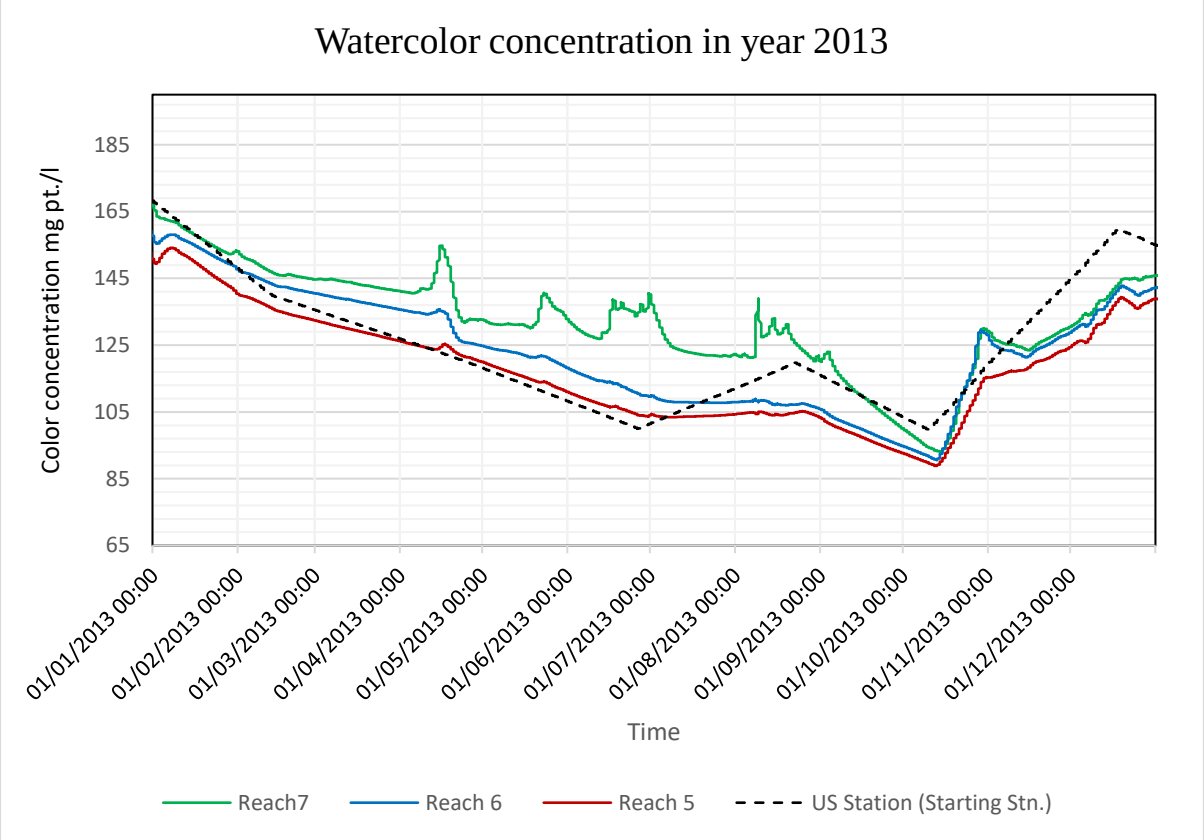

Figure 38 Color concentration variation in different reaches of Storån river in year 2013.

Figure 38 shows the variation of WCC in year 2013 in different reaches of Storån River. The broken black line is the WCC at the beginning of the simulation whereas the red curve, blue curve and green curve are the WCC in Reach 5, Reach 6 and Reach 7, respectively. Reach 6 starts just after joining River 6 to main river and Reach 7 starts just after River 7 (*Figure 13).* Here from the simulation results, it has been seen that the WCC in all reaches started lowering down from the initial date of the year up to mid of October and rose again when there was increase in discharge in the river.

Up to mid-October, the variation trend of WCC in Reach 5 and Reach 6 are similar (*Figure 38)*. But in the case of Reach 7, the WCC pattern was different from the others and there was a sharp increase in WCC from mid-April. This reach (green curve) also has some undulations with peaking of lowering down of WCC in a short period of time. This might be due to the high concentration of water even for a short period of time in the sub-catchment.

After the mid-October, due to high river discharge, the WCC got increased most probably due to more flushing of the nutrients in the catchment by the river in heavy rainfall event. The export of DOC to surface waters during precipitation events, or snow melt, groundwater levels peak is at its highest (Laudon et al. 2011).

The effect of this catchment was also seen distinct as the joint of this river to the Storån river is near to the outlet of the river.

6.5. Watercolor concentration in high/low flood events

Previous sub-chapters show that higher discharge results in higher WCC in most cases. But the time for rainfall and high/low flood varies in every year (*Figure 33, Figure 35, Figure A. 2 and Figure A. 3)* due to varying climatic conditions. In this sub-chapter, the WCC in the events of highest and lowest flood for sample years (2012 and 2013) have been discussed.

Figure 39 shows the WCC along Storån river for extreme events for years 2012 and 2013. Each curve shows the WCC on the specific dates as shown in the legend.

Following the figure, the curves start from the left in US boundary and goes to the right in the DS Boundary. The WCC value seems to be constant in every river station in a reach and then gets dropped or elevated rapidly. It is due to that, the tracer is conservative and there is no addition of flow in between reaches, so there is negligible effect of transport mechanism within a reach. Also, no further chemical reaction was considered in the river and the change in concentration due to other reasons were neglected. The WCC is almost same value of in every reach was due to the quick equilibrium time for mixing of the water in the river joints.

The vertical drop of the concentration is due to the rapid mixing of water from two sources in each river joints. The reason for this can be related to the lower dispersion coefficient. If the dispersion coefficient were higher for say 100 m^2/s, the change in WCC after a reach could have been less rapid and the change pattern of WCC could have been seen as shown in *Figure 4*. As the dispersion coefficient is taken from Fischer empirical formula was calculated lesser than 20 m^2/s in most of the river stations, the rapid change of the WCC was found as nearly vertical line as shown in *Figure 39.*

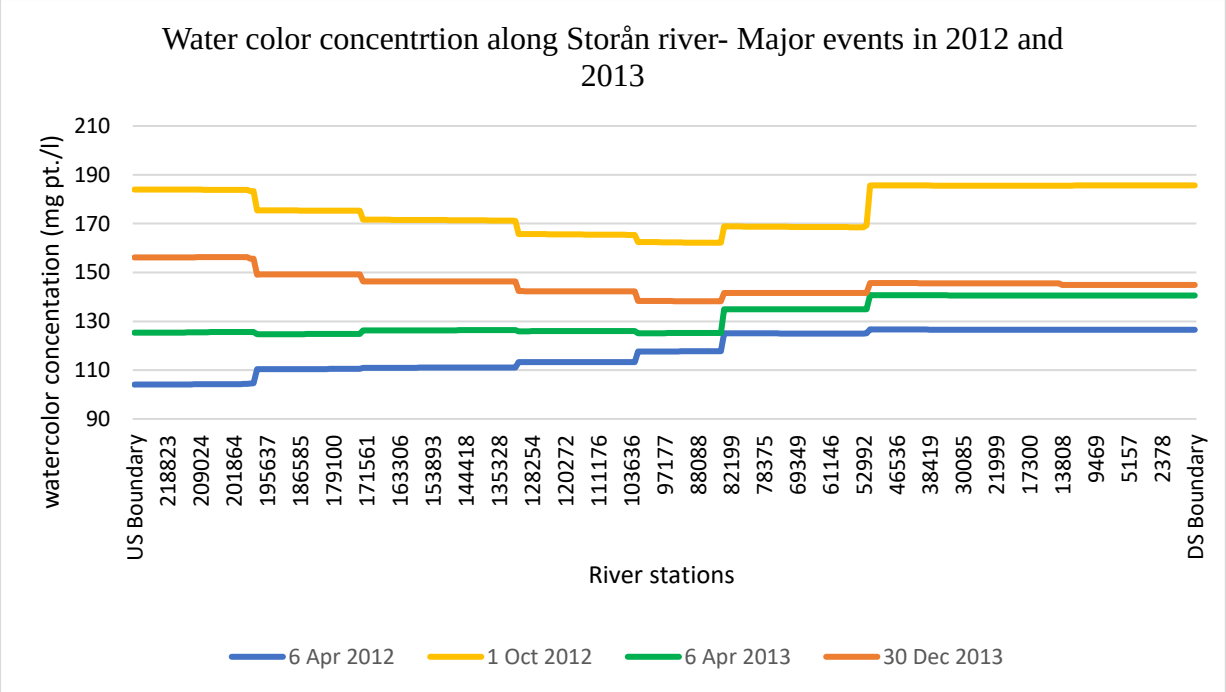

Figure 39 Watercolor concentration for high and flow events for year 2012 and 2013.

The lowest and highest flows in the last reach as per SMHI for years 2012 and 2013 were taken for the study. For year 2012, date of 6th April ($Q_{min\ 2012}$ = of 5.02 m^3/s) and 1st October ($Q_{max\ 2012}$ = 23.5 m^3/s)

and for year 2013, date of 6th April ($Q_{min\ 2013}$ = 3.19 m^3/s) and 30th December ($Q_{max\ 2013}$ = 26.3 m^3/s) were taken.

For $Q_{min\ 2012}$ (blue curve) and $Q_{min\ 2013,}$ (green curve), the WCC went on increasing up, starting from US boundary to DS boundary (Figure 39). In spring, there was less WCC concentration in the outlet of lake Flatten (at the starting of simulation), and it increased gradually after joining other tributaries. For $Q_{min\ 2012}$, the WCC started from 100.2 mg Pt./l at US station and after the simulation, the WCC was 126.47 mg Pt./l. Similarly, $Q_{min\ 2013}$ has 125.3 mg Pt./l at US station and 144.85 at DS station after the simulation. The graphical variation of WCC for 6th April 2012 is shown in *Figure 40*.

But for $Q_{max\ 2012}$ (yellow curve) and $Q_{max\ 2013,}$ (orange curve), WCC went on decreasing from starting up to RS 82199 (Reach 5), then started increasing up to DS station. It was seen that there was no significant change in the WCC in those two dates. $Q_{max\ 2012}$ had WCC of 156.19 mg Pt./l at US station, and it was just change of -12 mg Pt./l at the DS station. For $Q_{max\ 2013}$, the WCC at US station and DS station was almost the same i.e. 185 mg Pt./l. In the high flood, it was seen that the WCC at the outlet of Flatten was much more than of April.

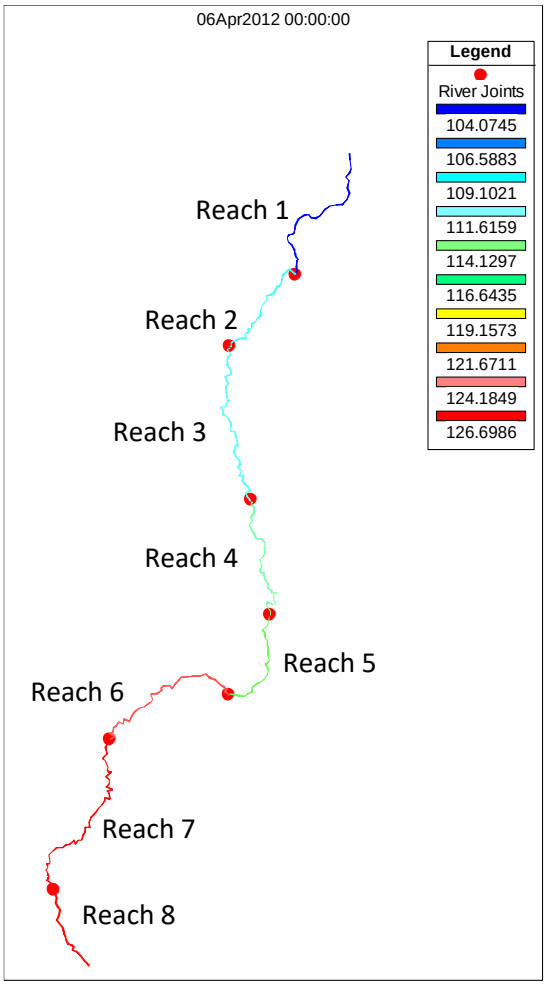

Figure 40 Graphical Illustration of WCC variation on 6th April 2012.

The graphical illustration of the WCC variation for remaining extreme events is shown in *Figure B. 13.*

Based on the available data, it can be discussed that, the flux of WCC and discharge was lower for the high flood in 2012 and 2013 up to Reach 5. After joining R_6 and R_7, the flux increased as these two rivers have comparatively higher WCC concentration. Also, River R_6 and R_7 is the main tributary of the river, resulting high flux added to the river. This behaviour further support that the R_6 and R_7 has much more influence in WCC in the river.

From the *Figure 40, and* Figure *B. 15,* it can be discussed that, in reference to of extreme events, the WCC has been increased after joining peat soiled rich rivers R_6 and R_7, the WCC has been increased after Reach 5. This also support the result showed by Mattsson et al. in 2005, that peat material is source for the carbon source to the river. Also, the terrain of Storån river is comparatively flat in Reach 6, Reach 7 and Reach 8 (*Figure 12*) and there exists large agricultural land in the banks of the river. This might also be the possible reason for increase in the WCC, as agricultural land use has positive impact for the WCC (Kritzberg et al., 2019, Klante et al., 2021).

7. MODEL LIMITATIONS AND UNCERTAINTIES

The model is just the simplification or idealizations of reality thus is not always able to create a realistic natural phenomenon. As the methodologies used in the model consist of many simplifications and assumptions, there might be lots of uncertainties in the model.

The quality of data collection for discharge and watercolor is the major limitation of produced work in this report. As described in *Section 4.4*, Due to absence of discharge measuring stations, all the analysis are based on the S-HYPE model approached given by SMHI. Similarly, the frequency of the color data is very low, and the measured data were also not measured at the same time to have a fair comparison. Likewise, assumptions described in *Section 4.5* may also be taken as the limitation of the study.

Another limitation is about the lesser river cross-sections survey or lesser bathymetric survey data of the river. As described in *Section 5.1*, the DEM of the river and its banks were developed by the bathymetric survey of 18 river cross-sections only. So, the DEM does not resemble the real scenario even terrain above the water level was taken from LiDAR data as described in *Section 4.1.1*. This is a reason that, the model has similar cross-sections in the reaches. Also, the structure existing in the river like Bridge, Bridge foundation, hydropower weir, energy dissipating structures, river training were not considered, which may have effect on the transport process of materials and has effect on the hydraulics of the river system.

Storån river is a meandering river and there exists lots of oxbow lakes, depressions in many locations. As the model is 1D, it was hard to represent the braided channel and oxbow lakes. As the model consist of lesser number of cross-sections (1 in average of 200 meters), depressions and other features existing in between two cross-sections could not be shown. Also, 1-D analysis restrict the lateral flow of water from the main channel to other sinks and depressions in the river section and assumes that water also flow from these depressions to the following cross-sections.

A minimum time step and minimum cell size are very crucial to get finer results (Brunner, 2016) but in this model, the unsteady flow have been analyzed in the time step of 1 hour and time step for water quality simulation was taken 2 hours due to long simulation time and software limitations. Likewise, there are about just 333 cross-sections altogether for 67 km river and just three cross-sections in each tributary. It seems that the number of cross-sections and cells are very less to address the complexity of the simulation. This may have some uncertainties while simulating the material transport process.

While calibrating, for hydraulic-steady analysis was carried out with only one sample date and for water quality model, just few sample dates were taken due to unavailing of the data series as discussed in *Section 5.2.2*. The calibration of the water quality analysis was only done qualitatively. The model lacks the validation process.

8. CONCLUSION AND RECOMMENDATION

In this study, 1-D hydrological model and water quality model of Storån river basin from south of lake Flatten to lake Bolmen were developed in HEC-RAS. The topography was built by the LiDAR file and bathymetric survey in multiple river sections through the SONAR method. Watercolor concentration and daily varying discharge from the outlet of lake Flatten as well other main tributaries were taken from SLU and SMHI respectively. Then the model was simulated for hydraulic model first, then simulation of tracer analysis from the multiple sources was simulated for available four years color data.

The output simulation data of HEC-RAS and long-term data were analysed to see the variation of material transport with respect to time-varying water discharge from the Storån river to lake Bolmen. To conclude this study as clearly as possible, the research questions have been answered thoroughly which have been stated in section *1.3*.

From the results and discussion, it can be concluded that the brownification in river Storån and its tributaries varies in time and space at a wide range. The material causing the brown color to water is in increasing trend, possibly due to climate change, seasonal variation and change of land-use and land cover change, like increase and change of forest pattern in the catchment. Though, the exact pattern of the variation of WCC only due to runoff just from four years of simulation is hard to explain, but in general, it was found that higher watercolor concentration was found in higher discharges during the autumn and winter seasons. The possible reasons for this may be due to the high mobilization of carbon and metal like Fe and more acid deposition in the wet season. In summer and spring, the WCC at downstream are lower in comparison with the wet seasons. Furthermore, it seems that tributary R_7 has a distinct effect for the WCC variation in the river followed by R_6.

Storån river, being the main tributary for Lake Bolmen, increasing the level of browning in Storån certainly could go browning the lake above the limit for aquatic animals and it seems that drinking water treatment cost will further increase in the future. So, it could be necessary to modify the treatment processes ahead of time to save money, treatment complexity, and other efforts. In the worst-case scenario, another source of drinking water may need to find if the treatment process is not feasible to act against the brownification.

The larger number of cross-sections is crucial for understanding the actual topography of the river. Further, larger resolution data for the color data are vital for a better analysis. The frequency of the color data is just 4-12 times a year, even though this can change in every hour (Jennings et al., 2009). Due to data limitation, detail analysis in each tributary could not be investigated in the same detail. This report also recommends for more color measurements and field campaigns in future in the river and its tributaries.

The wetland plays an important role in nutrition retention (Kritzberg et al., 2019). For the catchment of River R_2 and R_4, which possess large wetland areas of Store Mosse Nationalpark, data stations can be established nearby in the park to study the effect of wetlands in material transport. Experimental verification for dispersion coefficient could be done for some corrections to have a good assurance mixing process like advection and diffusion. Further, 2D modelling could be done to include other hydraulic processes like eddies and lateral flows in the river. One focus should be done to include the bathymetric data for tributaries too. As river R_7 has a distinct effect on the WCC variation in the river, further study in this tributary could be fruitful to understand the material transport in detail.

BIBLOGRAPHY

American Public Health Association (APHA), American Water Works Association (AWWS) and Water Environment Federation (WEF), (1999), 'Standard Methods for the Examination of Water and Wastewater', 23rd Edition.

Antonopoulos, V. Z., Georgiou P. E., Antonopoulos Z. V. (2015), 'Dispersion Coefficient Prediction Using Empirical Models and ANNs'. *Springer International Publishing Switzerland. Enviromental. Process.*

Arheimer B., Donnelly C., Strömqvist J. (2013),' Large-Scale Effects Of Climate Change On Water Resources In Sweden And Europe', *VATTEN – Journal of Water Management and Research 69:201–207*

Bandini F., Olesen D., Jakobsen J., Kittel C. M. M., Wang S., Garcia M., and Bauer-Gottwein P. (2018), 'Bathymetry observations of inland water bodies using a tethered single-beam sonar controlled by an Unmanned Aerial vehicle', *Hydrology Earth System Science, 22, 4165–4181*.

Borgström, A. (2020), 'Lake Bolmen past, present, and future, Aquatic ecology', Department of Biology, Lund University.

Brunner, G. W. (2016), 'HEC-RAS River Analysis System- User manual. US Army Corps of Engineers', Institute for Water Resources, Hydrologic Engineering Centre (HEC).

Brunner, G. W. P.E. (2008), 'Common Model Stability Common Model Stability Problems When Performing Problems When Performing an Unsteady Flow Analysis', Hydrologic Engineering Centre.

Chapra, S.C. (1997), 'Surface Water Quality Modeling'. *McGraw-Hill, Inc.*, New York.

Conserve Energy Future (2021), 'What is Water Pollution?' (Online) Available *at https://www.conserve-energy-future.com/sources-and-causes-of-water-pollution.php* [Accessed 25 01 2021].

Creed, I. F. et al. (2018), 'Global change-driven effects on dissolved organic matter composition: Implications for food webs of northern lakes.' *Glob Change Biology, Volume 24, Issue 8*, pp: 3692–3714.

Czernuszenko W. (1987), 'Dispersion of pollutants in rivers', *Hydrological Sciences Journal*, 32:1, 59-67.

Davidson, E. & Janssens, I., (2006), 'Temperature Sensitivity of Soil Carbon Decomposition and Feedbacks to Climate Change', *Nature. 440. 165-73. 10.1038/nature04514.*

Deeper (2021), 'Deeper Smart Sonar CHIRP+' [Online]. Available at *https://deepersonar.com/se/se_se/produkter/smart-sonar-chirp-plus* [Accessed 17 03 2021].

Deeper (2021b), 'How Sonars Work: Key Aspects to Know'. [Online] Available at *https://deepersonar.com/us/en_us/how-it-works/how-sonars-work* [Accessed 17 03 2021].

Degerman, E., Andersson M., Häggström H., and Persson P. (2011), 'Salmon and Sea Trout Populations and Rivers in Sweden Baltic Marine Environment Protection Commission – Helsinki Commission', *Baltic Sea Environment Proceedings No. 126B,* Helsinki Commission -Baltic Marine Environment Protection Commission.

Ekström, S. (2013), 'Brownification of freshwaters-the role of dissolved organic matter and iron', Doctoral Thesis, Department of Biology Aquatic Ecology, Lund University.

Engineer Paige (2021), 'HEC-RAS Boundary Conditions', [Online] Available at *https://engineerpaige.com/hec-ras-boundary-conditions/* [Accessed 17 03 2021].

Frycklund K., (1998), 'Artificial recharge of groundwater for public water supply-Potential and limitations in Boreal conditions', Dissertation Royal Institute of Technology Stockholm.

Graneli, W. (2012), R. W. Herschy, & R. W. Fairbridge 'Brownification of Lakes. In L. Bengtsson', *Encyclopaedia of Lakes and Reservoirs (pp. 117–119). Springer, Netherlands*.

Haaland S., Hongve D., Laudon H., Riise G., Vogt RD. (2010), 'Quantifying the drivers of the increasing-colored organic matter in boreal surface waters', *Environment Science Technology. 2010 Apr 15;44(8):2975-80.*

Harris County Flood Control District (HCFCD) 2018, 'The HEC-RAS Unsteady Modelling Guidelines'.

Hedström, P., Bystedt, D., Karlsson, J., Bokma, F. & Byström, P. (2017), 'Brownification increases winter mortality in fish', *Oecologia* 183(2), 587–595.

Hikersbay (2021), ä Jönköping Sweden weather' [Online] Available at *http://hikersbay.com/climate/sweden/jonkoping?lang=en* [Accessed 21 03 2021].

IHSS (2008), 'International Humic Substances Society' [Online]. Available at: *https://ihss.humicsubstances.org* [Accessed 13 06 2021].

Inyinbor, A., Adebesin, B., Oluyori, A., Adelani-Akande, T., Dada, A. O., Oreofe, A. (2018), 'Water Pollution: Effects, Prevention, and Climatic Impact', 10.5772/intechopen.72018.

Jennings, E., Järvinen, M., Allott, N., Arvola, L., Moore, K., Naden, P., Aonghusa, C., Noges, T.,iina & Weyhenmeyer, Gesa. (2009), 'Impacts of Climate on the Flux of Dissolved Organic Carbon from Catchments'.

Jönsson, L. (2006), 'Receiving water hydraulics', Water Resource Engineering, Lund University.

Kazanjian, G., Brothers, S., Köhler, J., Hilt, S. (2019), 'Incomplete resilience of a shallow lake to a brownification event', *Cold Spring Harbour laboratory. bioRxiv.*

Klante, C. & Larson, M. & Persson, K. M. (2020), 'Brownification in Lake Bolmen, Sweden, and its relationship to natural and human-induced changes' [01 03 2021], Department of Water Resource Engineering, Lund University. *(Remarks: Unpublished)*

Knorr, K. H. (2013), 'DOC-dynamics in a small headwater catchment as driven by redox fluctuations and hydrological flow paths—Are DOC exports mediated by iron reduction/oxidation cycles?' *Biogeosciences*, 10, 891–904.

Kritzberg, E.S., Hasselquist, E.M., Škerlep, M. et al. (2019), 'Browning of freshwaters: Consequences to ecosystem services, underlying drivers, and potential mitigation measures', *Ambio* 49, 375–390(2020)

Länsstyrelsen (2006), 'Metaller i Storån 2002-2004', Meddelande NR 2006:01, Länsstyrelsen I Jönköping län.

Länsstyrelsen (2021), 'Vatteninformationsystem, Sverige' [Online] Available at. *https://ext-geoportal.lansstyrelsen.se/standard/?appid=3e0dd9145e6e44f298111f47f5b4184d* [Accessed 31 03 2021]

Lantmäteriet (2021b), 'SWEREF 99 Projections'[Online] Available at*: https://www.lantmateriet.se/zh-tw/maps-and-geographic-information/gps-geodesi-och-swepos/Referenssystem/Tvadimensionella-system/SWEREF-99-projektioner/* [Accessed 18 01 2021].

Laudon, H., Berggren, M., Ågren, A.,Buffam, I.,Bishop, K., Grabs, T., Jansson, M., Köhler, S. (2011), 'Patterns and Dynamics of Dissolved Organic Carbon (DOC) in Boreal Streams: The Role of Processes, Connectivity, and Scaling. Ecosystems', *Ecosystems* 14. 880-893.

Lindgren, F. (2019), 'Lakes are browner in the south than in the north of Sweden despite similar levels of dissolved iron', Master thesis, Environmental Science, Högskolan I Hamstad.

Lintern A., Webb J.A., Ryu D., Liu S., Bende-Michl U., D., Waters P. L., Wilson P. and Western A. W. (2013), 'Key factors influencing differences in stream water quality across space'. *WIREs Water*, Volume 5, Issue 1 e1260.

Marinwatersheds (2021), 'Hydrology and Hydraulic (H&H) Modeling' [Online]. Available at *https://www.marinwatersheds.org/resources/projects/hydrology-and-hydraulic-hh-modeling* [Accessed 12 05 2021].

Mattsson, T., Kortelainen, P. & Räike, A, 'Export of DOM from Boreal Catchments: Impacts of Land Use Cover and Climate'. *Biogeochemistry 76, 373–394.*

Meyer-Jacob, C., Michelutti, N., Paterson, A. M., Cumming, B. F., Keller, W. (Bill), Smol, J. P. (2019), 'The browning and re-browning of lakes : Divergent lake-water organic carbon trends linked to acid deposition and climate change', *Scientific Reports.*

Merkuryeva, G., Merkuryev, Y., Sokolov, B.V., Potryasaev S., Zelentsov, V.A., Lektauers, A. (2015), 'Advanced river flood monitoring, modelling, and forecasting', *Journal of Computational Science*, Volume 10, Pages 77-85, ISSN 1877-7503.

Muluneh Ertiro Tumdedo (2010), 'Dynamics of Humic Substance in Bolmen Lake, Sweden', Master Project, Lund University.

Naden Pamela S. (1989), 'Statistical Modelling of Water Colour in the Uplands: The upper Nidd catchment 1979-1987', *Environmental Pollution*. Vol. 60, pp. 141-163.

Naturvardsverket (2021), 'About Store Mosse National Park', [Online] Available at *https://www.sverigesnationalparker.se/park/store-mosse-nationalpark/nationalparksfakta/*. [Accessed 13th May 2021].

Nieminen M., Palviainen M., Sarkkola S., Laurén A., Marttila H., Finér L. 'A synthesis of the impacts of ditch network maintenance on the quantity and quality of runoff from drained boreal peatland forests', *Ambio. 2018 Sep;47(5):523-534.*

Persson, K. M. (2011), 'On natural organic matter and lake hydrology in Lake Bolmen', Sydvatten AB and Water Resources Engineering, Lund University.

Ploum, S. W., Laudon, H., Peralta-Tapia, A., & Kuglerová, L. (2020), 'Are dissolved organic carbon concentrations in riparian groundwater linked to hydrological pathways in the boreal forest?', *Hydrology and Earth System Sciences*, 24(4), 1709–1720.

Ponce, (2021), 'Steady vs Unsteady Flow With HEC-RAS', [Online] Available at *http://ponce.sdsu.edu/legacy_tales_steady_unsteady_hec_ras.html* [Accessed 17 03 2021].

Rolf, D., Vogt, E. G., Andersen, D. O., Clarke, N., Gadmar, T., Bishop, K., Lundstrøm, U., Starr, M. (2001), 'Natural Organic Matter in the Nordic countries', *Nordtest Report.* TR 479.

SGU (2021), 'Maps Generator' [Online] Available *at https://apps.sgu.se/kartvisare/kartvisare-berggrund-1-miljon.html* . [Accessed 31 03 2021].

SHMI (2020), 'HYPE: Our Hydrological Model'. [Online] Available at *https://www.smhi.se/en/research/research-departments/hydrology/hype-our-hydrological-model-1.7994* [Accessed 19 01 2021].

SLU (2003). 'The color of water, Department of Environmental Assessment', SLU, Norwegian Institute for Water Research.

SMHI (2021), 'Hydrological Predictions for the Environment' [Online]. Available at *https://www.smhi.se/forskning/forskningsenheter/hydrologisk-forskning/hype-1.557* [Accessed 17 03 2021].

Spellman, F.R. (2013). 'Handbook of Water and Wastewater Treatment Plant Operations' (3rd ed.). CRC Press.

Statistikmyndigheten (2021), 'Statistikdatabasen', [Online] Available at *http://www.statistikdatabasen.scb.se/ pxweb/sv/ssd/*. [Accessed 13 05 2021].

Sundman, A. (2014), 'Interactions between Fe and organic matter and their impact on As(V) and P(V)', Department of Chemistry, Umeå University.

Tang, T., Strokal M., Michelle, T.H. van Vliet, Seuntjens, P., Burek, P., Kroeze, C., Langan S., Wada Y. (2019), 'Bridging global, basin and local-scale water quality modeling towards enhancing water quality management worldwide', *Current Opinion in Environmental Sustainability 2019*, 36:39–48.

Temnerud, J., Hytteborn, J. K., Futter, M. N., & Köhler, S. J. (2014), 'Evaluating common drivers for color, iron and organic carbon in Swedish watercourses', Ambio, 43(SI), 30–44.

Thurman E.M. (1985), 'Organic Geochemistry of Natural Waters', Volume 2. Kluwer Academic Publishers.ISBN : 978-94-010-8752-0

Weyhenmeyer, G. A., Prairie, Y. T., Tranvik, L. J. (2014), 'Browning of Boreal Freshwaters Coupled to Carbon-Iron Interactions along the Aquatic Continuum' *PLOS ONE 9(2): e88104.*

Williamson, C. E. et al. (2015), 'Ecological consequences of long-term browning in lakes', *Scientific Reports.*

Williamson, R. (2001) 'Transport and Fate of Contaminants in Surface Water', University of California Agricultural Extension Service and the California Department of Health Services.

Wit H. A., Valinia S., Weyhenmeyer G.S, Futter M. N., Kortelainen P., Austnes K., Hessen O, Räike A., Laudon H., and Vuorenmaa J., *Environmental Science & Technology Letters* 2016 *3* (12), 430-435.

World Weather & Climate Information (2021), 'Average monthly snow and rainfall in Jönköping (Jönköping County)' [Online]. Available at *https://weather-and-climate.com/average-monthly-precipitation-Rainfall,jonkoping,Sweden* [Accessed 21 03 2021].

Zeng, Yu-hong & Huai, Wen-xin. (2013), 'Estimation of longitudinal dispersion coefficient in rivers. *Journal of Hydro-environment Research. 8*. 10.1016/j.jher.2013.02.005.

APPENDIX

Appendix A: Tables and Figures

Table A. 1 Manning's Value Chart

Type of Channel and Description	Minimum	Normal	Maximum
Natural streams - minor streams (top width at floodstage < 100 ft)			
1. Main Channels			
a. clean, straight, full stage, no rifts or deep pools	0.025	0.030	0.033
b. same as above, but more stones and weeds	0.030	0.035	0.040
c. clean, winding, some pools and shoals	0.033	0.040	0.045
d. same as above, but some weeds and stones	0.035	0.045	0.050
e. same as above, lower stages, more ineffective slopes and sections	0.040	0.048	0.055
f. same as "d" with more stones	0.045	0.050	0.060
g. sluggish reaches, weedy, deep pools	0.050	0.070	0.080
h. very weedy reaches, deep pools, or flood ways with heavy stand of timber and underbrush	0.075	0.100	0.150
2. Mountain streams, no vegetation in channel, banks usually steep, trees and brush along banks submerged at high stages			
a. bottom: gravels, cobbles, and few boulders	0.030	0.040	0.050
b. bottom: cobbles with large boulders	0.040	0.050	0.070
3. Floodplains			
a. Pasture, no brush			
1.short grass	0.025	0.030	0.035
2. high grass	0.030	0.035	0.050
b. Cultivated areas			
1. no crop	0.020	0.030	0.040
2. mature row crops	0.025	0.035	0.045
3. mature field crops	0.030	0.040	0.050

Source :http://www.fsl.orst.edu/geowater/FX3/help/8_Hydraulic_Reference/Mannings_n_Tables.htm

Table A. 2 Yearly, min, max color concentration for station Storån Inlopp Bolmen

Year	Yearly average color conc. (mg Pt./l)	Max conc. (mg Pt./l)	Min conc. (mg Pt./l)	Max conc. /Min conc.	Standard deviation	Month of maximum watercolor	Month of minimum watercolor
1985	159	240	110	2.18	40.9	Sept	Feb
1986	139	160	90	1.78	21.5	Feb/May	Oct
1987	185	350	100	3.50	89.7	Oct	May
1988	161	250	120	2.08	43.1	July	June
1989	157	250	120	2.08	32.5	Aug	April
1990	176	300	100	3.00	56.0	July	April
1991	132	175	110	1.59	18.6	Nov	May
1992	109	150	60	2.50	26.6	Feb	Oct
1993	180	350	85	4.12	99.3	Oct	May/June
1994	127	200	85	2.35	29.0	Dec	Sept
1995	146	200	75	2.35	36.9	N/A	N/A
1996	134	170	80	2.13	26.2	July	Oct
1997	141	230	85	2.71	36.3	Nov	April
1998	216	400	125	3.20	89.6	Oct	Mar/April/May
1999	265	500	150	3.33	110.0	Aug	Mar
2000	181	275	100	2.75	59.5	July	April
2001	206	450	125	3.60	88.6	Sept	Mar/May
2002	174	300	85	3.53	78.3	Aug	Oct
2003	175	250	100	2.50	58.4	May/July	Feb/Mar
2004	209	400	120	3.33	93.0	Aug	June
2005	193	400	125	3.20	74.7	Aug	July
2006	167	260	100	2.60	46.6	Dec	May
2007	261	500	150	3.33	123.5	July	Dec
2008	152	220	75	2.93	48.4	Nov	Oct
2009	213	400	120	3.33	97.1	July/Aug	Feb/April/June
2010	238	550	140	3.93	119.3	Aug	Jan
2011	243	400	120	3.33	97.4	Oct	April
2012	215	350	120	2.92	64.7	June	April
2013	170	240	80	3.00	44.1	May	Oct
2014	235	500	140	3.57	101.3	Aug	April
2015	179	300	120	2.50	55.7	July	April
2016	133	184	70	2.63	34.7	Nov	Oct
2017	248	324	171	1.89	108.2	Oct	May
2018	169	191	146	1.31	31.8	May	Nov
2019	265	600	100	6.00	163.3	Dec	Aug

Table A. 3 Information about bridges existing in Storån

Name	Easting	Northing	Location	Nearby River Stations in HEC-RAS
B1*	423182.566	6327240.986	Dannäsvägan	7451
B2*	422919.067	6329448.343	Slättö	19190
B3*	423405.999	6329964.465		23059
B4*	425066.193	6333038.036	Ekenäs Väg Torskinge Plåtslageri AB	46536
B5*	425419.300	6334579.318	Slättövägen near Ästorp	56260
B6*	427315.711	6336027.568	Kvarnagård near Forshedaverken AB	70184
B7*	429180.217	6336215.026	Brogatan near ICA Nära Ässet	79200
B8*	429484.974	6335945.986	Galvanovägen near Emab i Forsheda AB	80977
B9*	430463.789	6335932.459		87329
B10*	430615.330	6336030.113	Trelleborg Mixing Forsheda AB near Qstar Fuel Station	88088
B11*	430945.965	6337871.269	Right Turn from MFS Technology AB	98799
B12*	430891.605	6340897.252	Värnamo NV 331 72 Värnamo near Hökhult	119275
B13*	430569.066	6342442.595	Värnamo NV	128234
B14	430473.884	6342906.270	Värnamo NVNear B13	130535
B15*	429875.499	6344796.566	331 72 Kulltorp near Thomas Kurtsson	144418
B16*	429402.183	6346206.041	330 31 Kulltorpnear H Johansson	153893
B17*	429571.386	6346561.910	330 31 KulltorpNear High Caparral Camping	157389
B18	429525.449	6347098.691	Gnosjö S Near Big Bengt Musuem	160050
B19	430511.333	6349570.098	Gnosjö S Tyngel	181619
B20*	431086.946	6350364.844	Gnosjö S, 330 33 Hillerstorp, 330 33 Hillerstorp next to Kulltorpsvägen	187402
B21*	431360.328	6350800.684	Gnosjö S 330 33 Hillerstorpnear Restaurang Ågård	191515
B22*	431666.963	6351045.158	330 33 Hillerstorp near Ågårds Farm cafe	192951
B23*	432076.578	6352222.914	Storgatan 58 330 33 Hillerstorp	202425
B24*	432140.214	6353236.005	Gnosjö S near ICA Nära	209024
B25*	432473.002	6353568.248	Brogatan 330 33 Hillerstorp	212524
B26	432779.280	6353399.293	Gnosjö S near Hamnkyrkan	213962
B27	433021.250	6353522.757	330 33 HillerstorpNear Hamnkyrkan	209024
B28	434069.015	6354602.794	Sven Björns väg 330 33 Hillerstorp	221251

**Bridges from where SONAR measurement was done during field survey.*

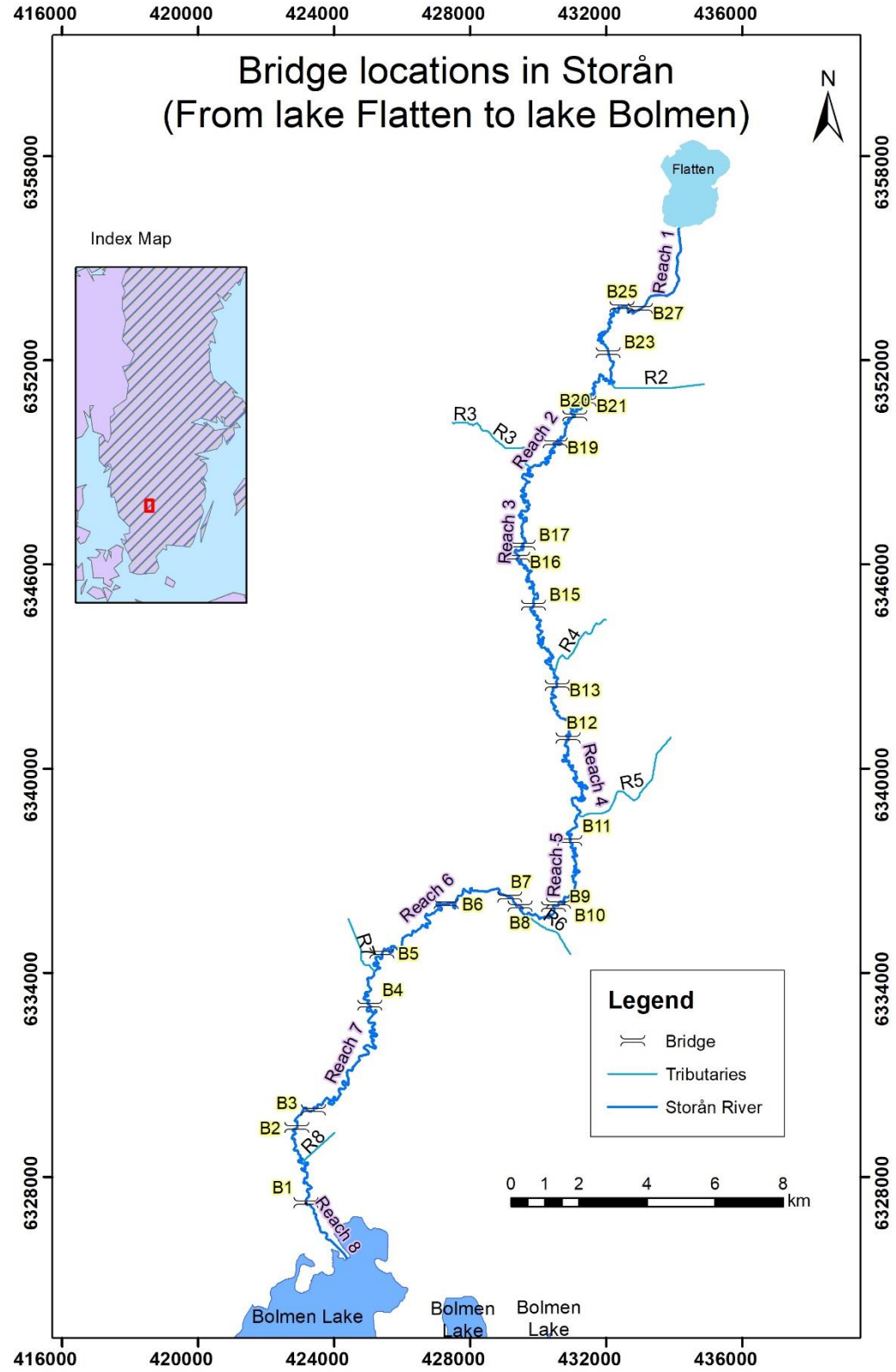

Figure A. 1 Location of Bridges along in the Storån

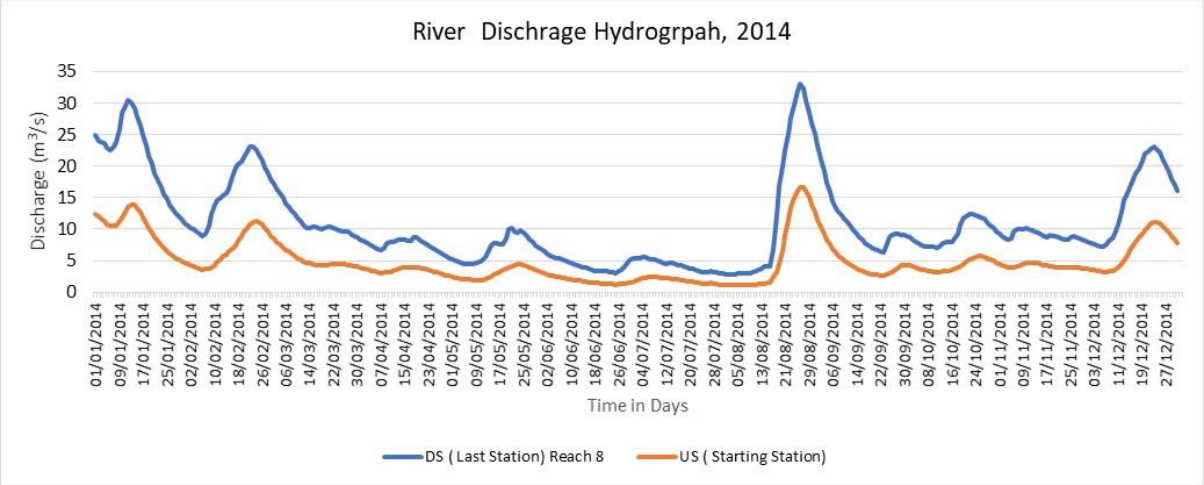

Figure A. 2 Daily River discharge hydrograph for year 2014

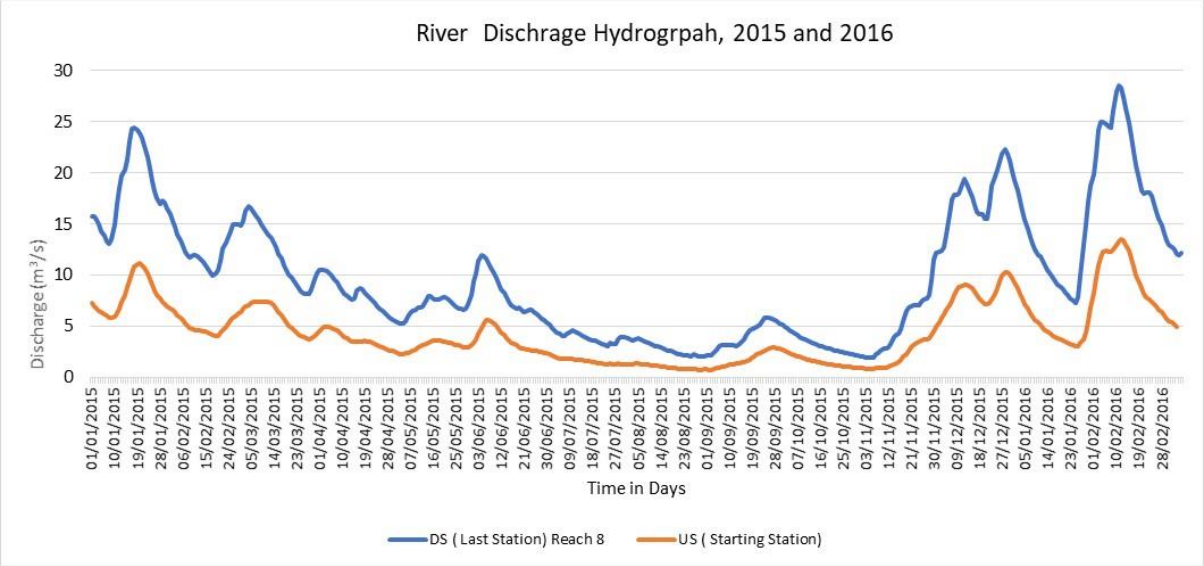

Figure A. 3 Daily River discharge hydrograph for year 2015 and 2016 (Feb)

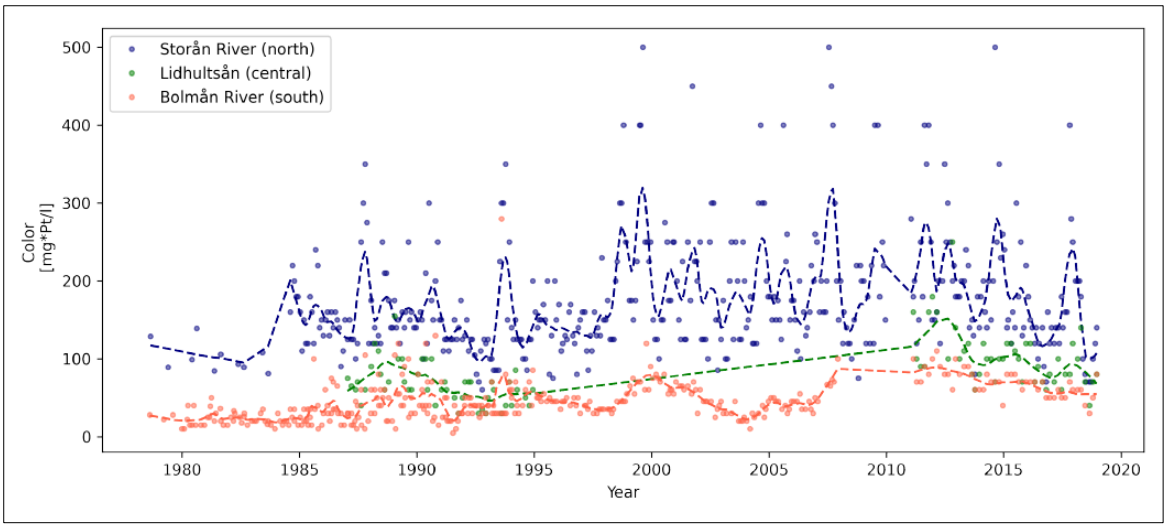

Figure A. 4 Long-term color trend of the main tributaries of Lake Bolmen (Klante et al., 2021,Remarks : Unpublished, Permission taken form the author)

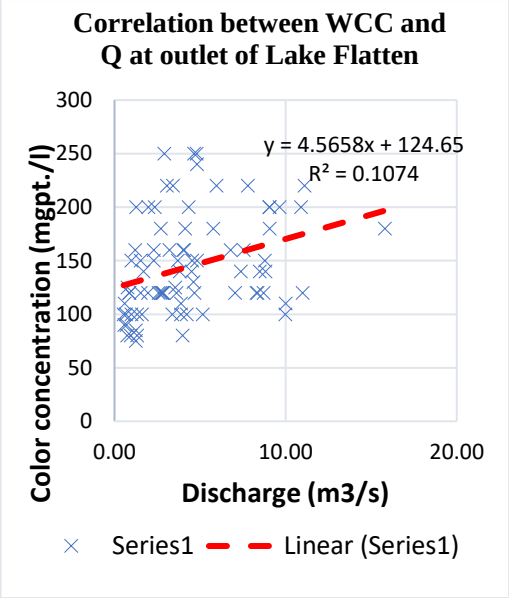

Figure A. 5 Correlation of river discharge and watercolor concentration for outlet of lake Flatten (r=0.32)

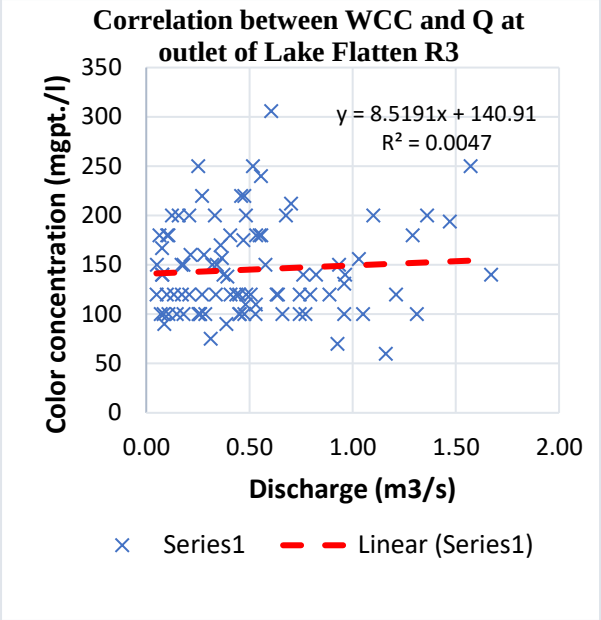

Figure A. 6 Correlation of river discharge and watercolor concentration for R3 (r=0.068)

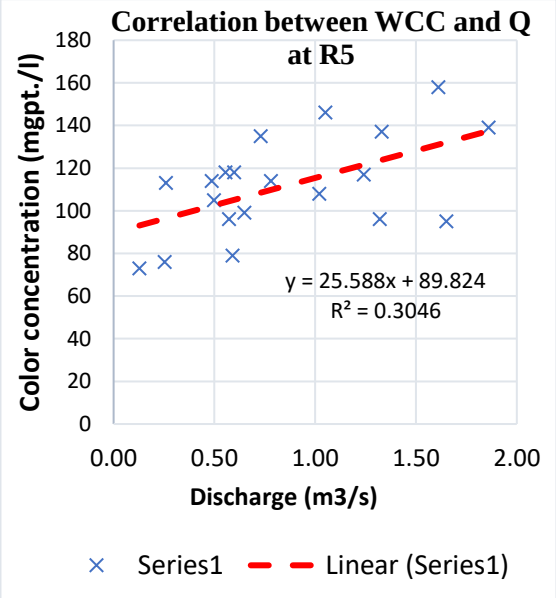

Figure A. 7 Correlation of river discharge and watercolor concentration for River R5 (r=0.55)

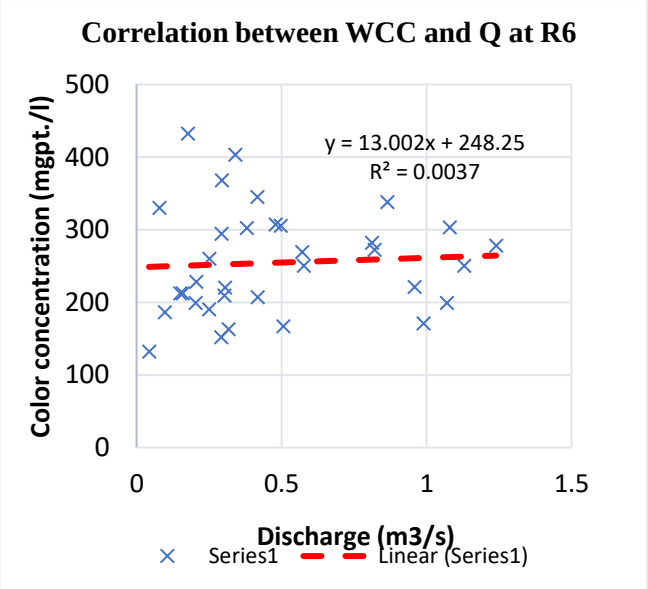

Figure A. 8 Correlation of river discharge and watercolor concentration for R6 (r=0.06)

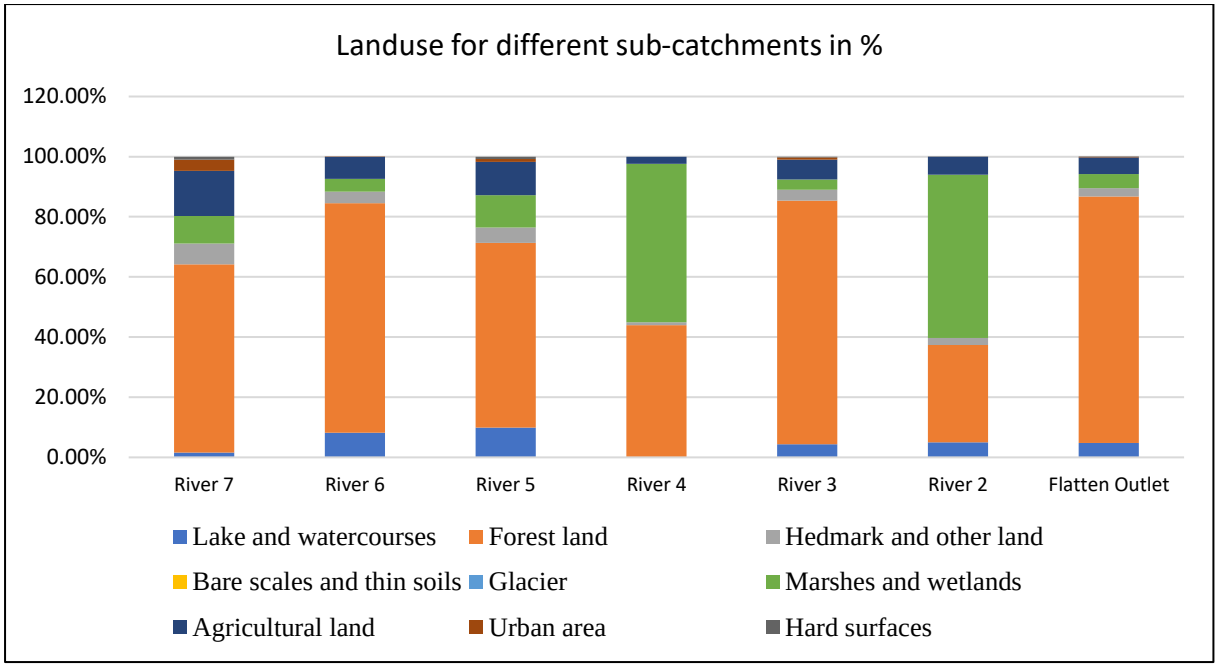

Figure A. 9 Land use for main tributaries of Storån (Source: SMHI).

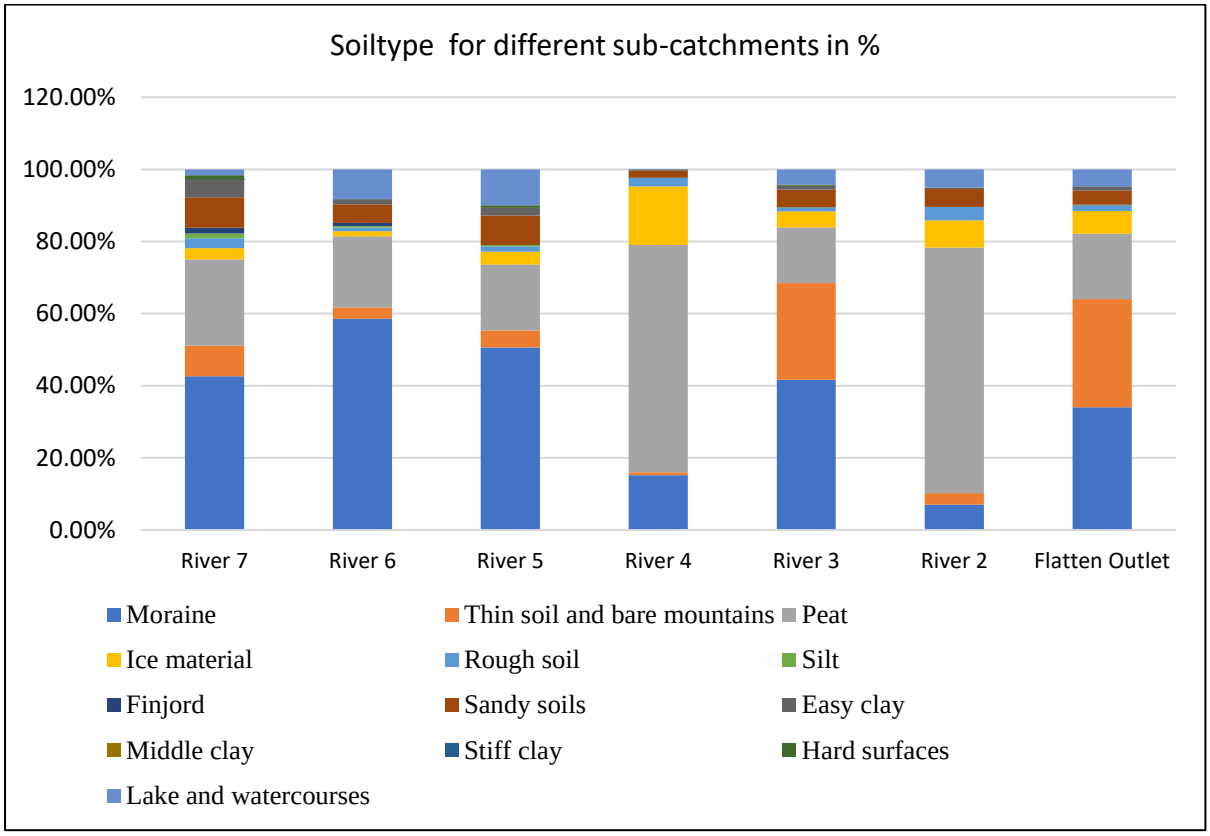

Figure A. 10 Soil type for main tributaries in Storån (Source: SMHI).

Table A. 4 Land use and soil type area for each tributary and reach catchments (Source: SMHI).

Land use in %	**River 7**	**River 6**	**River 5**	**River 4**	**River 3**	**River 2**	**River 1**	**Reach 8**	**Reach 7**	**Reach 6**	**Reach 5**	**Reach 4**	**Reach 3**	**Reach 2**	**Reach 1**
Lake and watercourses	1.60	8.23	9.94	0.02	4.32	4.99	4.76	1.84	0.51	0.37	0.30	0.35	0.30	0.62	0.78
Forest land	62.56	76.30	61.43	43.94	81.11	32.38	82.01	35.14	51.37	69.14	66.35	73.02	60.02	56.38	64.31
Hedmark and other land	6.97	3.78	5.09	0.93	3.54	2.30	2.77	10.77	6.60	5.21	8.01	4.36	4.80	10.38	7.25
Bare scales and thin soils	0.00	0.00	0.00	0.00	0.00	0.00	0.00	0.00	0.00	0.00	0.00	0.00	0.00	0.00	0.00
Glacier	0.00	0.00	0.00	0.00	0.00	0.00	0.00	0.00	0.00	0.00	0.00	0.00	0.00	0.00	0.00
Marshes and wetlands	9.11	4.28	10.77	52.76	3.47	54.30	4.64	3.08	25.35	12.65	2.37	13.40	23.69	10.17	7.80
Agricultural land	15.01	7.41	11.04	2.35	6.56	5.98	5.59	49.16	16.17	7.65	21.17	8.87	7.48	14.46	9.99
Urban area	3.70	0.01	0.98	0.00	0.73	0.00	0.20	0.00	0.00	4.07	1.10	0.00	3.70	5.73	5.98
Hard surfaces	1.04	0.00	0.74	0.00	0.27	0.05	0.03	0.00	0.00	0.91	0.69	0.00	0.00	2.26	3.89
Catchment Area (km2)	57.54	34.21	59.21	31.55	35.50	48.66	282.15	2.41	21.90	23.40	15.95	15.82	21.30	6.44	20.81
Yearly Average Q (m3/s)	**1.122**	**0.640**	**0.995**	**0.805**	**0.579**	**1.048**	**1.048**	**0.04**	**1.147**	**0.741**	**0.987**	**0.711**	**0.8**	**0.835**	**4.165**
Soil type in %	**River 7**	**River 6**	**River 5**	**River 4**	**River 3**	**River 2**	**River 1**	**Reach 8**	**Reach 7**	**Reach 6**	**Reach 5**	**Reach 4**	**Reach 3**	**Reach 2**	**Reach 1**
Moraine	42.64	58.61	50.61	15.23	41.65	7.04	34.01	5.28	12.53	27.51	43.04	38.26	21.21	17.09	28.82
Thin soil and bare mountains	8.52	3.09	4.72	0.79	26.85	3.19	30.05	3.11	2.02	1.25	1.37	3.08	7.79	4.82	9.25
Peat	23.87	19.77	18.29	63.02	15.41	68.08	18.12	28.75	45.08	38.19	12.53	26.88	40.81	22.35	19.21
Ice material	3.08	1.38	3.57	16.23	4.43	7.59	6.26	6.35	12.08	16.54	14.79	17.88	7.35	22.46	18.28
Rough soil	2.81	0.95	1.51	2.40	1.18	3.71	1.54	5.46	11.50	6.83	3.83	4.53	14.98	16.02	10.20
Silt	1.35	0.44	0.34	0.04	0.03	0.00	0.04	0.89	1.34	0.27	0.70	0.53	0.34	0.00	0.01
Finjord	1.57	0.89	0.00	0.00	0.00	0.00	0.17	0.00	0.01	0.68	2.38	0.01	0.04	0.00	0.00
Sandy soils	8.44	5.18	8.14	1.94	4.83	4.99	3.90	39.74	11.30	6.12	16.76	6.23	6.00	13.65	8.88
Easy clay	4.88	1.42	2.12	0.34	1.04	0.37	1.07	8.58	3.57	1.26	3.10	2.20	1.13	0.73	0.68
Middle clay	0.00	0.00	0.00	0.00	0.00	0.00	0.00	0.00	0.00	0.00	0.00	0.00	0.00	0.00	0.00
Stiff clay	0.19	0.04	0.00	0.00	0.00	0.00	0.04	0.00	0.04	0.06	0.51	0.05	0.05	0.00	0.00
Hard surfaces	1.04	0.00	0.74	0.00	0.27	0.05	0.03	0.00	0.00	0.91	0.69	0.00	0.00	2.26	3.89
Lake and watercourses	1.60	8.23	9.94	0.02	4.32	4.99	4.76	1.84	0.51	0.37	0.30	0.35	0.30	0.62	0.78

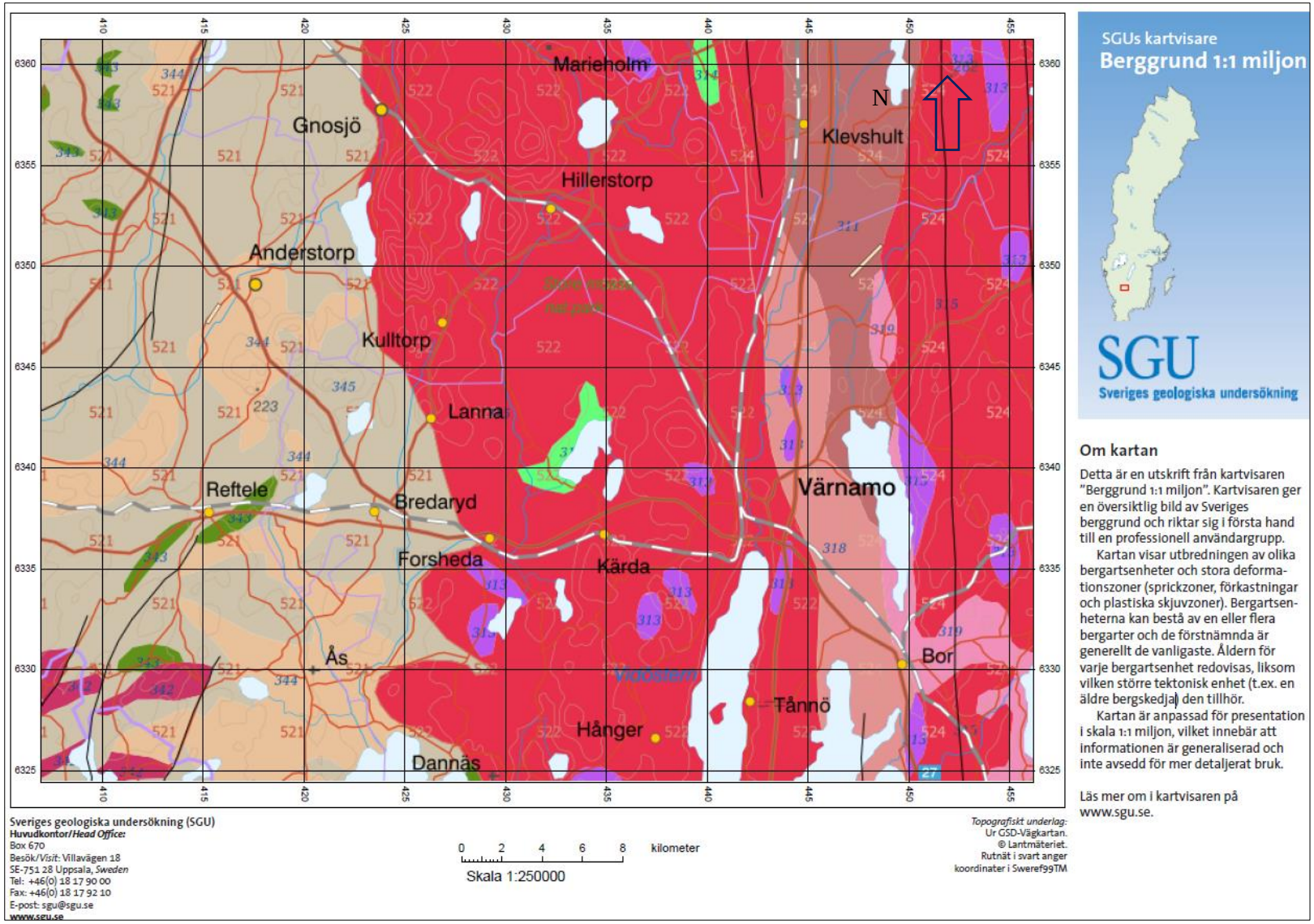

Figure A. 11 Geological Map (Bedrock) of the study area (1/2)

Figure A. 12 Geological Map (Bedrock) of the study area (2/2)

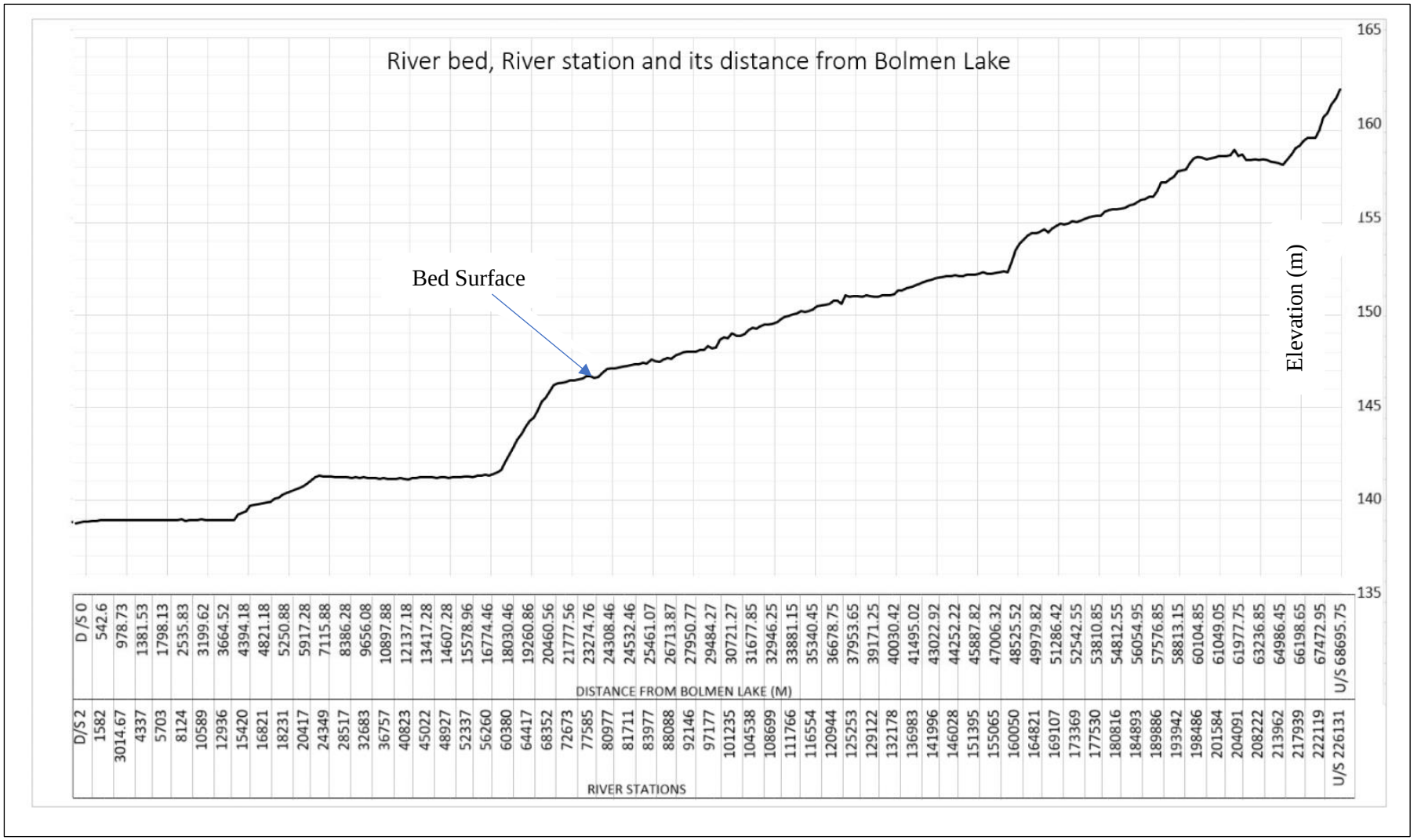

Figure A. 14 River profile along with chainage and river

Appendix B: Simulation Result and Calibration results

Result from RAS -mapper

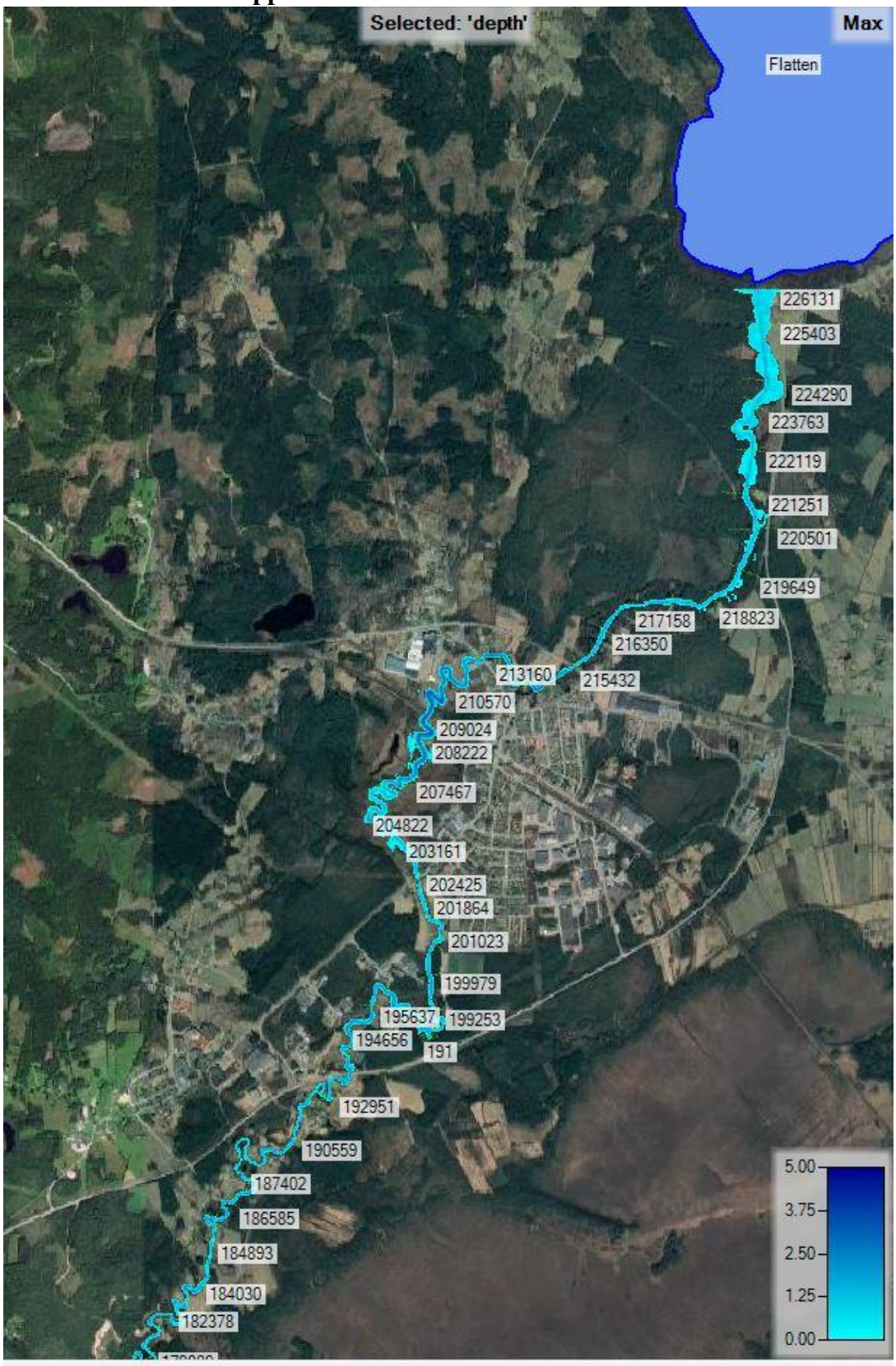

Figure B. 1 Depth mapping for simulation result for maximum water surface profile for year 2004-2019 (1/5)

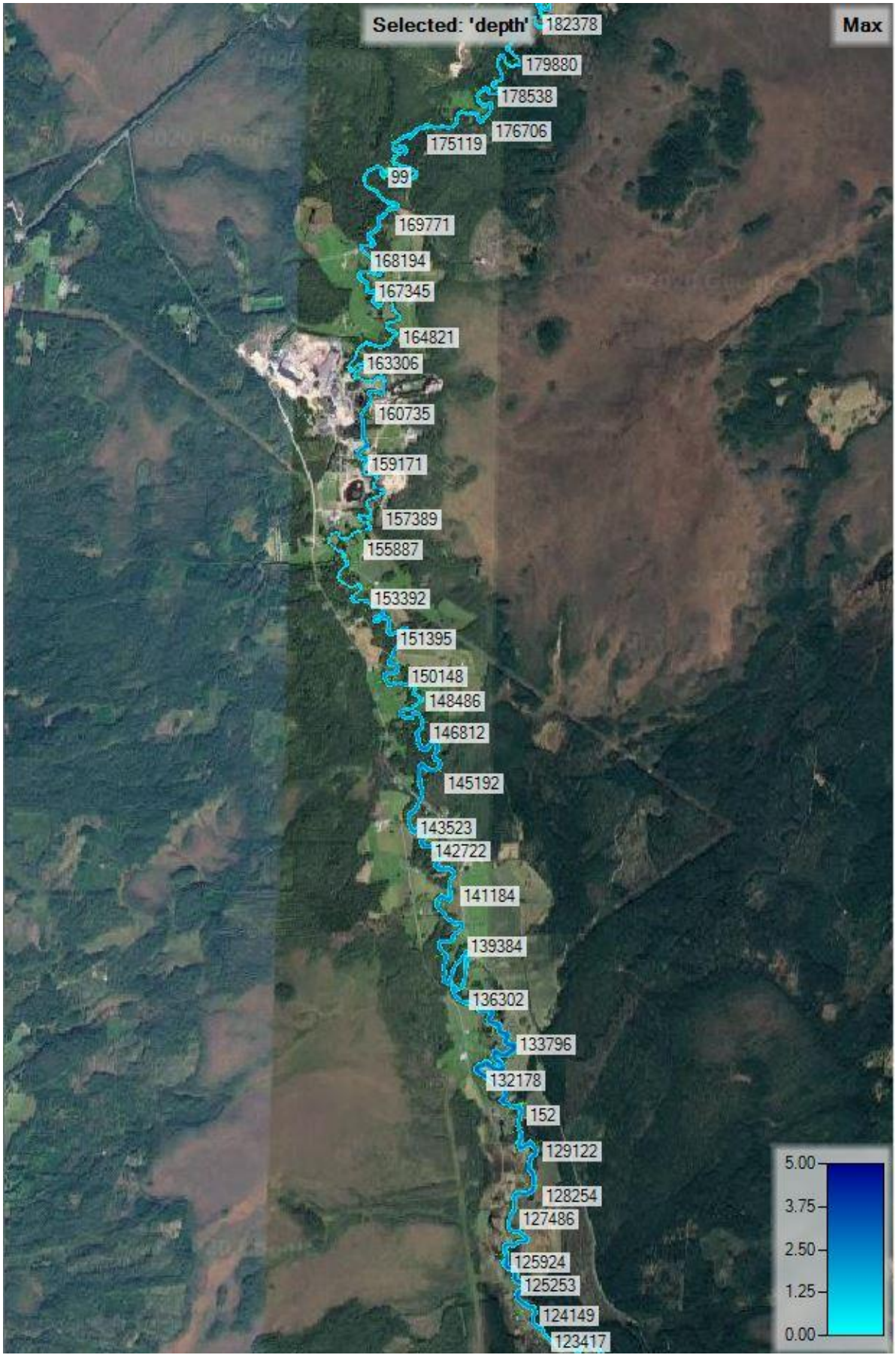

Figure B. 2 Depth mapping for simulation result for maximum water surface profile for year 2004-2019 (2/5)

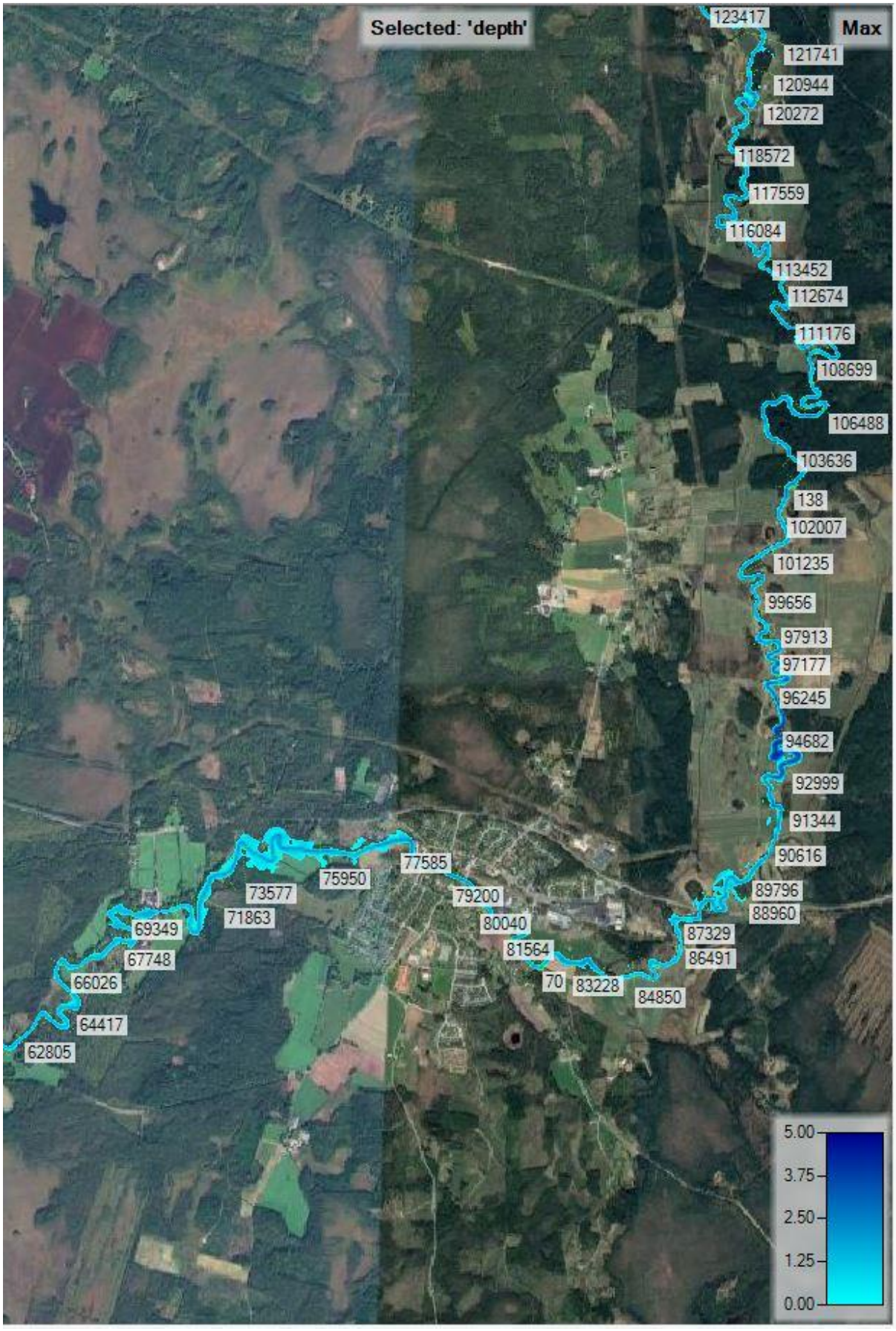

Figure B. 3 Depth mapping for simulation result for maximum water surface profile for year 2004-2019 (3/5)

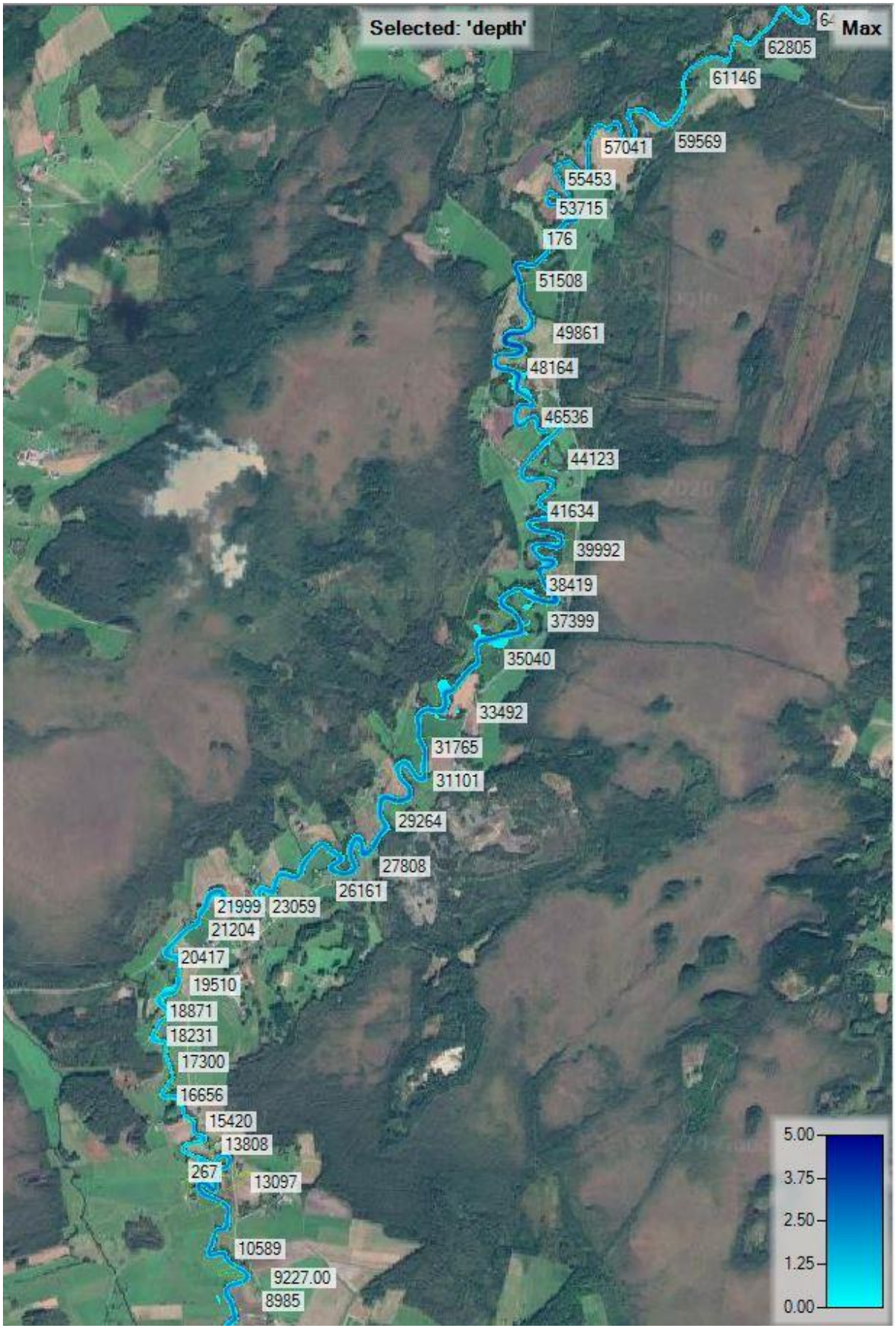

Figure B. 4 Depth mapping for simulation result for maximum water surface profile for year 2004-2019 (4/5)

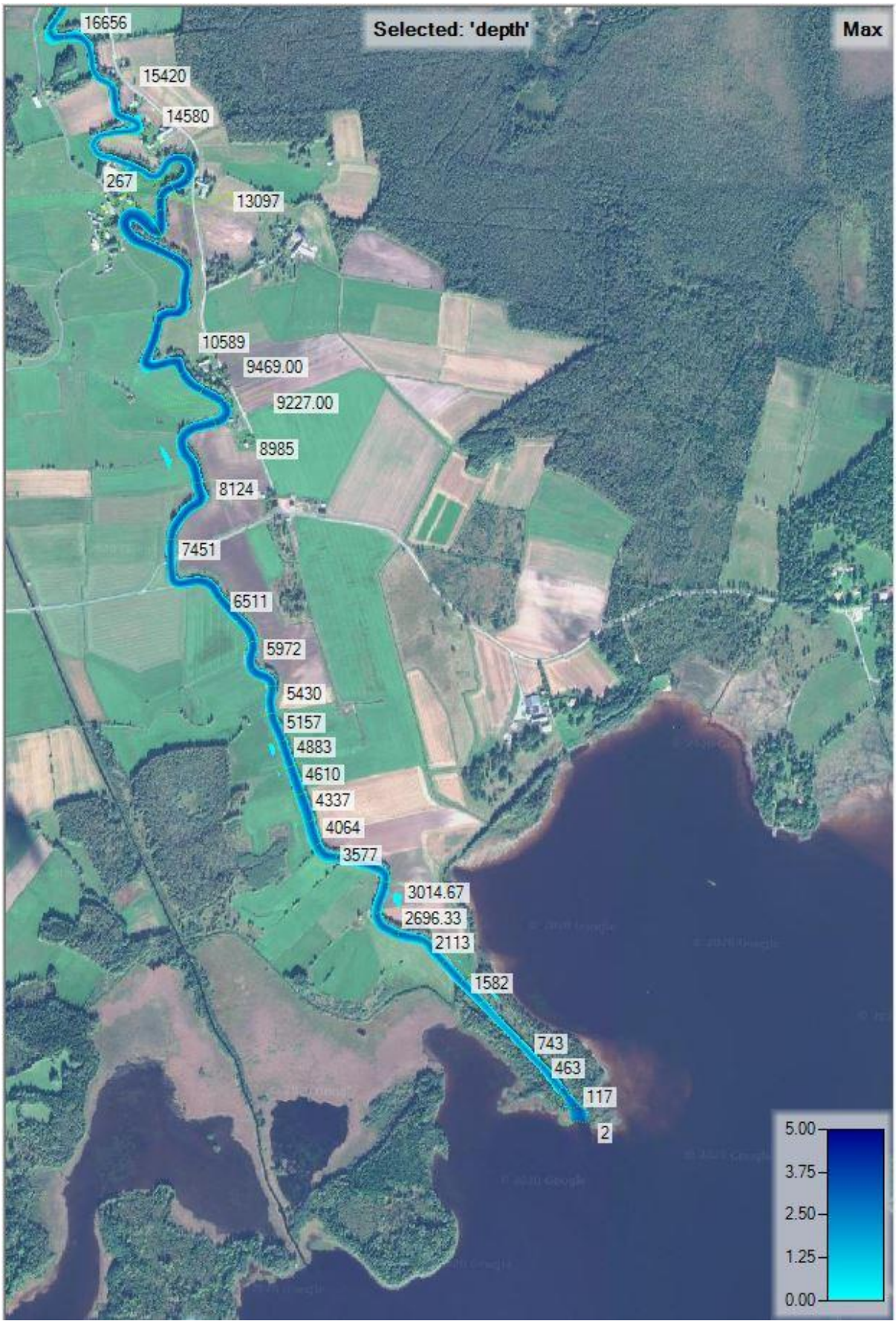

Figure B. 5 Depth mapping for simulation result for maximum water surface profile for year 2004-2019 (5/5)

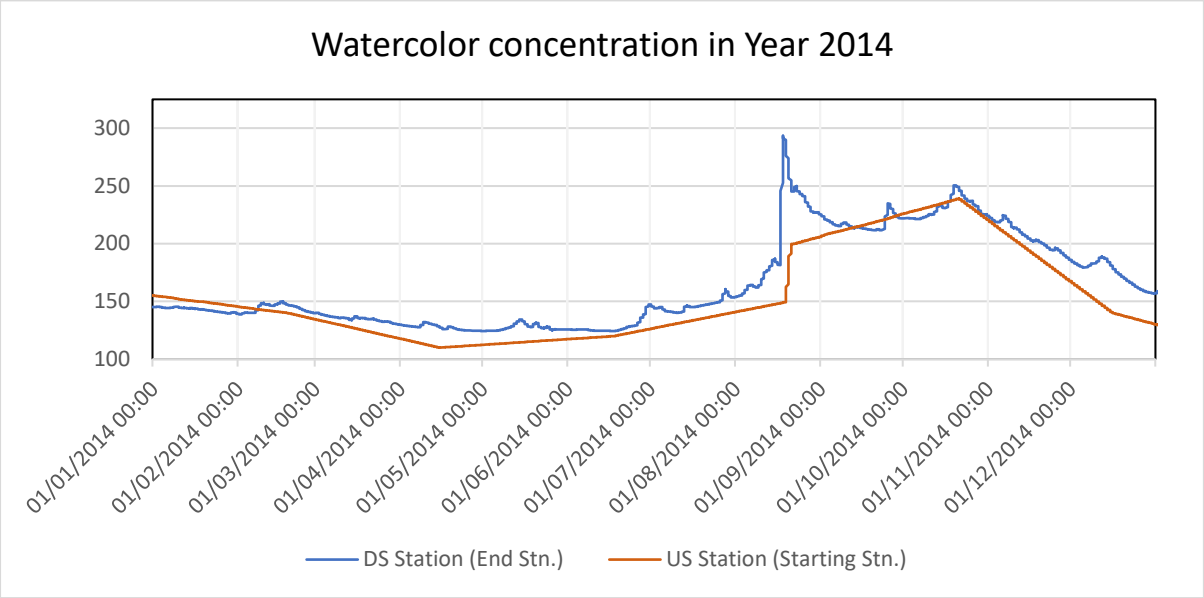

Figure B. 6 Simulation Results for the watercolor concentration in 2014 for US and DS stations

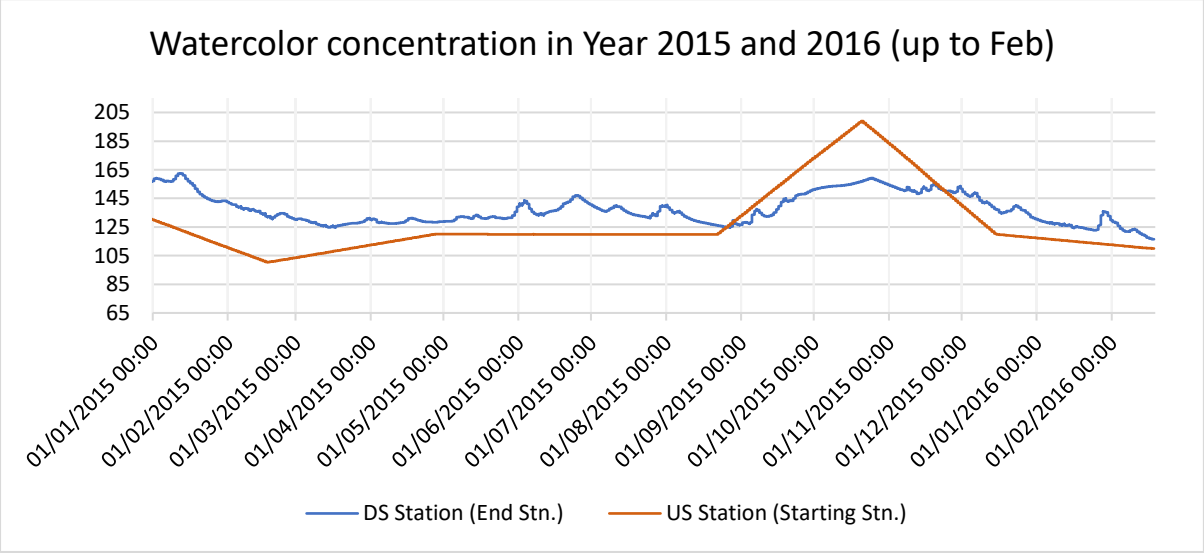

Figure B. 7 Simulation Results for the watercolor concentration in 2015 and 2016 for US and DS stations

Calibration Results Samples

The time taken for equilibrium condition is 2 days 11 hours (D =computed from Fischer Equation).

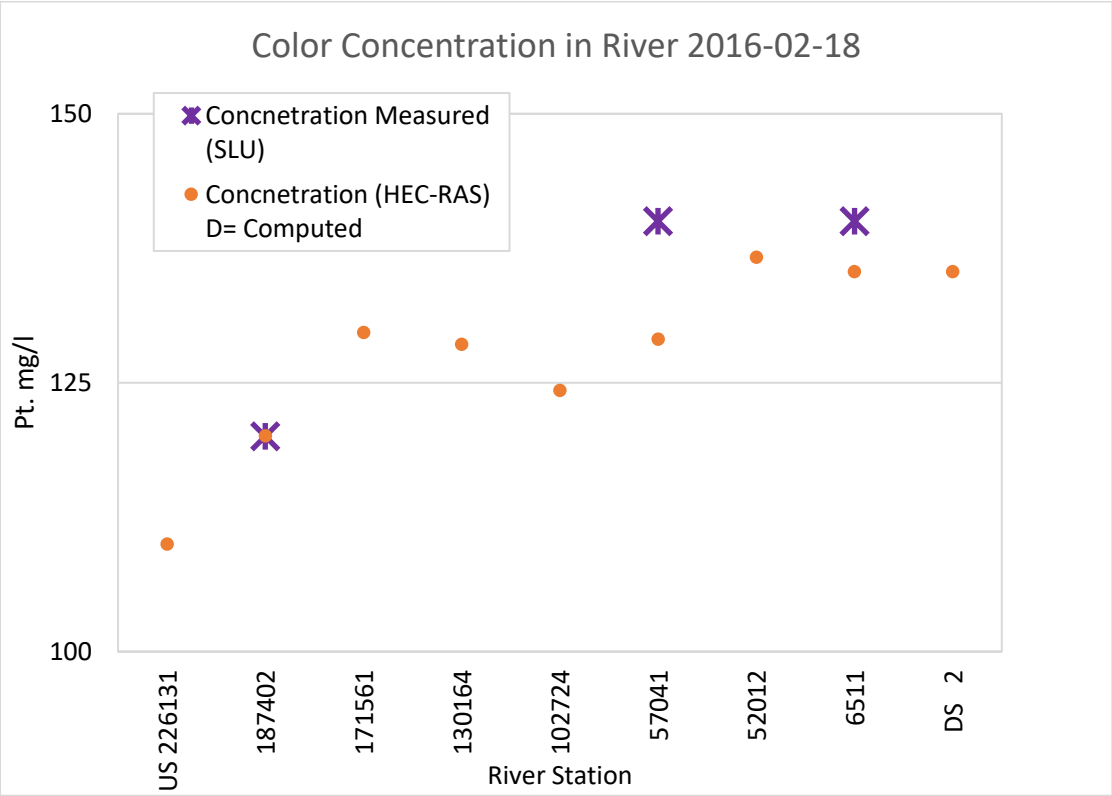

Figure B. 8 Calibration Results for color data of 2016-02-18

Table B. 1 Calibration Results for color data of 2016-02-18

RS	Station	Discharge (m^3/s)	Dispersion Coefficient (Computed)	Concentration (HEC-RAS) D= Computed	Concentration Measured (SLU)
1	226131	10	100.000	110.000	-
2	187402	11.7	3.956	107.940	120
3	171561	13.3	5.274	119.020	-
4	130164	14.5	4.343	117.118	-
5	102724	16.7	4.643	114.330	-
6	57041	18.3	1.873	119.950	140
7	52012	20.5	3.560	128.560	-
8	6511	20.7	8.665	127.319	140
8	2	20.7	26.702	127.312	-

The time taken for equilibrium condition is around 2 days 8 hours.

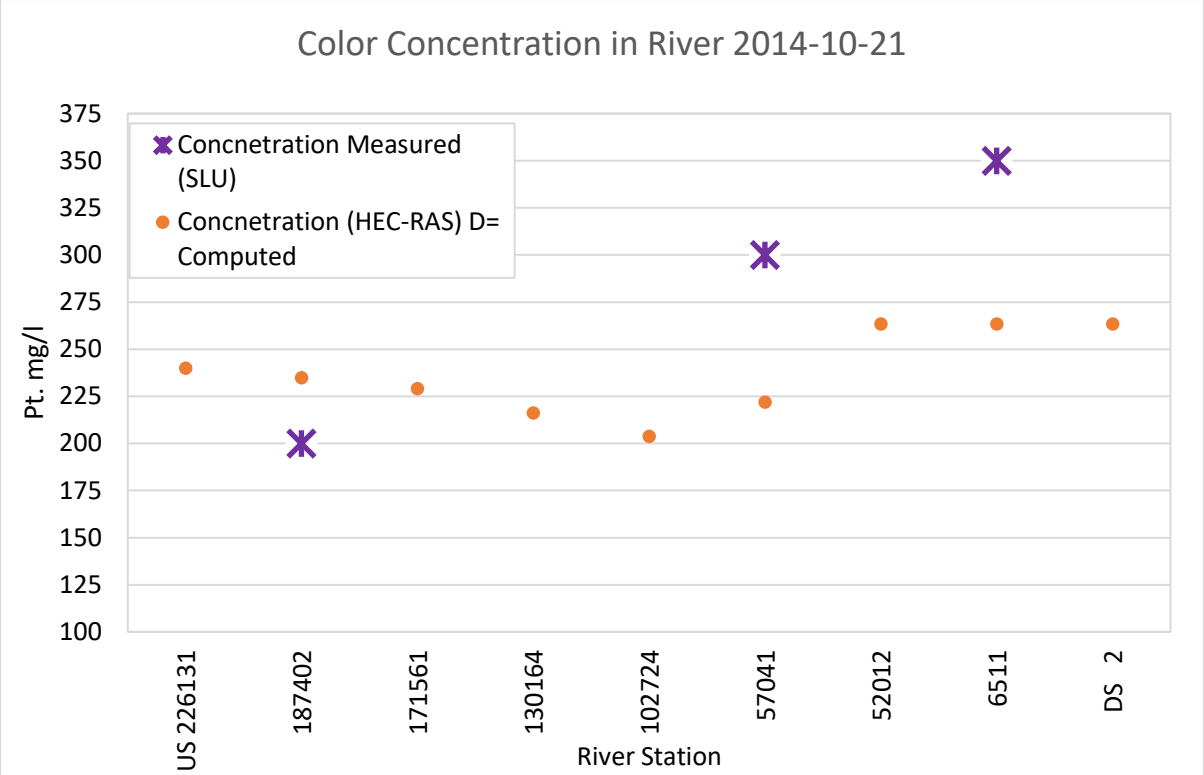

Figure B. 9 Calibration Results for color data of 2014-10-21

Table B. 2 Calibration Results for color data of 2016-02-18

RS	Station	Discharge (m^3/s)	Dispersion Coefficient (Computed)	Concentration (HEC-RAS) D= Computed	Concentration Measured (SLU)
1	US 226131	4.82	21.42381	240.00	
2	187402	5.87	4.165122	217.15	200
3	171561	7.05	4.769931	214.30	
4	130164	8.22	3.512584	200.14	
5	102724	9.36	3.832441	189.64	
6	57041	10.3	1.335775	209.13	300
7	52012	12.1	2.239512	252.42	
8	6511	12.1	6.813588	252.42	350
8	DS 2	12.1	15.60819	252.42	

The time taken for equilibrium condition is around 2 days 22 hours.

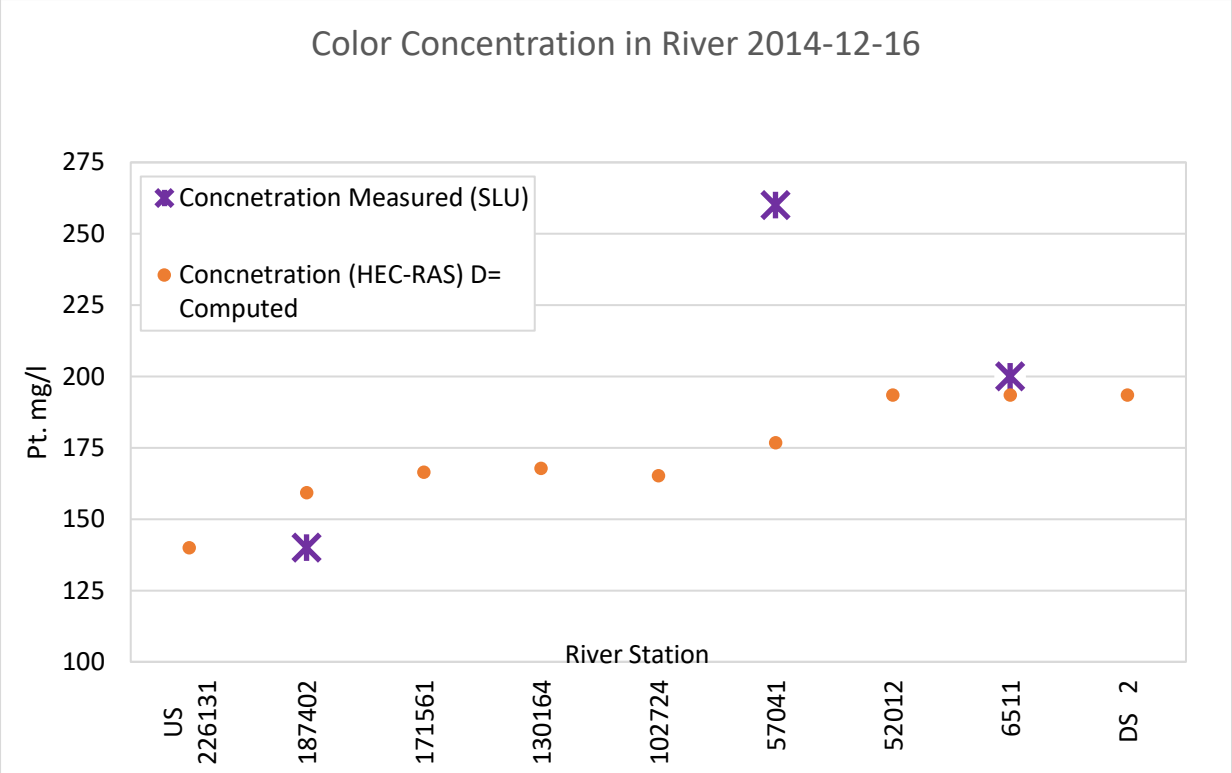

Figure B. 10 Calibration Results for color data of 2014-12-16

Table B. 3 Calibration Results for color data of 2014-12-1

RS	Station	Discharge (m^3/s)	Dispersion Coefficient (Computed)	Concentration (HEC-RAS) D= Computed	Concentration Measured (SLU)
1	US 226131	7.39	100.000	140	
2	187402	8.63	4.035	140.87	140
3	171561	10.5	5.119	151.35	
4	130164	12	4.195	150.68	
5	102724	13.6	3.889	150.13	
6	57041	15.1	1.620	163.25	260
7	52012	18	2.790	182.085	
8	6511	18	8.212	182.08	200
8	DS 2	18	23.219	182.08	

The time taken for equilibrium condition is around 2 days 13 hours.

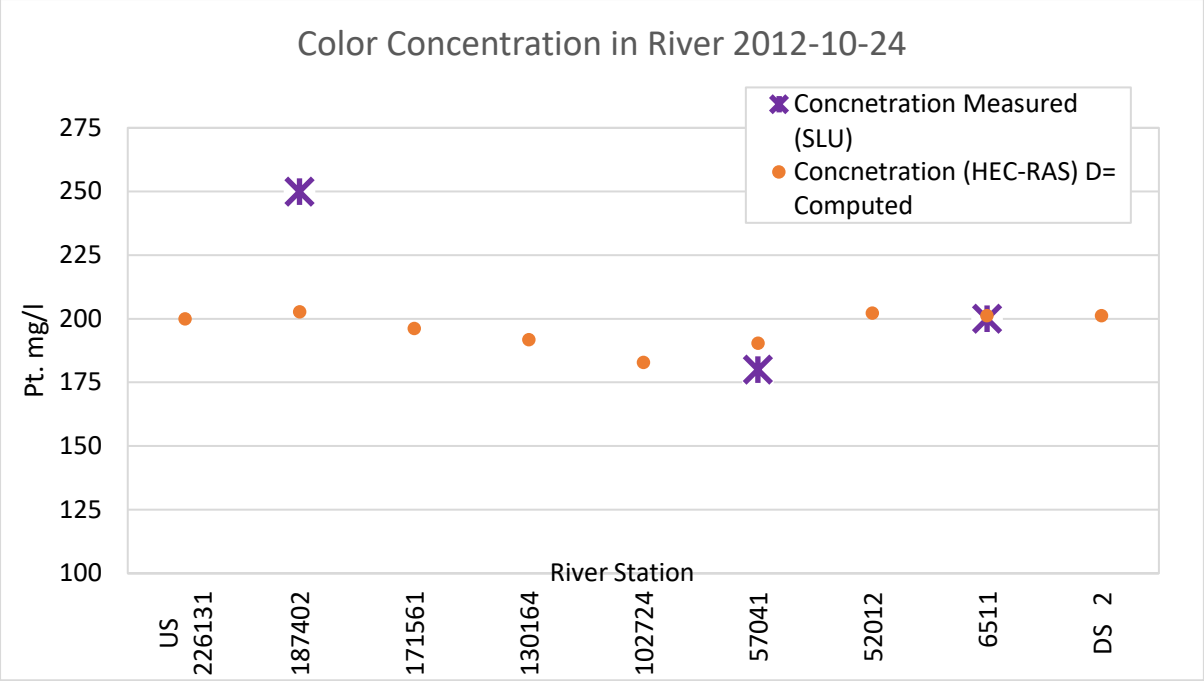

Figure B. 11 Calibration Results for color data of 2012-10-24

Table B. 4 Calibration Results for color data of 2012-10-24

RS	Station	Discharge (m^3/s)	Dispersion Coefficient (Computed)	Concentration (HEC-RAS) D= Computed	Concentration Measured (SLU)
1	US 226131	8.71	100	200	
2	187402	9.949	3.980065	187.15	250
3	171561	11.5	5.243503	182.58	
4	130164	12.6	4.290829	177.1634	
5	102724	13.9	4.322461	169.98	
6	57041	15.2	1.73551	178.65	180
7	52012	17.5	2.858935	191.795	
8	6511	17.6	8.31987	190.75	200
9	DS 2	17.6	23.99276	190.759	

The time taken for equilibrium condition is around 2 days 9 hours.

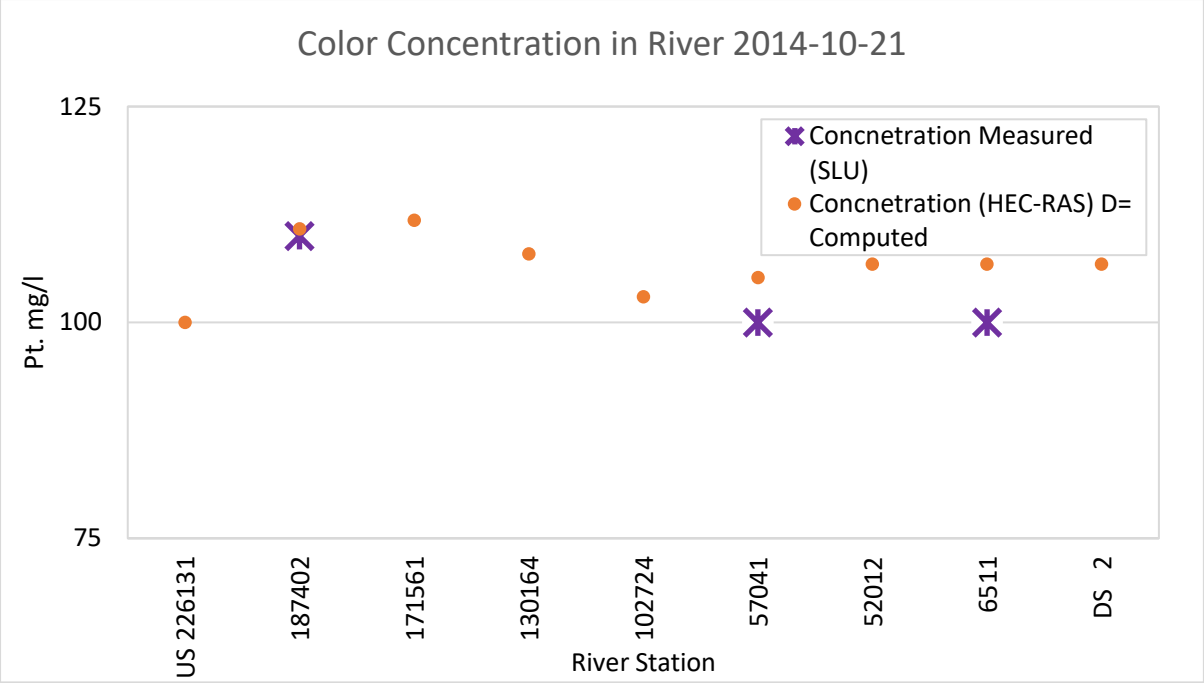

Figure B. 12 Calibration Results for color data of 2013-10-09

Table B. 5 Calibration Results for color data of 2013-10-09

RS	WQ	Discharge (m^3/s)	Dispersion Coefficient (Computed)	Concentration (HEC-RAS) D= Computed	Concentration Measured (SLU)
1	US 226131	4.82	6.2470	100.0000	
2	187402	5.87	2.4584	91.5200	110
3	171561	7.05	2.5850	94.6300	
4	130164	8.22	3.5140	95.5600	
5	102724	9.36	2.5822	102.9544	
6	57041	10.3	0.5934	105.2060	105
7	52012	12.1	0.9310	106.7470	
8	6511	12.1	1.1238	106.7464	110
8	DS 2	12.1	1.8575	106.7463	

The time taken for equilibrium condition is around 2 days 21 hours.

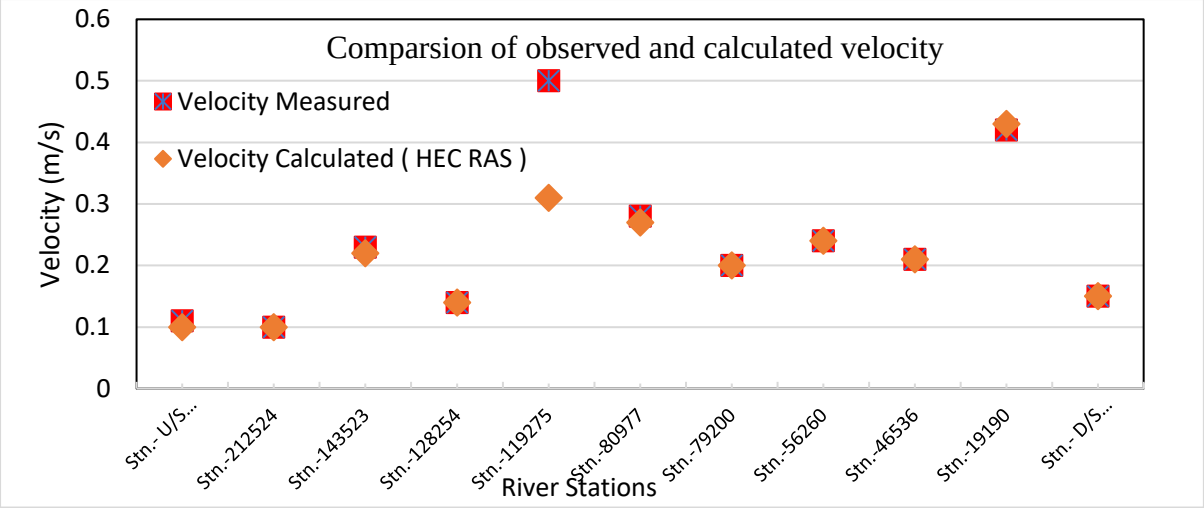

Figure B. 13 Comparison of the observed and computed velocity in different river stations.

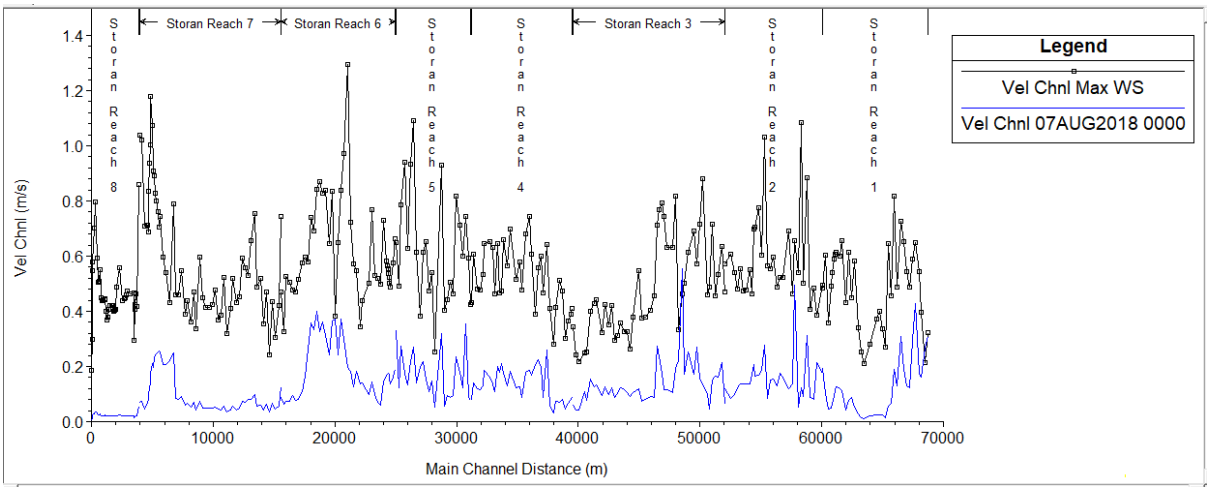

Figure B. 14 Velocity plot corresponding to the maximum water surface and lowest water profile (Aug. 7, 2018)

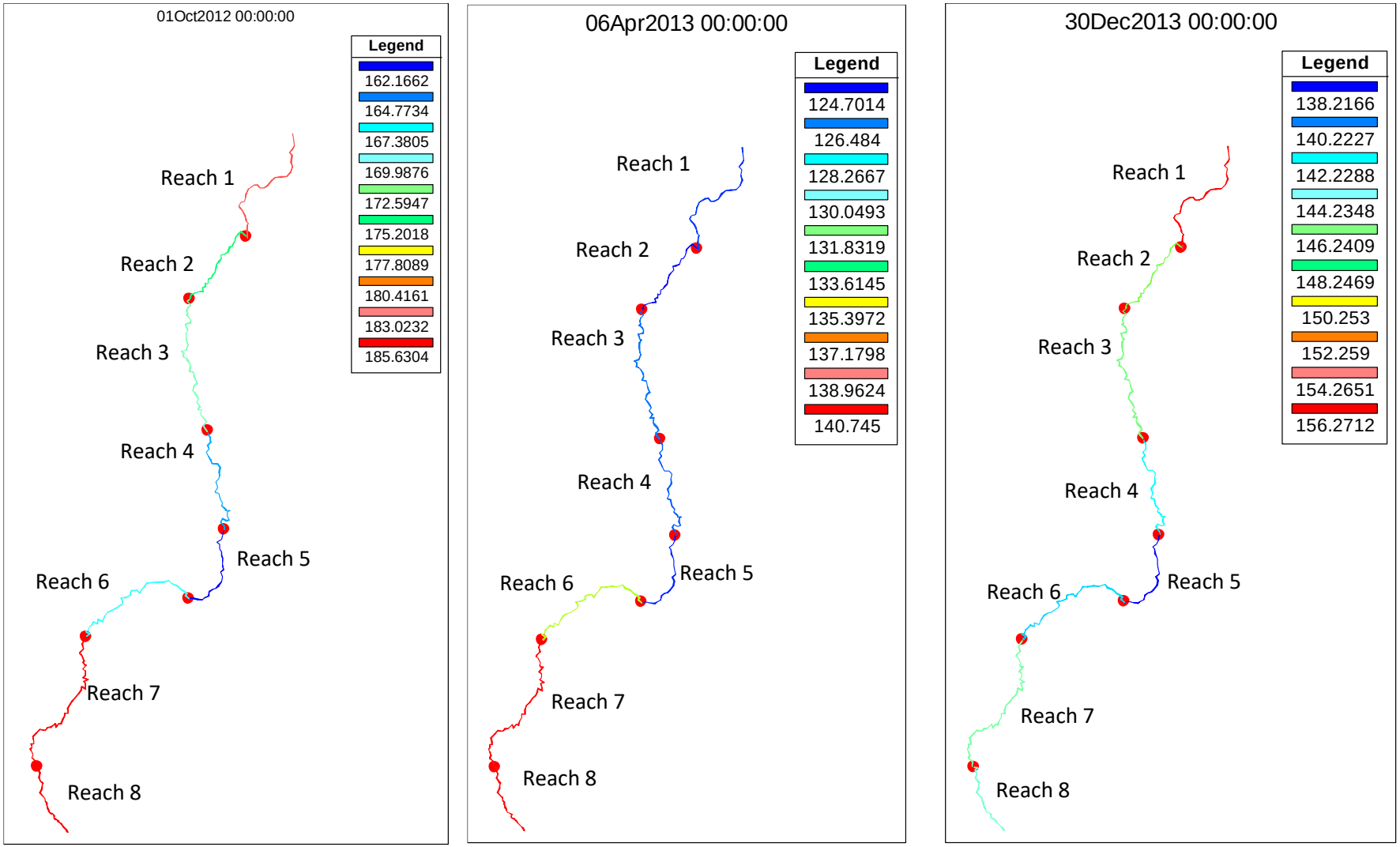

Figure B. 15 WCC variation in extreme events in year 2012 and 2013

Appendix C: Photographs

Figure C. 1 Storån near river station 46536, Bridge code: B4

Figure C. 2 Storån near river station 56260, Bridge code: B5

Figure C. 3 Storån (upstream) near river station 70184, Bridge code: B6

Figure C. 4 Storån (downstream) near river station 70184, Bridge code: B6

Figure C. 5 Storån near river station 80977, Bridge code: B8

Figure C. 6 Storån near river station 87329, Bridge code: B9

Figure C. 7 Storån near river station 88088, Bridge code: B10

Figure C. 8 Storån near river station 128254, Bridge code: B13

Figure C. 9 Storån (downstream) near river station 154562, Bridge code: B16

Figure C. 10 Storån (upstream) near river station 154562, Bridge code: B16

Figure C. 11 Storån (downstream) near river station 157889, Bridge code: B17

Figure C. 12 Storån near river station 202425, Bridge code: B23

Figure C. 13 Storån near river station 209024, Bridge code: B24

Figure C. 14 Storån (downstream) near river station 212524, Bridge code: B25

Figure C. 15 Storån (downstream) near river station 213962, Bridge code: B26

Figure C. 16 Store Mosse National Park located in the catchment of river Storån. Picture credit: Clemens Klante